DISS. ETH NO. 22756

Decentralized Electricity Storage Scenarios in LowExergy ZeroEmission Buildings and Communities

A thesis submitted to attain the degree of
DOCTOR OF SCIENCES of ETH ZURICH
(Dr. sc. ETH Zurich)

presented by

Diego Alexander Sandoval Vargas

MSc. ETH Zurich
born on 13.03.1984
citizen of Colombia

accepted on the recommendation of:

Prof. Dr. Hansjürg Leibundgut, examiner
Prof. Dr. Konstantinos Boulouchos, co-examiner

2015

Decentralized Electricity Storage Scenarios in LowExergy ZeroEmission Buildings and Communities

Diego Sandoval

Para mi familia

Il semble que la perfection soit atteinte non quand il n'y a plus rien à ajouter, mais quand il n'y a plus rien à retrancher.

Antoine de Saint Exupéry

Contents

Abstract

THIS dissertation is devoted to the definition of distributed electricity storage scenarios in a community consisting of *lowExergy* buildings.

Residential buildings are responsible for a substantial and steadily growing share of the overall electricity consumption. The ability to control the timing and magnitude of the aggregate buildings' consumption is acquiring critical relevance. This importance is justified in the pivotal role that buildings play in defining the shape and composition of the final electricity demand, and the impact they have on the electrical system existing and projected infrastructure. Distributed electrical storage is an elegant, economical, and technically-feasible way to introduce a degree of responsiveness with the residential buildings' demand without compromising the users' comfort.

The fundamental constituents in the analyses presented in this dissertation are an aggregation of *lowExergy* buildings and the electricity retailer with whom the buildings have a commercial relation. This thesis comprises three main blocks: 1) the proposition of a pricing policy aimed to stimulate a power-aware consumption, and consequently peak-shave the total electricity profile. 2) The simulation of the electricity profile that a *lowExergy* community will exhibit. And 3) the determination of the optimal amount of decentralized electrical storage and PV necessary to meet the retailer's objectives and allowing users to obtain a profit from the dynamic electricity tariff.

The first part of the thesis is concerned with the simulation of the electricity profile that a *lowExergy* community will exhibit. The simulation reflects a scenario in which thermal space-conditioning and domestic hot water production have been completely electrified. We followed a statistical approach to represent a variety of characteristics that buildings pertaining to a *lowExergy* community are expected to implement. The electricity profile's shape and composition in those buildings was found to be dictated mainly by the occupancy schedules. Each occupant was modelled as a stochastic agent, using a two-state Markov process. This approach results in plausible electricity profiles that simultaneously account for the heterogeneity found across different buildings and converge, in the aggregate view, in a well-known, quasi-deterministic profile.

The second part of the thesis is dedicated to the determination of the optimal battery and PV investment. The first model is formulated from the users' perspective. A rational user, facing a demand-based electricity tariff that separately penalizes energy and power, can use this model as a strategic tool to find the optimal amount of battery and PV she has to incur in order to minimize costs. The model revealed that the electricity tariff results

in an equilibrium, in which users invest between 20% and 25% of the total cost in battery and PV. Battery and PV are both important and interdependent upon each other, but the investment in battery is more than twice as large than the one in PV. The PV and the battery input power were found to be mainly related to the objective of reducing the energy cost. On the other hand, the battery capacity and output power were found to be associated with the peak reduction objective. Users invest less than 10% of the total battery investment share in the battery input power. This fact indicates that contrary to a battery usage driven by the price volatility, which is proposed in many models, the battery is used as a power to energy buffer. Energy is slowly stored in the battery and rapidly released at critical peak hours.

The second model simultaneously addresses the users' and the retailer's perspectives. This model has the form of a hierarchical bilevel optimization (BLP). The final equilibrium is not only determined by the electricity tariff and the user's reaction to it, but is additionally constrained by the retailer's strategy and profit objectives. The retailer's active control on the prices results in a profit recovery of approximately 6%. The battery investment is still larger than the one in PV, but the difference between the two shares decreases when the retailer becomes an active player. The ratio between battery and PV investments under this model was found to be approximately 1.8:1.

On the whole, the findings of this dissertation are a contribution to understanding the role of buildings in the operation and planning of the electrical system. The results suggest that a power-aware electricity tariff, in conjunction with a meaningful deployment of distributed batteries and PV, is more favorable and can accrue more benefits for society than the mere massive deployment of grid-tie PV.

Zusammenfassung

In dieser Dissertation werden Szenarios für die dezentrale elektrische Energiespeicherung in einem Verbund von LowExergy-Gebäuden ausgearbeitet. Wohngebäude sind für einen beträchtlichen und wachsenden Teil des Stromverbrauchs verantwortlich. Die Beeinflussung der zeitlichen Verteilung und des aggregierten Ausmasses dieser Verbraucher ist von kritischer Bedeutung für die gesamte Elektrizitätnachfrage und für die Anforderungen an die existierende und zukünftige Infrastruktur. Die dezentrale Elektrizitätsspeicherung ist eine elegante, ökonomische und erprobte Technologie, die die Laststeuerung von Wohngebäuden ohne Komforteinbussen ermöglicht. Die zentralen Aktoren in der Analyse dieser Dissertation sind die einzelnen LowExergy-Gebäude und das Elektrizitätsversorgungsunternehmen (EVU) mit welchem eine Geschäftsbeziehung besteht.

Diese Arbeit ist in drei Teile gegliedert: 1) Die Definition einer Preispolitik, die darauf abzielt die Spitzen des Gesamtverbrauchs zu brechen. 2) Die Simulation von Lastprofilen eines Verbundes von LowExergy-Gebäuden. Und 3) die Ermittlung der optimalen Grösse des dezentralen Speichers und der Photovoltaikanlage (PV) für das Erreichen der Ziele des EVU bei gleichzeitiger Reduktion der Kosten seiner Kunden durch die neue Preispolitik.

Die Simulation der Lastprofile basiert auf einem Szenario, in dem die Erzeugung von Raumwärme und Warmwasser komplett elektrifiziert ist. Variierende Eigenschaften der einzelnen LowExeregy-Gebäude sind als stochastische Simulationsparameter eingebunden. Es stellt sich heraus, dass der Lastverlauf dieser Verbraucher hauptsächlich vom Anwesenheitsverhalten der Bewohner abhängig ist. Die Bewohner werden einzeln, mit Hilfe von Markowprozessen mit zwei Zuständen modelliert. Das Resultat dieser Methodologie sind plausible Lastprofile, die gleichzeitig die Heterogenität der Gebäude abbilden und zu einem vorhersehbaren, quasi-deterministischen aggregierten Profil konvergieren.

Der erste Teil des Optimierungsproblems ist aus der Sicht der Verbraucher formuliert. Das resultierende Modell kann als strategisches Werkzeug zur optimalen Dimensionierung von Batterie und PV-Anlage verwendet werden, um die Kosten im Umfeld eines dynamischen Strompreismodells zu minimieren. Es wird gezeigt, dass die Elektrizitätspreise in einem Equilibrium sind, wenn die Verbraucher zwischen 20% und 25% der Gesamtkosten in Batterie und PV-Anlage investieren. Batterie und PV-Anlage sind beide wichtig und abhängig voneinander, aber die optimale Investition in die Batterie ist mehr als doppelt so gross wie in die PV-Anlage. Die Resultate zeigen, dass die Dimensionierung der PV-Anlage und die Wahl der Einspeiseleistung der Batterie hauptsächlich das Ziel der Energiekostenreduktion beeinflussen. Demgegenüber wird das zweite Ziel, die Reduktion der

Lastspitzen, hauptsächlich durch die Optimierung der Kapazität und die Ausgabeleistung des Speicherelements erreicht. Die optimale Investition in die Einspeiseleistung der Batterie beträgt weniger als 10% der Gesamtinvestition in den Speicher. Dies deutet darauf hin, dass die Batterie eine Pufferwirkung zwischen Leistung und Energie hat und ihr Betrieb, nicht wie in vielen Modellen angenommen, durch Preisvolatilität bestimmt wird. Energie wird langsam gespeichert und während den Spitzenzeiten schnell abgegeben.

Das zweite Model umfasst die Sicht der Verbraucher und des EVU gleichzeitig. In diesem Fall wird das Gleichgewicht zusätzlich durch die Strategie und die Gewinnziele des EVU beeinflusst und nicht nur durch den Stromtarif und die darauffolgende Reaktion der Verbraucher bestimmt. Ein aktives Eingreifen des EVU in die Tarife steigert seine Gewinne um etwa 6%. Auch wenn das EVU der aktive Akteur wird, bleibt die optimale Investition in die Batterie grösser als in die PV-Anlage, aber dieser Unterschied schrumpft auf ein Verhältnis von etwa 1.8:1.

Im Grossen und Ganzen sind die Erkenntnisse dieser Dissertation ein Beitrag zum Verständnis der Rolle von Gebäuden im Betrieb und in der Planung des Elektrizitätsversorgungssystems. Die Resultate zeigen, dass ein leistungsabhängiger Stromtarif in Kombination mit einem koordinierten Einsatz von dezentralen Batterien und PV-Anlagen vorteilhafter ist als ein blosser Ausbau von netzabhängigen PV-Anlagen.

Acknowledgments

I would like to express my warmest gratitude to my *Doktorvater*, Prof. Dr. Hansjürg Leibundgut, for having invited me to join his group and to be part of his vision. I am sincerely thankful for his guidance, support, and for all the freedom I enjoyed to develop my own ideas and pursue many interesting projects.

I want to express my sincerest thanks to my co-examiner, Prof. Dr. Konstantinos Boulouchos. I very much enjoyed our discussions, his feedback and recommendations have proven very useful.

I also want to extend my thanks to Prof. Dr. Dr. E.h. Dr. h.c. Werner Sobek, who acted as a third examiner of my thesis.

I had the benefit of many inspiring discussions with my colleague Antonio Sánchez-Ihl, he encouraged me to investigate many interesting topics and provided me constantly with critical feedback.

I would like to extend my warmest thanks to my colleagues Philippe Goffin and Jonas Ruggle. We were involved in very many interesting academic and entrepreneurial endeavors. Jonas and Philippe provided me with extremely useful feedback and recommendations.

I enjoyed a most inspiring and familiar academic environment. I was regularly involved in very interesting and enriching discussions with my colleagues. It was very pleasurable to work and exchange ideas with Vera Schmidt, Luca Baldini, Marc Bätschmann, Niklaus Haller, Christoph Meier, João Nogueira, Kim Moon Keun, Matthias Mast, Georg Putzi, Volker Ritter, Lester Ullman, Marcel Brülisauer, and Forrest Meggers.

I am deeply thankful to the International Centre of Physics CIF, especially to Prof. Dr. Eduardo Posada-Flórez and José García-González, and to the Colombian Institute for Development of Science and Technology COLCIENCIAS that granted me a scholarship for studies abroad.

I also want to thank several friends and fellows who provided me either with valuable recommendations or support: Valérie Gass, Arno Schlüter, Jimeno Fonseca, Daren Thomas, Clayton Miller, Zoltan Nagy, and all the fellows at the A/S Chair at ETH Zurich. Vaggelis Vrettos and Marina González-Vaya from the Power Systems Laboratory at ETH Zurich. And finally, my friends and colleagues from BS2 AG and the Building Technology Park Zurich; digitalSTROM, in particular, provided me with residential consumption data.

I want to thank to Arvindan Thekkadath, Advait Godbole and Abhishek Rohatgi, who read an early version of this thesis's introduction, and Martín Mosteiro-Romero, who proof-read some sections of my manuscript and provided me with several stylistic corrections.

Like all important milestones in my life, this goal would not have been possible without the unconditional love and support from my family. Immense *gracias* to my parents Edgar and María Eugenia, my sisters Johana and Gisella, and my brother Fernando.

Finally, I would like to thank Gabrielė for her love and support, for being my music and my muse.

Zurich, 2015 vasara

List of Acronyms

AMI Advanced Meter Infrastructure

AS Ancillary Services

BLP Bilevel Program

CDD Cooling Degree Day

CO_2 Carbon Dioxide

COP Coefficient of Performance

CPP Critical Peak Pricing

CTP Critical Time Pricing

DHW Domestic Hot Water

DOD Depth of Discharge

DR Demand Response

DSE Distributed Storage Element

DTMC Discrete Time Markov Chain

EAC Equivalent Annual Cost

EV Electric Vehicle

HDD Heating Degree Day

HP Heat Pump

IBP Incentive Based Program

KKT Karush-Kuhn-Tucker

LP Linear Program

MB Marginal Benefit

MBHE Membrane Borehole Heat Exchanger

MC Marginal Cost

MIP Mixed Integer Program

MPCC Mathematical Problems with Complementarity Constraints

MPEC Mathematical Problems with Equilibrium Constraints

NLP Nonlinear Program

NPV Net Present Value

OAT One at a Time

OPF Optimal Power Flow

PHS Pumped Hydro Storage

PV Photovoltaic

RTP Real Time Price

SOC State of Charge

TBR Time Based Rate

TOU Time of Use

TRY Typical Reference Year

List of Figures

List of Tables

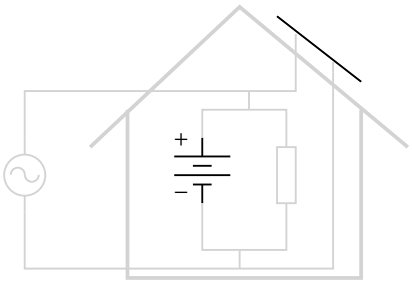

Chapter 1

Introduction

Buildings are not isolated entities, they are constituents of larger and more complex systems. The relation between a building and its environment can be characterized in terms of the different interactions and synergies that take place at the building's boundaries. Buildings make up neighborhoods, urban landscapes, and are connected to a wide range of district utilities. There is a constant interaction in the form of energy, mass, and information between the building and its surroundings.

One such interaction is at the interface between the building and the electrical grid. The electrical grid is a complex system connecting generators to consumers. Due to the nature of electricity, generation and consumption have to be balanced on a per-second basis. Historically, all operations necessary to keep the grid in balance were carried out from the generation side. However, a series of developments that have taken place during the last years have highlighted the pivotal role of flexible loads on balancing the grid [21, 67].

In the last decades, several socioeconomic, technological, and political events have restructured the energy scenario. The advent of renewables, the phasing out of nuclear power plants, and a variety of policies favoring a low carbon society reshaped the energy landscape and imposed new challenges that emphasize the necessity of a flexible, controllable, and responsive demand side.

The different operations, techniques, and approaches aimed at making buildings flexible and controllable are collectively referred to as Demand Response (DR) [30, 32, 66]. Essentially, DR provides the possibility of shifting electricity consumption between peak and off-peak periods and, more accurately, of matching the building's load with the available generation on a real-time basis. There are multiple ways in which these objectives can be met [19, 30, 48, 66]. This thesis focuses on the introduction of Distributed Storage Elements (DSEs) only.[1] A DSE provides the required flexibility and responsiveness, while decoupling the DR objectives from the building operational requirements and constraints.

This thesis will explore several DR interactions between the electrical grid and buildings implementing an electrical battery. The main focus of this thesis will be to determine the optimal size of this battery. An extensive adoption of battery technologies in residential buildings requires both a technical and an economic analysis, it has to consider the aggregation of a plurality of buildings, their interaction with the grid, and the required policy

[1] Throughout this document, the terms 'DSE' and 'battery' are indistinctly used.

and business framework.

A flexible electrical load is a very important aspect of the role of buildings in the transition towards a clean energy society. It is not the only one though. If buildings are going to contribute to paving the way towards a low carbon society, the form and amount of the consumed energy have to be regarded as relevant factors as well. The migration towards clean technologies will result in the electrification of several processes formerly driven by fossil fuels, e.g., space conditioning. In this context, reducing the share of electricity consumed, or increasing the share of electricity generated, is as well a goal of great importance.

Photovoltaic (PV) modules on solar roofs are a widespread feature of today's architecture. The rooftop segment has experienced a sustained growth in recent years. In 2013, the residential rooftop segment accounted for 22% of the total PV market in Europe, representing more than 2.4GW of the total installations [20]. Simultaneously, reports, laws, and recommendations stimulating or enforcing the installation of solar roofs continue to emerge [25]. In the light of this context, some natural questions arise:

1. *Is the dimension of a battery element affected by the available on-site generation?*

2. *Is the idea of deploying DSEs in line with a massive deployment of rooftop PV? Does it pursue overlapping, complementary, or contradictory objectives?*

Batteries and PV are not competing but complementary technologies; PV provides local electricity generation, while batteries provide storage functionality. A policy enforcing a massive adoption of PV might not necessarily be the best or the only way to tackle the challenges that are inherent in the current and future energy scenario. On one hand, electrical storage, or a combination between electrical storage and PV, offers a greater load control potential than PV alone. On the other hand, there is still a seasonal energy imbalance that neither PV nor batteries can alleviate.

Motivated by the complementary nature and the inter-dependencies between the battery selection and the amount of available on-site generation, the battery dimension problem will be tackled in tandem with the PV one. The following questions are relevant to this research:

1. *What is the optimal investment in batteries and PV in low exergy (lowEx) residential buildings?*

2. *What is the recommended organizational framework to coordinate a meaningful deployment of batteries and PV?*

3. *What is the resulting interplay between the electrical grid and buildings implementing DSEs?*

1.1 Problem Description

This thesis deals with the definition of an electricity scenario in which an aggregation of buildings have adopted *lowEx* standards, including the electrification of space-conditioning processes. This *lowEx* community will claim similar energy shares, but will exhibit a different electrical consumption structure than today's buildings using conventional heating and cooling systems. Each of these buildings has a commercial relation with the aggregating entity that supplies the electricity, hereinafter also referred to as 'retailer'. The first part of the problem basically consists in the extrapolation of the $2Sol$ (see Section 2.1) building paradigm to the concept of *lowEx* community, and the identification of the resulting interaction with the retailer.

The interaction with the retailer is important given the increased share of electricity claimed by buildings under the previously described scenario. It is also important in terms of the accompanying challenges, such as coordination of the distribution infrastructure, stability, and planning of future grid investments. The second part of the problem comprises the definition of a mechanism that allows the retailer to influence the aggregate consumption pattern, i.e. to control, to some extent, the aggregate electricity profile. Under the assumption that this objective can be achieved by combining a pricing policy and the deployment of DSEs, this investigation deals with the definition of such policy and deployment mechanisms.

This thesis is devoted to the definition of a mathematical model, aimed at calculating the optimal power and energy of a DSE, as well as the optimal installed power of a PV element, pertaining to a building implementing the $2Sol$ principles. The model has to contemplate each building's individual perspective as well as the perspective of the retailer aggregating a community consisting of several such buildings. The goal of this model is to find the optimal investment in battery and PV elements that have to be undertaken by individual buildings and by the retailer.

1.2 Research Hypothesis

Hypothesis 1: Given a *lowEx* community, whose buildings are aggregate by an electricity utility through a commercial relation, it is possible to introduce a level of control upon the final electricity profile. This goal can be achieved by providing an adequate price signal and by deploying DSEs.

Hypothesis 2: In the presence of a price signal explicitly addressing energy and the maximum daily power, a rational user will choose to install a combination of battery capacity and PV, provided she can reduce costs or obtain an economic profit.

Hypothesis 3: It is possible to devise a Demand Response mechanism that brings economic benefits to the final consumers, and simultaneously makes the retailer more

competitive.

1.3 Thesis Objective

The main objective of this investigation is to devise the operative principles of a *lowEx* community, in which the retailer's DR objectives, namely responsiveness, peak-shaving, and control of the aggregate electricity profile, are achieved by means of a pricing policy and DSEs. The resulting mechanism has to contemplate both the individual buildings' and retailer's perspectives. This objective involves several other complementary objectives.

1. To simulate the electricity profile of a community consisting of *lowEx* buildings.
2. To define a pricing policy allowing the aggregating entity to indirectly control the final electricity consumption pattern.
3. To introduce an explicit differentiation between energy and power in the electricity tariff.
4. To find the optimal battery and PV size implemented by each building as a response to the pricing policy.
5. To determine the correlation between the dimension of PV and battery elements.

1.4 Thesis Methodology

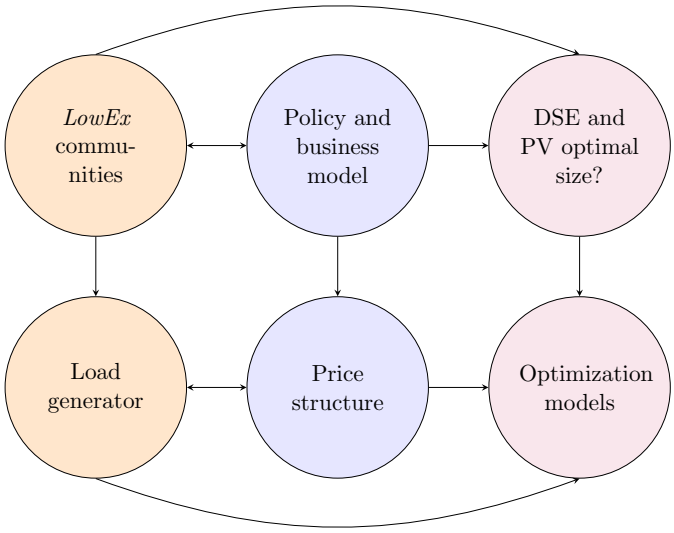

Figure 1.1: Milestones and methodology

The results presented in this thesis are based on the formulation of mathematical models. These models attempt to represent both the physical and the economic mechanism governing the relation between *lowEx* residential buildings and the electricity retailer aggregating them.

The methodology adopted in this work, illustrated in Figure 1.1, consists in the definition of three milestones: a policy-related one, relative to the construction of a price signal explicitly addressing energy consumption and maximum power; a load generator attempting to represent the electricity pattern of a *lowEx* community; and a mathematical model aimed at finding the dimension of the optimal PV and battery capacity from both the individual buildings' and the retailer's viewpoint.

Milestone 1: from *lowEx* buildings to *lowEx* communities. The problem of anticipating the resulting electricity profile that a *lowEx* community will exhibit is approached by combining bottom-up and top-down methodologies. This approach offers the possibility to model the heterogeneity displayed by individual buildings, while simultaneously converging to the desired aggregate figures.

Milestone 2: commercial relation between the buildings and the retailer. The formulation of the economic framework is approached by proposing a business model defining the commercial relation between the users and the retailer. We assume that the aggregating entity has a strong incentive to peak-shave, and in general control, the total consumption pattern. The proposed pricing scheme favors the adoption of DSEs and PV as a way to meet the DR objectives without compromising the user's comfort.

Milestone 3: distributed electrical storage as DR driver. Building on the first two milestones, the final part of this dissertation is devoted to attaining a model to determine the optimal amount of PV and DSEs that has to be deployed. We consider both the user's and the aggregating entity's perspective. The model follows a cost-based approach. A cost-based approach constitutes a lower bound for further scenarios, in which additional non-economic incentives, such as environmental awareness, are considered.

1.5 Thesis Scope

The research presented in this thesis is formulated in the context of the temperate climatic conditions predominant in Switzerland, Swiss building characteristics and standards, and the composition and characteristics of the Swiss electrical system. The models and results are general enough to be extrapolated to different locations and conditions, but the underlying assumptions apply mainly to the temperate climate of Central Europe.

(a) Number of buildings (b) Constructed area

Figure 1.2: Distribution of residential and non-residential buildings in Switzerland [37]

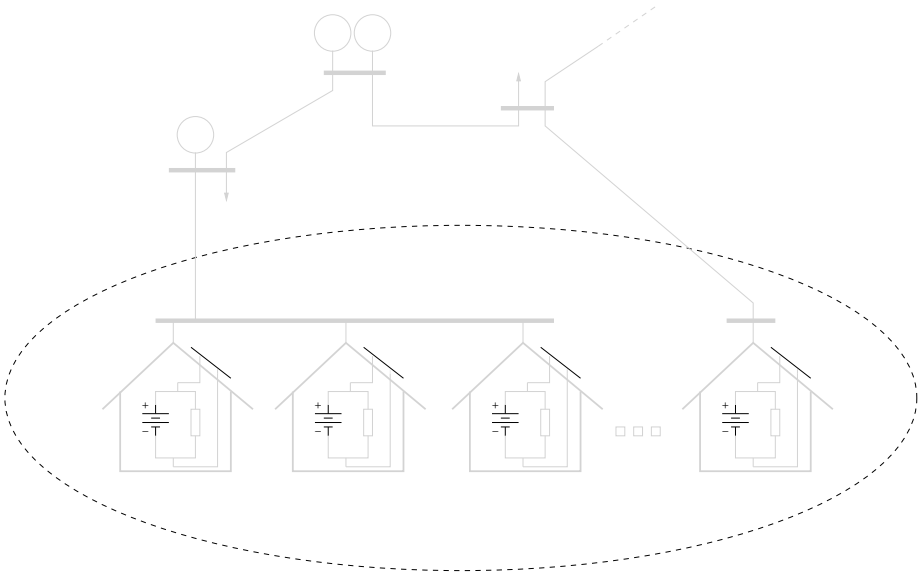

Figure 1.3: Definition of the problem's boundary conditions

This thesis prioritizes one particular type of building paradigm; buildings are assumed to comply, completely or to some extent, with the guides and principles dictated by the $2Sol$ methodology, described later in Section 2.1. The main focus is on residential buildings, even if office buildings are considered as well. The majority of buildings in Switzerland are residential (see Figure 1.2).

The fundamental block in the presented analyses is a residential building implementing a DSE and, optionally, a PV element. The objectives pursued in this thesis require considering a system larger than each individual building. This system must include the aggregation of hundreds or thousands of buildings and consider their interplay with the electrical grid. The electrical grid is not explicitly modelled. The interaction between the buildings and the grid is accounted for in terms of the economic relation and the transactions occurring between the individual buildings and the retailer. The boundary condition

is thus selected to encompass a collection of buildings and one segment of the entity to which the buildings are subordinated. The resulting system is illustrated in Figure 1.3.

1.6 Thesis Context and Energy Scenario

The ultimate goal of *lowEx* buildings and communities is to reduce the significant share of the final CO_2 emissions for which the building sector is responsible.[2] Closely related to this objective is the imperative necessity of replacing heating systems fired by fossil fuels. Additionally, the current structure of the electrical system, the limited capacity reserves, and the nature of several generation technologies impose the requirement that buildings be controllable, such that the grid utility can better coordinate the dispatch of the available power and energy resources to supply the buildings' loads.

The role of DSEs as power and energy regulators acquires special relevance in the context of a *lowEx* community. It has to be understood not only under the circumstances of the current situation, but under those of a scenario in which room-heating processes have been, partially or completely, electrified. The electrification of the room-conditioning processes will substantially reduce the CO_2 emissions produced in buildings, but will impose additional challenges upon the electrical grid. These challenges will have the form of an even larger seasonal energy imbalance, and a possibly higher instantaneous load power during the critical peak hours. A DSE is not a generator, so it can do little or nothing to alleviate the seasonal energy imbalance. The same applies for PV elements, as solar radiation is scarce during the heating period. The main contribution of DSEs will be to serve as a coordination tool, allowing a better match between the buildings' load and the grid instantaneous conditions. This matching can be achieved by differentiating and independently controlling two variables: power and energy. Under the assumption that users give a very high value to their comfort, this flexibility can only be introduced by relying on a storage mechanism: a DSE.

This section hypothesizes different energy scenarios, in which the aforementioned electrification of buildings' heating and cooling systems has taken place. The construction of this scenario is based on the Swiss national electricity statistics [11, 37].

1.6.1 *LowEx* Communities

A *lowEx* community is an agglomeration of buildings implementing practices and standards aimed at reducing their exergy consumption and their direct CO_2 emissions. *LowEx* buildings combine passive and active approaches to optimize the building's exergetic performance, and to balance the energy flows between the building and its environment. Achiev-

[2] The building sector accounts, in industrialized countries, for roughly one third of the final energy consumption, and a similar proportion of CO_2 emissions [44]. In Switzerland, for instance, the building sector is responsible for 49% from the total fossil fuel consumption [27], and claims 31.6% of the total electricity consumption [37].

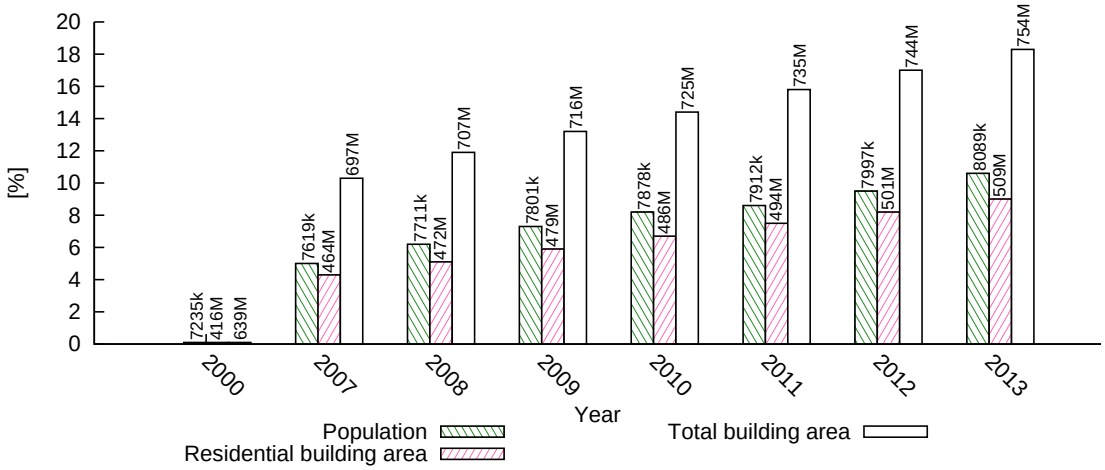

(a) Increment in the population, total buildings area [m^2], and residential buildings area [m^2] with respect to year 2000. Numbers on top of the bars indicate the absolute figures in the corresponding period, in thousands [k] and millions [M] respectively.

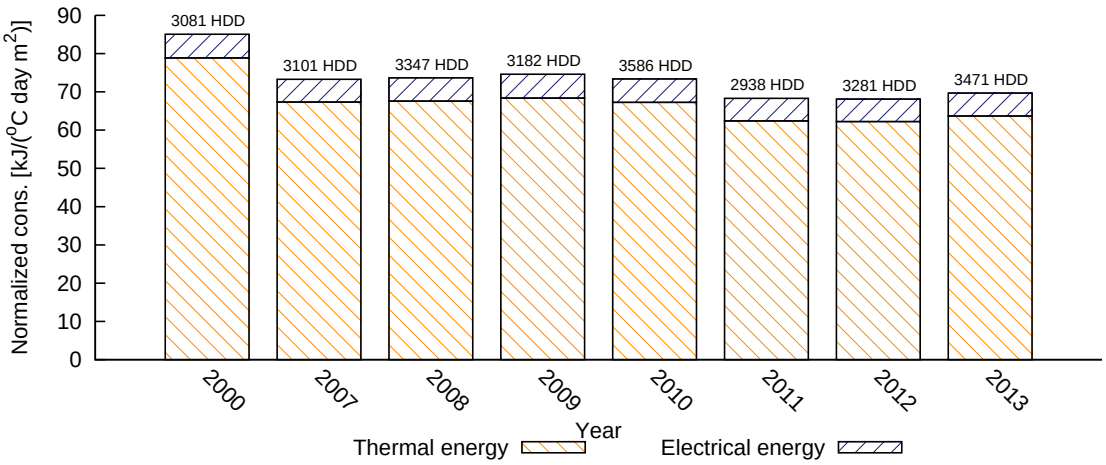

(b) Normalized consumption in buildings per total constructed area [m^2] and total Heating Degree Days (HDD)

Figure 1.4: Evolution of factors influencing the energy consumption in buildings in Switzerland. Data source: [37].

ing a *ZeroEmission* operation implies among others the electrification of fossil-fuel-driven space-heating processes.

The core component in a *lowEx* building is a low temperature heating system, implementing a Heat Pump (HP) with high Coefficient of Performance (COP). A high COP results in a lower fraction of electrical energy required to supply the building heating demand. *LowEx* buildings are further described in Section 2.1.

The following section explores the impact of a massive deployment of HPs in the context of the current Swiss energy scenario and the accompanying challenges regarding the energy and power resources.

1.6.2 Swiss Energy Scenario

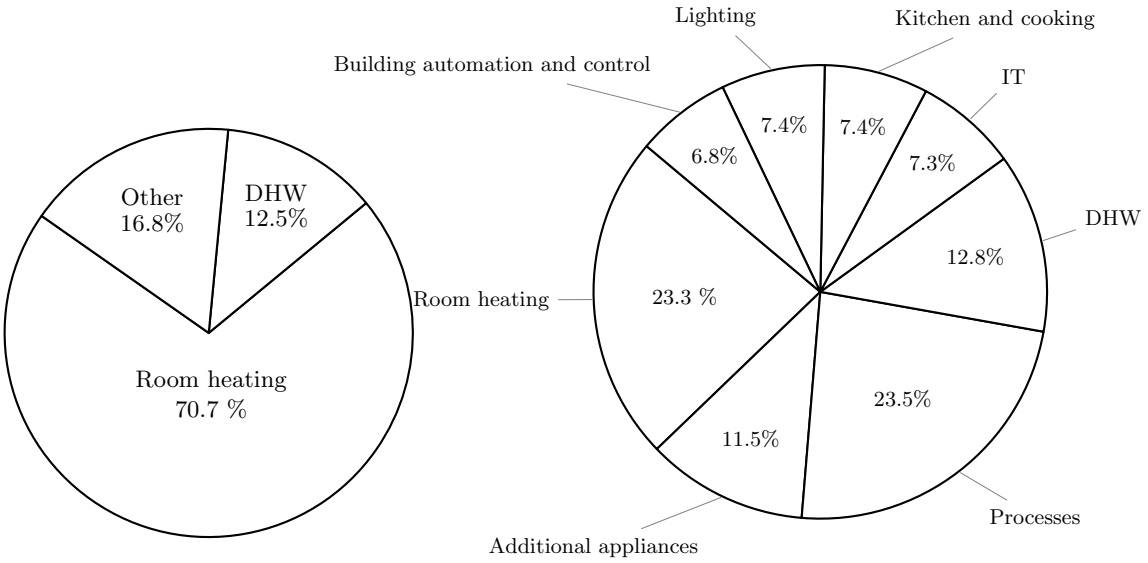

(a) Total energy shares (b) Electricity shares

Figure 1.5: Households total energy and electricity shares in Switzerland in 2013. Data source: [37].

The development of the energy consumption claimed by the building sector exhibits a strong correlation with different socioeconomic factors, including population and economic growth, and the accompanying increment in the total constructed area. Figure 1.4 illustrates the evolution of the building sector energy consumption in Switzerland since 2000. The total consumption figures do not increase monotonically, mainly due to the dependence of heating on weather variables. Figure 1.4b evidences that no significant change in the buildings characteristics and technology has taken place in the periods 2007-2010 and 2011-2013.

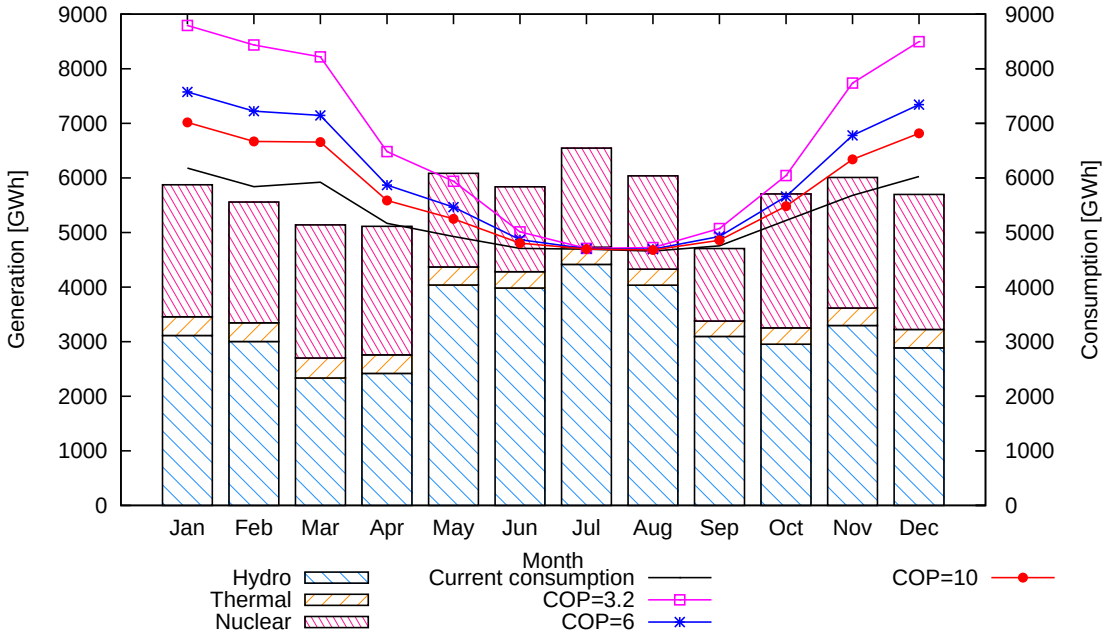

Figure 1.6: Projected increment in the electricity consumption in Switzerland if all room heating is provided by HPs. Current HPs and electrical heating systems are not considered. Current consumption and generation data for reference year 2013 [11, 37].

Even if DSEs cannot contribute to balancing out the seasonal energy imbalance imposed by heating requirements, they can play a significant role in adequately using the available power resources. Understanding the future role of buildings, and their interaction with the electrical system, requires extrapolating the current state of both the electrical grid and the buildings technology to the future, and hypothesizing about possible developments.

The dominating energy driver in residential buildings in Switzerland, as can be appreciated in Figure 1.5a, is room heating, claiming 70.7% of the total energy consumed (182.4 PJ), followed by Domestic Hot Water (DHW) preparation with 12.5% (32.2 PJ) [37]. If all the heating provided today by fossil fuels were going to be immediately replaced by HPs, the resulting monthly energy consumption would look like the one depicted in Figure 1.6. The seasonal pattern in the generation (indicated by the bars) is governed by the economic optimization of the water reservoirs. The lower COP considered in the scenarios depicted in Figure 1.6 corresponds to the current average (COP=3.2). The heating demand is distributed over the year using the average monthly Heating Degree Days (HDDs) of 40 different locations in Switzerland.

Figure 1.7 illustrates the evolution of installed HPs in Switzerland and their corresponding average COP. In 2013, the number of HPs reported in the Swiss office of statistics was 224657, which provide 5519 GWh_{th}, with an installed power of 3325 MW_{th} and 891 MW [11]. This corresponds to an average installed power of 3.96 kW (14.8 kW_{th}) and 1659

full-load hours.

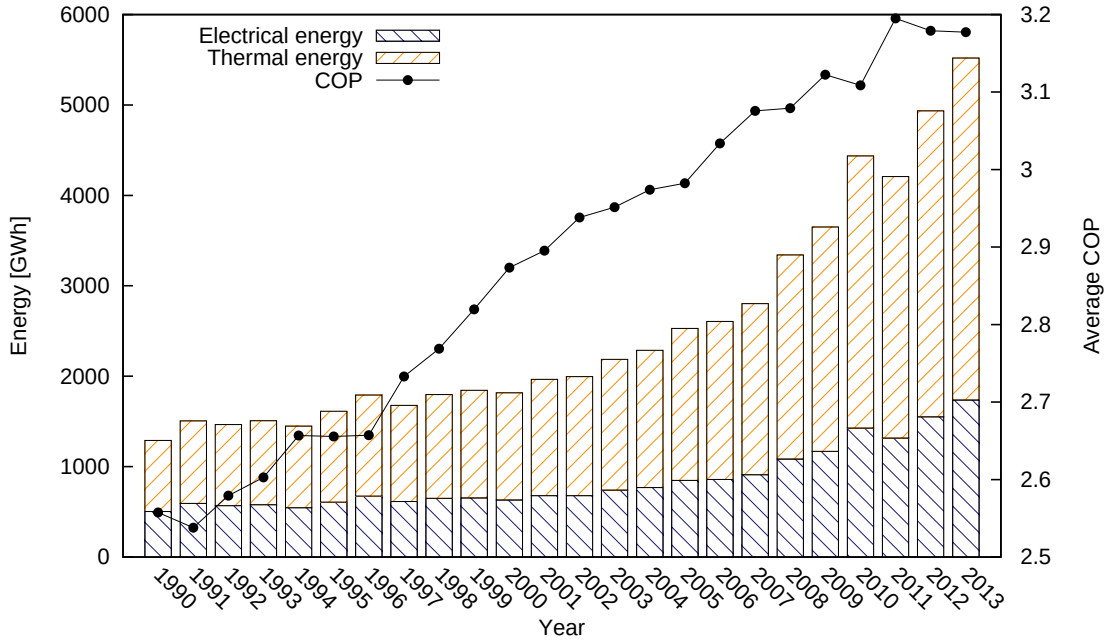

Figure 1.7: Evolution of the HP energy consumption and average COP in Switzerland. Data source: [11].

The total electricity share claimed by buildings has increased in average 1.3% per year [11]. Assuming the same growth and considering the projections from [11], it is possible to extrapolate the scenarios presented in Figure 1.8. Figure 1.8 hypothesizes, both in terms of energy production and available installed power, how a HP adoption scenario is likely to be. The scenarios displayed in Figure 1.8 assume that the heat amount corresponding to room heating —50600 GWh_{th} (182.4PJ)— is gradually converted to HP systems, and deployed within the depicted 8-year period. This additional energy corresponds to approximately 30.5 GW_{th}, if 1659 full-load hours are considered. In this scenario, neither DHW preparation nor the existing HPs, which already provide 5519 GWh_{th}, are included. The power scenario corresponds to a situation in which the additional power is added on top of the current instantaneous load without considering any kind of coordination or load time-shift.

1.7 Literature Review

This section provides a concise overview of the state of the art in different topics related to *this* dissertation. Besides enumerating relevant literature in the fields that constitute *this* dissertation's background, a parallel is established between some selected references and

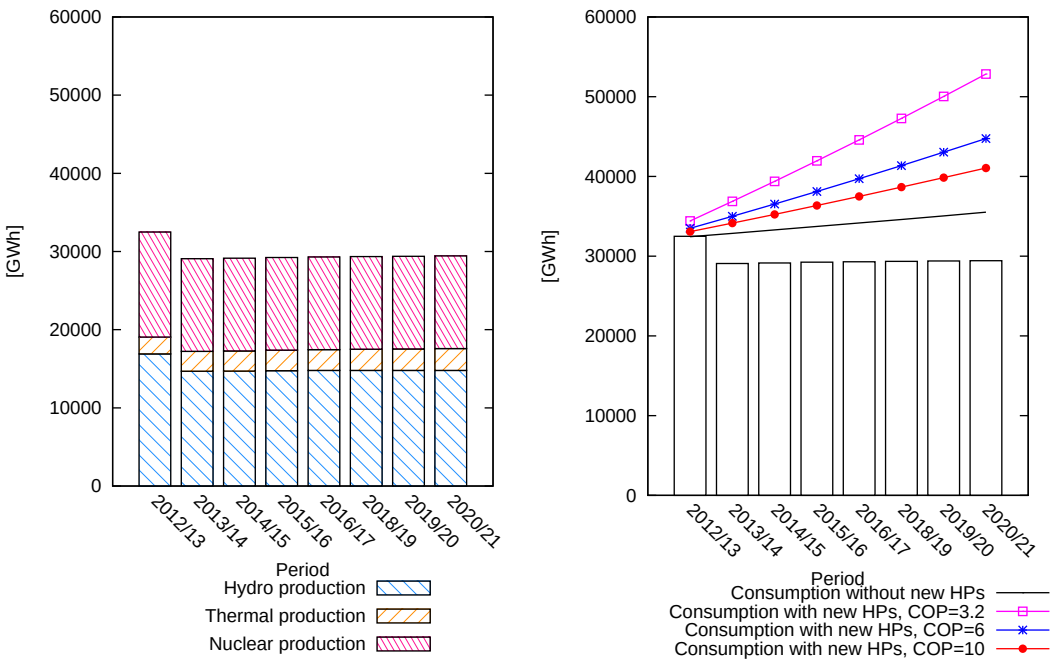

(a) Generation projection [11]

(b) Consumption projection

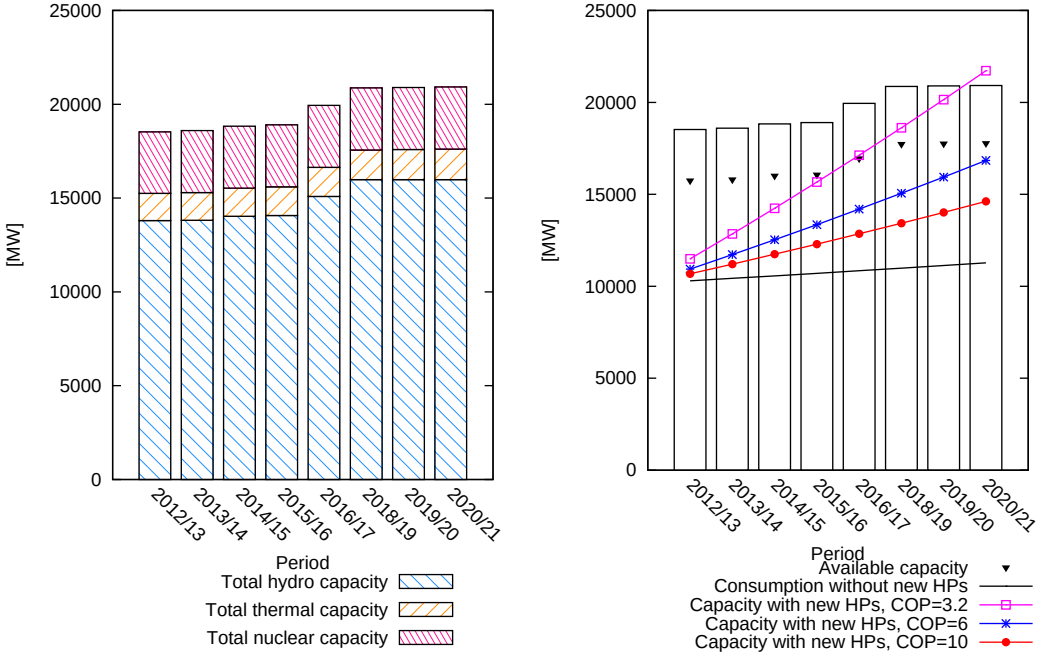

(c) Capacity projection [11]

(d) Additional capacity projection

Figure 1.8: Projected increment in the consumption and installed capacity (data source: [11]). The consumption and available capacity without HPs are estimated by extrapolating today's figures (2013). An annual increment of 1.3% in the consumption is considered. For the projected scenarios with HPs, it is assumed that the electrification of all residential heating systems is equally distributed throughout the considered period.

this work. This section ends with a summary of the dissertation's contribution to the field.

'DR' is the general term encompassing all strategies aimed at controlling the electrical system's demand side. The terms DR and Demand Side Management (DSM) are related concepts, on occasion used interchangeably. Over the years, the term DR has become a buzzword; the conveyed concept can be very vague and refer to a broad range of definitions.

References [30, 32] are early compendiums defining the basic DR ideas. Reference [30], in particular, highlighted the importance and potential of residential buildings in DR planning. Reference [48] is a more recent and comprehensive survey on existing DR programs; the paper elaborates on the concept of demand elasticity and presents a model to calculate the elasticity of different DR programs. Reference [12] further develops in the concept of demand elasticity and presents a study on the increment in economic efficiency resulting from the use of Real Time Prices in a competitive electricity market. Reference [66] explores different DR strategies, challenges, and opportunities in the context of the UK electricity market; the paper elaborates on drivers enabling adoption, barriers, and the effect of load curtailment programs on transmission and distribution grid investments. Chapters [14, 51, 61] provide DR case studies and business experiences from industry experts.

Reference [8] documents a DR program, a demand-based Time of Use (TOU) electricity tariff in Sweden, under which, "households pay a given price per kilowatt on the average of their three highest instances of demand in peak hours". The work reports that households received positively the demand-based tariff. The user's reaction consisted in an adjustment in their consumption habits.

Reference [18] provides a comprehensive review of electrical energy storage technologies for stationary applications. A considerable amount of battery-related literature has recently appeared, mainly in the context of Electric Vehicles (EVs), e.g., [16], and microgrids, e.g., [34]. Reference [9] presents a study on Li-ion batteries price development. Reference [10] explores the possibility of recycling EVs batteries in commercial buildings microgrids; the paper proposes an optimization model based on DER-CAM to find the dimension of the battery capacity. DER-CAM is a Mixed Integer Program written in the GAMS [15] language.

The idea of using DSEs in residential buildings is not new, the topic is already addressed in [40]. Reference [22] calculates the amount of electrical storage required to cope with a high penetration of variable renewables. Reference [41] presents a model aimed at finding the dimension of a battery for load peak-shaving in residential buildings; the model uses a high temporal resolution of 5 min. The proposed model is a scoping one that selects the battery based on simulation. Reference [58] presents a heuristic method to determine the optimal battery capacity in *lowEx* buildings located in the Zurich area. The method presented in the paper is based on the marginal peak reduction achieved by an incremental fixed battery storage capacity; it assumes an input and output power equal in magnitude to the storage capacity.

References [1–3] propose an arbitrage accommodation model for decentralized storage.

Reference [2] provides an exhaustive analysis on the impact of electricity price's forecast errors, and the impact of aggregate storage on the electricity prices. The work investigates the cost reduction potential of a demand-responsive consumption side under hourly prices, as well as the feasible amount of operable storage in a market. The model compares different scenarios with variable capacity, power, and technologies to identify potential cost reductions.

The literature related to the use of batteries in PV systems is copious. Reference [65] provides a detailed description of characteristics and differences across battery technologies; the paper addresses the importance of selecting the adequate battery in PV systems. Reference [26] provides another comprehensive list of storage options for PV. Reference [31] studies the economic viability of electrical energy storage, used in conjunction with PV, in residential buildings; the paper assumes a combination of constant battery, PV, and electricity prices scenarios.

There exist numerous references in the field of optimization and operations research. Concretely, references [57, 59] provide the necessary background for formulating stochastic programs. In the field of bilevel optimization, or Mathematical Problems with Complementarity Constraints, there also exists a broad range of literature, but only a small fraction of recent works provide concrete applied cases [7, 29, 35, 36]. These applications are formulated in the context of electricity markets. In the typical formulation, the lower level optimization corresponds to the market clearing, and the upper level to the strategy of some profit-maximizing agent.

1.7.1 Positioning of *this* Work

This dissertation constitutes a further step in the definition of the $2Sol$ system, and in general of *lowEx zeroEmission* buildings [42, 43, 47]. Specifically, this dissertation provides the framework for the introduction of short-term electrical storage, complementing and building on former works that already approached the seasonal storage problem [33, 56]. *This* work is the first attempt to explicitly study the interface between $2Sol$ buildings and the electrical grid, and the first to approach electrical storage within this building paradigm.

In contrast to direct load DR strategies [66], or approaches stimulating user's change in consumption habits [8], the approach adopted in *this* work strives to be independent from user's comfort. The responsiveness in the demand is introduced by means of DSEs, as in [1–3, 10, 41, 58]. In contrast to the models presented in [1–3, 31, 58], and as in [10], the DSE and PV are endogenous variables in the optimization, and therefore optimum values.

In the model presented in [41], the battery capacity and inverter size are calculated based on diminishing returns of energy vs. demand limit plots, for a set of fixed battery energy and power combinations. Data are not directly measured but estimated using a bottom-up approach. The battery is triggered based on a fixed peak, defined at 5kW,

which is part of a TOU tariff. The model simulates system failures as well. Reference [58] combines a stochastic optimization with a heuristic decision-making process to identify the most suitable battery capacity. The battery input and output power are assumed to be equal in magnitude to the battery capacity. In *this* dissertation, the battery-related variables and the amount of PV are the optimum result of an equilibrium, which constitutes the best response of a final consumer to the proposed price policy. *This* dissertation does not contemplate system failures. The evolution in the prices, or equivalently in the costs, are analysed by means of cost scenarios. The battery is sized as three independent variables, namely capacity, input, and output power.

The methodology used for calculating the battery costs in *this* dissertation is extracted from [3], and the battery costs for different battery technologies are taken from [1]. Our model does not consider PV electricity flowing from the building to the grid; therefore, feed-in tariffs or incentives are not relevant, as they are in [31]. *This* work proposes a demand-based dynamic tariff, using the price elements proposed in [50], but explicitly addressing energy and power. The main difference, regarding the costs, between *this* work and other battery dimension models, is that power is explicitly accounted for, and the elements selection does not entirely depend on the volatility of the prices or the feed-in tariffs as in [1–3, 31].

The pricing policy proposed in *this* dissertation is novel and constitutes a step towards a power-driven distribution business model. The tariff's two components provide two control dimensions, namely intraday and seasonal. The model presented in Chapter 4 implements a structure that superimposes daily and annual objectives in a single optimization, which constitute another contribution to the demand-based tariff analysis. The relationships found between DSE and PV are a contribution to understanding the autonomous use of locally-generated electricity.

The model presented in Chapter 5 is novel in the context of residential buildings and stationary battery applications. The models introduced in [7, 29, 35, 36] focus on the generation side and do not consider storage. In those models, the strategic investments belong to the upper level, while the lower level provides the nodal prices, as the result of a dc Optimal Power Flow (OPF). In *this* dissertation, the investments take place at the lower level, even though the policy maker is the upper one. The electrical grid is not explicitly modelled, mainly due to the temporal relation that is inherent to the battery operation.

1.8 Thesis Organization

The rest of this document is organized as follows: Chapter 2 introduces the necessary background and assumptions on which the subsequent chapters build on. The load generator simulating the electricity profile of a *lowEx* community is described in Chapter 3. Chapter 4 details the model formulated to determine the optimal battery and PV capacity from the individual user's perspective. The combined perspective of the users and the aggregating

entity is detailed in Chapter 5. Chapter 6 is devoted to the final discussion, remarks, and conclusions.

Additional material is provided at the end of this document. Appendix A describes in detail some aspects of the building simulation model presented in Chapter 3.

Chapter 2

Assumptions and Background

This chapter is a primer on the concepts that form the theoretical background of this dissertation. We introduce all the blocks that support our assumptions and that are necessary to develop the models presented in the subsequent chapters. Each assumption is enunciated and contextualized in the frame of a particular subject. The subjects discussed in this chapter include mathematical tools, technologies, as well as theoretical aspects.

The chapter is organized as follows: Section 2.1 describes the main ideas of the 2*Sol* system. Section 2.2 covers the basics of electrical energy storage. Section 2.3 provides a brief introduction to the power markets elements that are relevant to this investigation. Section 2.4 is a short introduction to the topic of Demand Response. Electricity prices are discussed in Section 2.5 and the assumed costs in Section 2.6. Section 2.7 introduces the basics of hierarchical optimization problems. Section 2.8 describes the structure of the time series used in the analyses. This chapter concludes with a summary of the assumptions.

2.1 *LowEx* Buildings

The 2*Sol* system defines guidelines and components for *lowEx ZeroEmission* buildings [42, 47]. This building paradigm is in line with the 2050 IPCC[1] CO_2 reduction objectives [43]. The ultimate goal of the 2*Sol* system is that *lowEx* buildings be operated emission-free during the coldest hour of the year without imposing a significant additional stress on the electrical grid (max 10-15% increment in the consumption), and respecting economics and aesthetics constraints [43].

Residential buildings can be characterized in terms of their thermal energy demand; primarily, space conditioning and DHW preparation. The main components in buildings complying with the 2*Sol* system are depicted in Figure 2.1. The HP operates in conjunction with the Membrane Borehole Heat Exchanger (MBHE) to provide a low temperature heating system. This topology results in a high COP and, consequently, a low fraction of electrical energy required to supply the buildings' heating and DHW demand.

We assume our buildings to comply, even if not thoroughly, with the topology defined by the 2*Sol* system. This assumption implies that we consider electrified heating and cooling

[1] Intergovernmental Panel on Climate Change

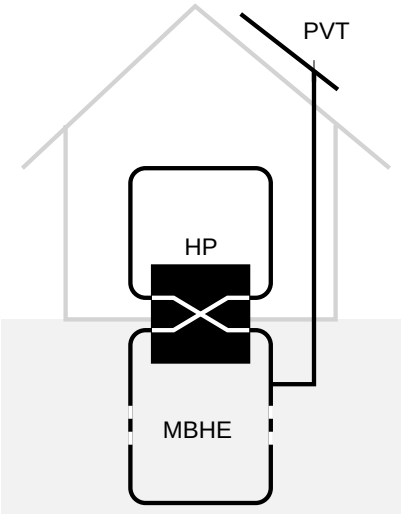

Figure 2.1: *LowEx* buildings as defined by the 2*Sol* system [43]

systems only. The regeneration of the MBHE is not explicitly considered in the models presented in this dissertation. The resulting electricity profile consists of the electricity due to lighting, appliances, and the HPs consumption.

2.2 Electrical Energy Storage

Electricity storage is a major driver for electricity markets, and a key component in the provision of electrical energy and in the reliability of the electrical system. Electricity storage allows decoupling the generation and consumption sides, by making the coordination between generation and consumption schedules much more flexible.

Figure 2.2 exemplifies the wide range of available storage technologies, with decentralized and centralized storage possibilities appearing at opposite extremes of this spectrum. Each technology has a different niche and characteristics that make it suitable for specific applications. These technologies can be classified according to their size, performance, efficiency, cost, availability, and so forth. A comprehensive list of the currently available electricity storage technologies is provided in [18].

Pumped Hydro Storage (PHS) dominates the energy storage scenario in some countries, among them Switzerland. This storage mechanism provides large amounts of energy and power, and has long deployment times and high investment costs associated with it. Despite the large volumes of energy that can be stored, this technology exhibits a great dependence on the geographical conditions and offers little or no room for further expansion. We argue that distributed electricity storage is better suited and more in line with a dynamic and controllable demand side, and with a grid scenario featuring micro grids and a high

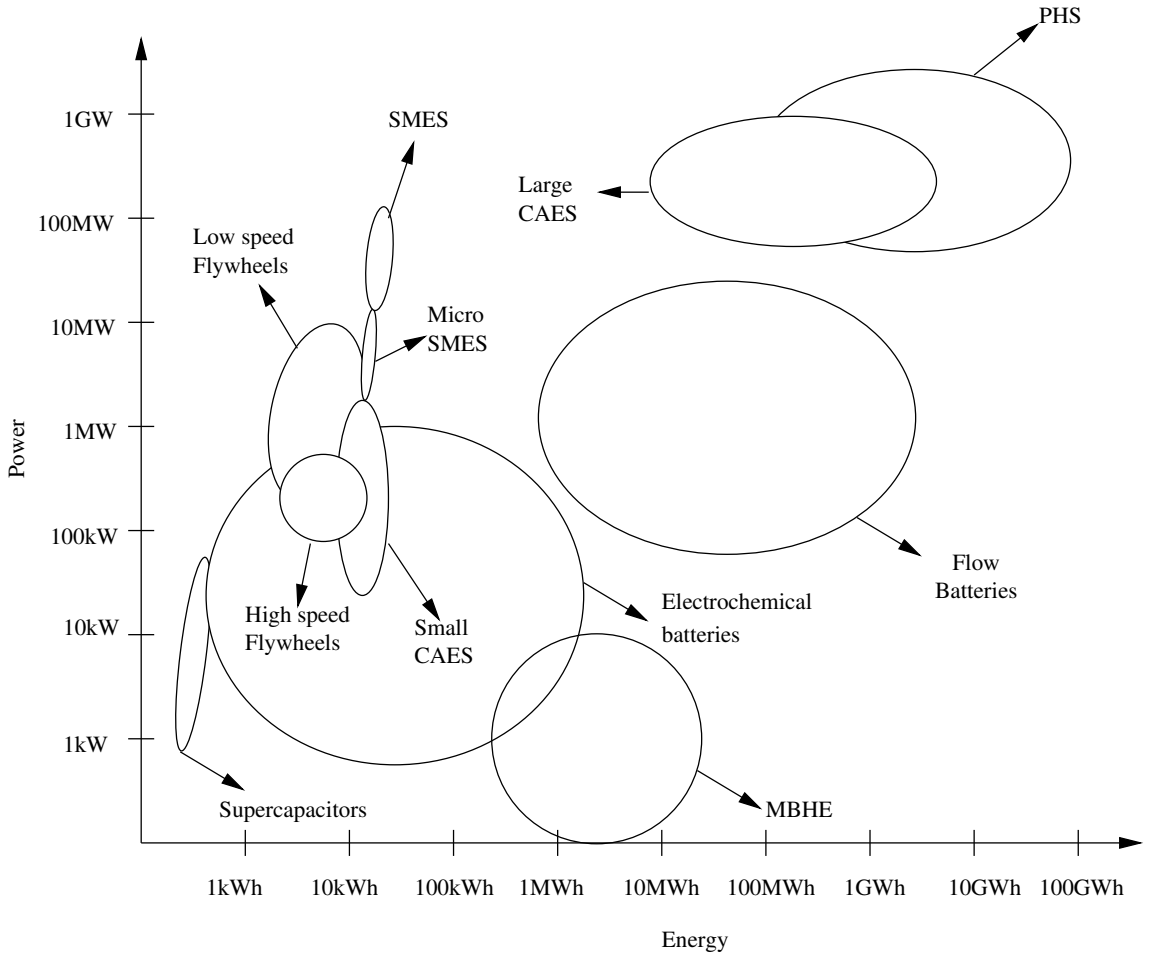

Figure 2.2: Application range for different energy storage technologies. Figure adapted from [46] and [56].

penetration of renewables. We consider decentralized storage systems only.

Our analyses focus mainly on Li-ion batteries, but can be applied to the electrochemical technologies depicted in Figure 2.3. We regard batteries as energy receptacles without explicitly modelling the intricate physical and chemical details of their operation. Our battery model comprises the energy, input power, and output power dimensions, the overall efficiency, and parameters that are known to play an important role in the battery aging, such as the number of complete cycles and the maximum Depth of Discharge (DOD) [3].

2.3 Power Markets

Despite the fact that the periodicity and seasonality observed in the electricity consumption can also be observed in other "conventional goods" [38], electricity exhibits characteristics

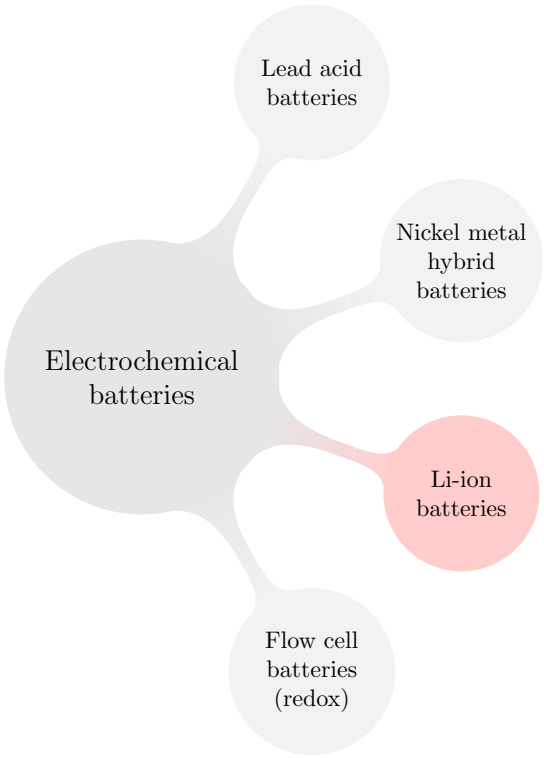

Figure 2.3: Electrochemical battery technologies. The analyses presented in this thesis focus mainly on Li-ion batteries.

that make it unique in many regards [5]:

- The flow of electricity is dictated by physical laws. Electricity flows can neither be controlled nor tracked. Additionally, losses occur in the delivery of electricity.
- Electricity cannot easily and economically be stored.[2] Electricity cannot be stored seasonally in the volume and scale required. As a consequence of this inability, prices exhibit seasonal and intra-day differences.
- Generation and consumption must match on a per-second basis. The electrical system is built in a way that a frequency deviation from the nominal value is virtually unacceptable.
- Users depend on the network to effectuate transactions. The fixed costs of the infrastructure are high, but the marginal costs are low, sometimes nearly zero.

In spite of the aforementioned characteristics, electricity is a commodity that can be traded. The place, real or virtual, at which the electricity transactions occur, is called a

[2]Different electricity storage technologies are discussed in Section 2.2.

power or electricity market. According to the mechanism used between the parties to trade electricity, power markets can be classified as follows [38]:

1. Bilateral trading
2. Electricity pools
3. Managed spot market

In a free, open market, producers submit offers and consumers submit bids. The market dynamics converge to a clearing price guaranteeing that all energy required is provided at the lowest possible cost. Once an offer or a bid gets accepted, the producer or consumer becomes liable, meaning that they have to meet their obligations, or otherwise incur financial penalties. In this work we assume a perfect competition market. In reality, however, market players can behave strategically and influence the market clearing outcome.

Among the different types of markets, two are relevant to this research: the day-ahead market and the balancing or intra-day market. The day-ahead market is cleared on a daily basis, one day in advance, and provides hourly prices. The intra-day market exists to compensate all deviations between scheduled production and consumption.

We differentiate between two related concepts: price formation and price structure. Price formation refers to the market participants interactions that result in the market clearing, while price structure refers to the tariff that final electricity consumers pay. The price structure is discussed in Section 2.5.2.

We consider an underlying electricity price formation mechanism with similar characteristics to those of an electricity pool. In our model, however, prices depend on the aggregate load level only. We regard this type of market as a partial equilibrium market, meaning that the merit order curve is assumed constant and known. This assumption is supported in that the changes in the generation technology are relatively slow. This assumption ignores the shifting effect of renewables on the price formation. Given the aggregate load level, a merit order curve is assumed that corresponds to the different segments of the load duration curve, as exemplified in Figure 2.4.

The second important assumption is in regard to the hierarchy in the supply chain. We assume users to have an economic relation with a retailer and not with the wholesale market directly, as depicted in Figure 2.5.

Traditionally, retailers buy electricity either through long-term contracts or at the spot market, but sell electricity at constant tariffs. These constant tariffs are the result of long-term forecasts and risk assessments. In our model, the retailer issues in advance hourly electricity prices, which are decoupled from the wholesale clearing prices and have the structure described in Section 2.5.2.

The reason for introducing the intermediate figure of a retailer is that users implementing DSEs will react to prices and accommodate their profiles in order to minimize costs.

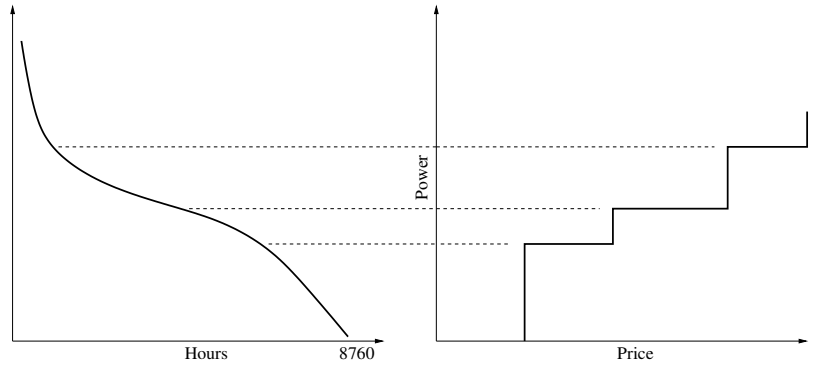

Figure 2.4: Merit order curve as a function of the duration load curve

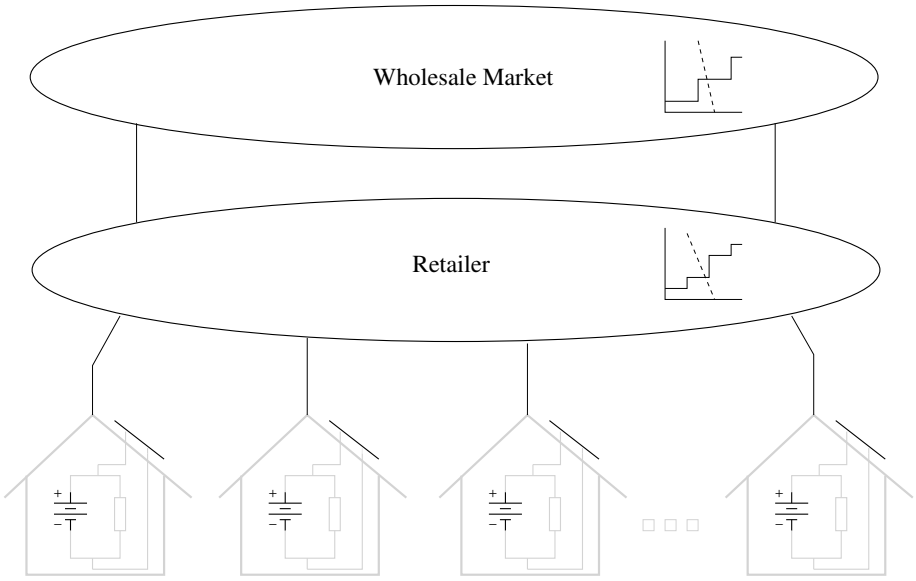

Figure 2.5: Assumed electricity market hierarchy

In other words, consumption is expected to be anti-correlated with the price signal when DSEs are present. This fact would result in a mismatch between scheduled generation and consumption. Having into account the aforementioned reasons, we propose the following mechanism:

1. The retailer issues hourly prices in advance. Those prices are structured according to the expected consumption without considering storage.

2. The retailer can anticipate how users implementing storage will react to the price signal and, accordingly, estimate the actual consumption.

3. The retailer trades electricity at the wholesale market according to its prediction. We are not interested in whether the retailer buys electricity only at the day-ahead or at

the intra-day market as well.

An alternative approach is to allow users to directly interact with the wholesale market. Due to the limitations exposed before, namely the necessity of keeping the balance between the generation and consumption, users have to declare in advance the amount of energy and the price they are willing to pay each hour, and meet these commitments in case their bids get accepted. In this scenario, users can anticipate that the price they will pay is proportional to their consumption and, consequently, solve a quadratic optimization. This approach is not considered, among other reasons, because the retailer figure guarantees risk insulation for the users.

2.4 Demand Response

In the classic microeconomics theory, the social optimum is attained when producers make their offers at a price that equals their Marginal Cost (MC) and consumers make their bids at a price that equals their Marginal Benefit (MB). Following this reasoning, electricity consumers will accommodate their demands to match their MB [38]. In reality, however, in the short term, residential buildings loads are inelastic. The elasticity is defined in terms of the quantity q and the price π as in (2.1). A good is considered inelastic if $|\epsilon| < 1$, and elastic if $|\epsilon| > 1$.

$$\epsilon = \frac{\frac{dq}{q}}{\frac{d\pi}{\pi}} = \frac{dq}{d\pi}\frac{\pi}{q} \tag{2.1}$$

DR is a general term encompassing a wide variety of approaches, aimed to control to different extents the demand side. When indirect load control is assumed, the nature of this control is closely related to the electricity prices structure. Figure 2.6 provides an overview of different DR programs [48] whose pricing schemes are further explained in Section 2.5.

Even under Real Time Prices (RTPs), residential buildings display low elasticity [12]. The low elasticity exhibited by buildings is in part due to the high value that users give to electricity, i.e. the value that consumers place on the availability of electrical energy is greater than the price of electricity, but is also due to the fact that electricity is inexpensive.

DSEs provide a way in which residential buildings can become flexible, i.e. elastic, without compromising users' comfort. This idea is illustrated in Figure 2.7. We regard the implementation of DSEs as a DR enabler and assume that the necessary infrastructure for coordinating the control actions is or is soon to be available. It has been claimed that there is little or any incentive for residential buildings to take part in the electricity market, mainly due to the costs of the associated Advanced Meter Infrastructure (AMI), as this cost would absorb all resulting benefits [38]. Nevertheless, we assume that as the result of the convergence of different DR and smart grid approaches, and the integration of power and IT companies, the AMI infrastructure will be ubiquitous.

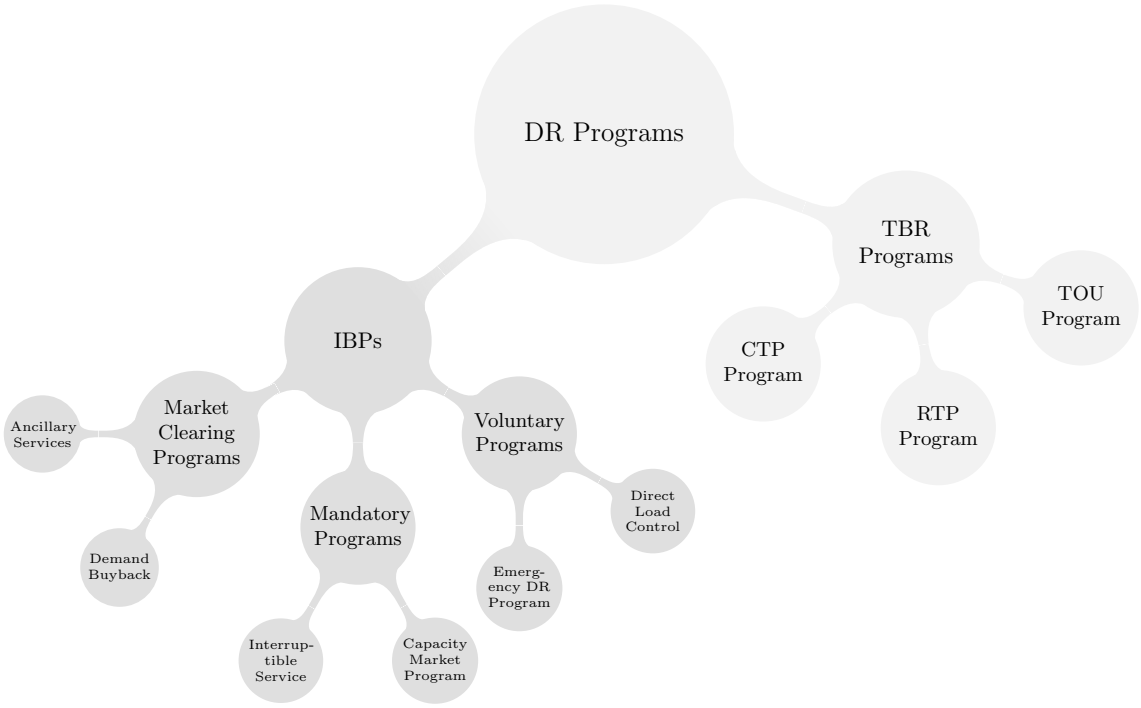

Figure 2.6: DR price schemes [48]

2.5 Electricity Prices

Our premise is that the main motivation for electricity consumers to take part in a DR program is the possibility of reducing their electricity costs or obtaining any other economic benefit.[3] This economic incentive is closely linked to the electricity prices' structure. This section explores the different pricing schemes that electricity consumers could face. Each one of these schemes addresses particular objectives and offers different advantages.

Residential buildings have historically paid a plain electricity tariff accounting mainly for the bulk energy consumed. The liberalization of the electricity market brought about almost no changes in this scheme, as final consumers continue to pay a plain tariff that insulates them from the market's dynamics. A plain electricity tariff provides no incentive to modify or time-shift the energy consumption, but offers consumers a shield against volatility and risk.

Figure 2.6 provides a summary of different dynamic pricing mechanisms. The most commonly used are the so called Time of Use (TOU) tariffs, which establish two or more price regions during the day or the week, and intend to address periods of critical load [48]. RTPs vary continuously on an hourly or sub-hourly basis, accounting for the wholesale price or for a combination between the market price and the instantaneous load level [50].

[3]There is, however, evidence suggesting that environmental concern is increasingly earning awareness [8].

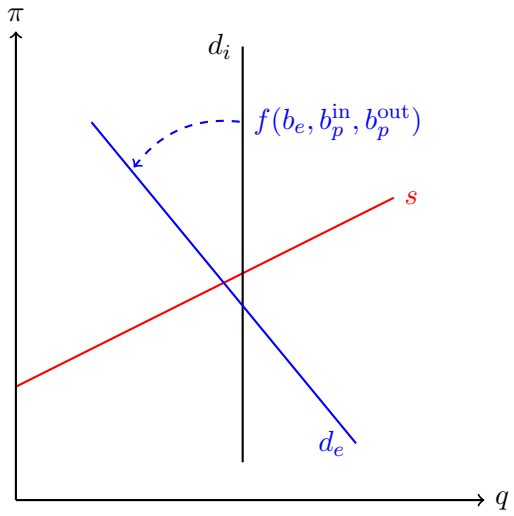

Figure 2.7: Expected effect of electricity storage on the elasticity of demand. s is the supply curve, d_i is the initial demand without storage, and d_e is the resulting demand with storage. The resulting elasticity is assumed to be a function of the storage energy b_e and the battery input and output power, b_p^{in} and b_p^{out}, respectively.

Critical Peak Pricing (CPP) on the other hand makes use of RTPs during critical periods only [48].

Dynamic electricity prices play a twofold role in DR or conservation programs. For the electricity consumers, dynamic prices offer a saving potential or similar economic incentive to take part in control programs. For the electricity utility, dynamic prices constitute a versatile control signal.

2.5.1 Composition of the Electricity Prices in Europe

Even if the wholesale electricity prices across Europe have declined by 35-40% during the last 7 years, the electricity prices that households face have increased in average 4% during the same period [68]. This contradictory fact is mainly due to market imperfections that allow the retailers to avoid passing the price reduction to the final consumers. Final electricity prices are expected to steadily grow until 2020 [68].

Figure 2.8 illustrates the composition of the electricity prices that final consumers pay across Europe. The energy costs comprise wholesale and retail costs. The wholesale costs are due to generation costs, construction of new power plants, maintenance, decommissioning, and so forth. The retail costs are associated with the sale of energy. The network costs encompass the cost of the transmission and distribution grid: maintenance, expansion, and Ancillary Services (AS).[4] The distribution grid claims most of the network costs, with

[4] Voltage and frequency control, compensation of losses, black start, among others.

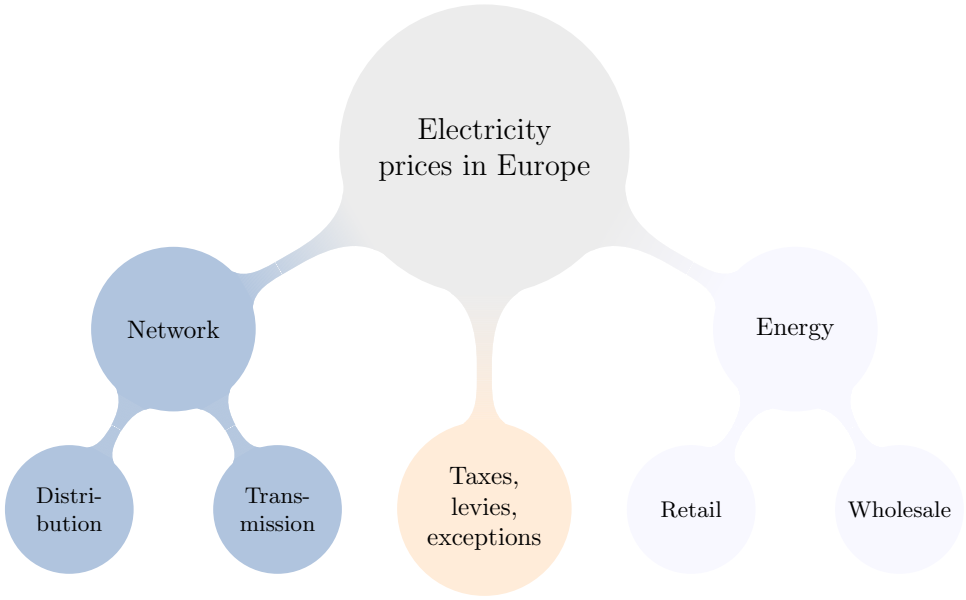

Figure 2.8: Electricity price components in Europe. Source: [68]

an average value greater than 80% across Europe [68]. The strong penetration of wind and solar generation has had a major impact in the grid utilization and energy production costs, the grid utilization component for households has increased by 18.5% [68].

We do not consider the tax element, which is not harmonized throughout Europe. This component tends to be higher in countries with high penetration of renewables such as Germany and Spain [68]. The resulting assumed cost structure is detailed in the following section.

2.5.2 Electricity Prices Structure

As stated in the previous section, final electricity prices account for both the energy consumption and the electrical grid utilization, i.e. energy and network costs. A modified version of the model proposed in [50] is introduced in (2.2), where c'_{g_i} is the resulting instantaneous price, $c^{\text{spot}}_{g_i}$ is the instantaneous spot market price, $x^{\text{total}}_{g_i}$ is the instantaneous load level, and $\overline{\mathbf{c}}^{\text{spot}}_g$ and $\overline{\mathbf{x}}^{\text{total}}_g$ are the mean values of the spot market prices and the load levels, respectively. $0 \leq \alpha \leq 1$ is a weighting factor. We consider $0.4 \leq \alpha \leq 0.6$. For comparison purposes, the value reported in [50] is $\alpha = 0.537$.

$$c'_{g_i} = \alpha \cdot \frac{c^{\text{spot}}_{g_i}}{\overline{\mathbf{c}}^{\text{spot}}_g} + (1-\alpha) \cdot \frac{x^{\text{total}}_{g_i}}{\overline{\mathbf{x}}^{\text{total}}_g}, \quad \forall c'_{g_i} \in \mathbf{c}'_g, \forall c^{\text{spot}}_{g_i} \in \mathbf{c}^{\text{spot}}_g, \forall x^{\text{total}}_{g_i} \in \mathbf{x}^{\text{total}}_g \tag{2.2}$$

In general, end electricity consumers will pay a tariff with the structure illustrated in

Figure 2.9.

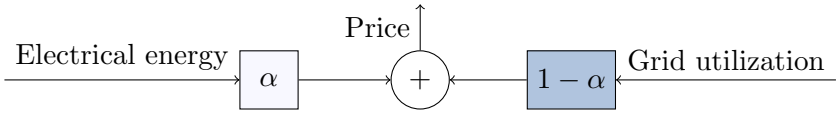

Figure 2.9: Price structure including energy and grid utilization components

There is evidence suggesting that demand-based tariff schemes represent a stronger economic incentive than conventional tariffs for electricity consumers to adjust their demand profiles [8]. In this dissertation we adopt a pricing model that explicitly addresses both the integral energy consumption and the maximum daily peak, irrespective of whether the prices are constant or dynamic.

We assume that users pay a tariff that reflects both energy consumption and grid utilization, as sketched in Figure 2.9. Given a price element c'_{g_i}, it can be split into energy consumption $\alpha c'_{g_i}$ and grid utilization $(1-\alpha)c'_{g_i}$ components. The reasoning behind our assumption is that the grid utilization component, integrated over one day, can be mapped to an element accounting for the maximum daily peak. This scheme results in hourly electricity $\mathbf{c}_g$ and daily peak $\mathbf{c}_g^{\max}$ price vectors. For one particular day d, with prices $\mathbf{c}_g^{d'}$ and total load $\mathbf{x}_g^{d,\text{total}}$, there correspond a vector of hourly energy prices $\mathbf{c}_g^d$, given by (2.3a), and a peak price $c_{g_d}^{\max}$, given by (2.3b). The hourly prices account for the electrical energy component, while the daily peak price is chosen to approximate the grid utilization contribution. This equivalence is illustrated in Figure 2.10, for a 1-day period.

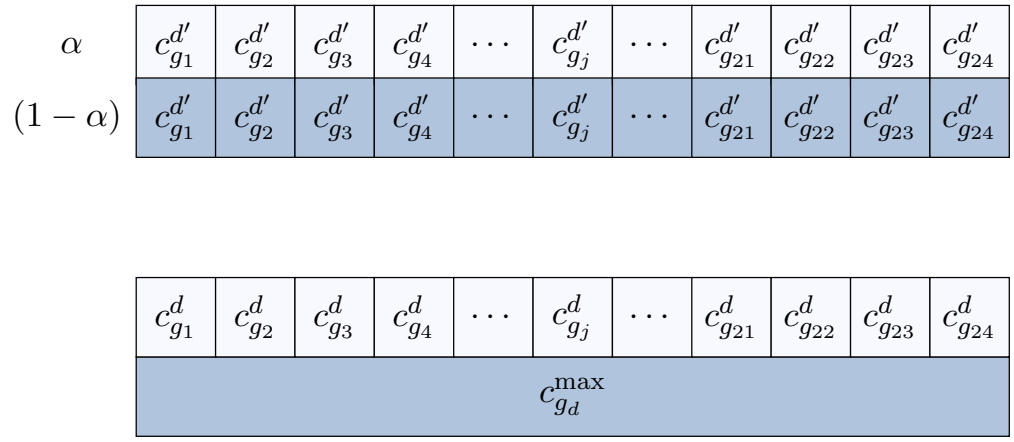

Figure 2.10: Price structure for day d. The light cells account for the hourly energy component. The shaded cells represent the hourly grid utilization component in the top plot, and the equivalent daily peak component in the bottom plot.

$$\mathbf{c}_g^d = \alpha \mathbf{c}_g^{d'} \tag{2.3a}$$

$$c_{g_d}^{\max} = (1-\alpha) \cdot \frac{\sum_{j=h_1}^{h_{24}} c_{g_j}^{d'} x_{g_j}^{d,\text{total}}}{\max \mathbf{x}_g^{d,\text{total}}} \tag{2.3b}$$

The electricity fee incurred by a particular building on day d is given by (2.4), where $\mathbf{x}_g^d$ is the vector of hourly electricity consumption, and $\mathbf{c}_g^d$ is the vector containing the corresponding prices (energy component). It is worth clarifying that $\mathbf{c}_g^d$ and $c_{g_d}^{\max}$ are calculated using the total load levels, i.e. the aggregation of all building loads, and that the $c_{g_d}^{\max}$ is only an approximation of the grid utilization component.

$$\text{Total daily cost} = c_{g_d}^{\max} \max \mathbf{x}_g^d + \sum_{j=h_1}^{h_{24}} c_{g_j}^d x_{g_j}^d \tag{2.4}$$

Finally, a remark is worth mentioning here, the proposed price is not a two-part tariff (a tariff consisting of per-unit price plus lump-sum fee). Instead, penalizing the peak represents a demand charge, i.e. our price structure constitutes a demand-based electricity tariff.

2.6 Costs Assumed in the Models

This section describes the structure and range of the costs used as inputs for the models developed in the subsequent chapters.

2.6.1 Definition

Table 2.1 introduces the parameters involved in the different cost calculations. Parameters labeled "input" are given or known, while parameters labeled "output" are calculated.

It is convenient to formulate both the battery and PV costs in terms of the Equivalent Annual Cost (EAC) (2.5), which in turn is defined in terms of the Net Present Value (NPV) and the annuity $A_{\tau,r}$. This metric allows comparing investments with different life spans τ. The life span considered for the battery and PV components is $\tau_y = 10$ [1] and $\tau_\phi = 25$ [31] years, respectively.

$$\text{EAC} = \frac{\text{NPV}}{A_{\tau,r}} \tag{2.5a}$$

$$A_{\tau,r} = \frac{1 - \frac{1}{(1+r)^\tau}}{r} \tag{2.5b}$$

The costs calculated in this section and used in the models introduced in the subsequent chapters are conveniently expressed on a per-day basis. The PV costs in (2.6) are based

Description	Symbol	Type	Units
Cost per battery capacity unit	c_e^k	Input	€/kWh
Cost per battery power unit	c_p^k	Input	€/kW
Battery maximum number of cycles	γ	Input	cycle
Battery calendar life	τ_y	Input	year
Daily per-unit battery energy fixed cost	$c_{b_e}^f$	Output	€/kWh day
Daily per-unit battery power fixed cost	$c_{b_p}^f$	Output	€/kW day
Battery marginal cost	$c_{b_e}^m$	Output	€/kWh
PV calendar life	τ_ϕ	Input	year
Cost per PV power unit	c_ϕ^k	Input	€/kW
Daily per-unit PV power fixed cost	c_ϕ^f	Output	€/kW day
Length of the analysis period	τ_d	Input	day
Discount rate	r	Input	%
Maintenance rate	m	Input	%

Table 2.1: Parameters involved in the battery and PV costs calculation

on the EAC metric.

$$c_\phi^f = \frac{1}{365 \text{ day}} \Big(\frac{1}{A_{\tau_\phi, r}} \cdot c_\phi^k \Big) \tag{2.6}$$

The EAC cannot be directly applied to the battery cost because the battery depreciation depends on both its calendar and cycling life. Additionally, the battery dimension process involves three independent variables instead of one: energy plus input and output power. The battery costs are then calculated on a slightly different way, according to the model derived in [3]. The battery costs are split according to the topology depicted in Figure 2.11, where the input and output powers can be ac/dc, dc/dc, or a combination of both.

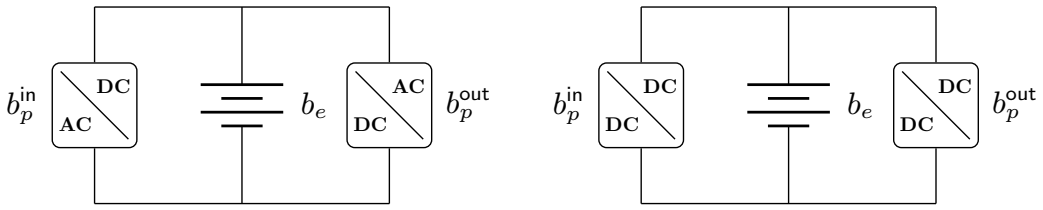

(a) ac/dc conversion (b) dc/dc conversion

Figure 2.11: Battery topology. b_e: battery capacity, b_p^{in}: input power, b_p^{out}: output power.

Equation (2.7a) defines the MC of storage, which is intended to account for the battery cycling life. Equations (2.7b) and (2.7c) define the fixed costs of the energy and power modules, respectively. The first two terms in these equations account for the maintenance and capital costs, while the additional term in (2.7c) is the depreciation of the input and output power modules. We assume that the input and output power modules have identical

costs.

$$c_{b_e}^m = \frac{c_e^k}{\gamma} \tag{2.7a}$$

$$c_{b_e}^f = \frac{1}{365\ \text{day}}\left(m \cdot c_e^k + r \cdot c_e^k\right) \tag{2.7b}$$

$$c_{b_p}^f = \frac{1}{365\ \text{day}}\left(m \cdot c_p^k + r \cdot c_p^k + \frac{1}{\tau_y} \cdot c_p^k\right) \tag{2.7c}$$

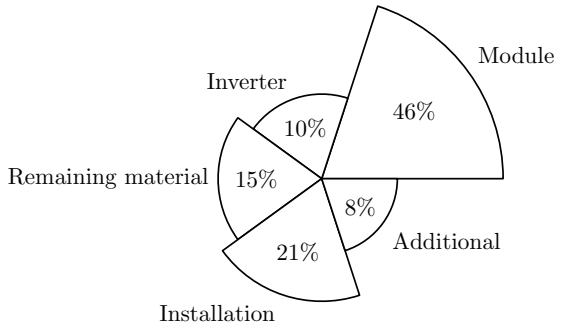

Figure 2.12: PV system costs [28]

2.6.2 Assumed Costs

Figure 2.12 depicts the PV system cost structure [28]. The PV costs c_ϕ^k are extracted from the projections presented in [31], whose figures are summarized in Table 2.2a. The cost reductions for 2017 and 2022, relative to 2013, correspond to a 15% and 30% decrease, respectively, which agrees with the figures reported for Switzerland in Table 2.2b [28].

Year	c_ϕ^k
2013	1700
2017	1430
2022	1190

(a) Projected PV costs in €/kW [31]

Year	**Reduction** [%]
2014	7
2016	12
2018	17

(b) Projected reduction in the PV costs relative to 2013 in Switzerland [28]

Table 2.2: PV cost development

The battery capital costs, i.e. c_e^k and c_p^k, are taken from the scenarios summarized in [1]. These figures are presented in Table 2.3 for three different electrochemical technologies.

Even if the battery markets for stationary and mobile applications have different dynamics, and the requirements of stationary applications are different from those of EVs,

Scenario	Technology	c_e^k	c_p^k	γ	b_η
Average	Lead-acid	175	175	2100	82
	Ni-Cd	550	177	7500	65
	Li-ion	650	315	7000	92
Best	Lead-acid	100	120	3000	85
	Ni-Cd	400	120	10000	70
	Li-ion	130	130	10000	95

Table 2.3: Battery costs in €/kWh and €/kW as reported in [1], where b_η is the overall efficiency.

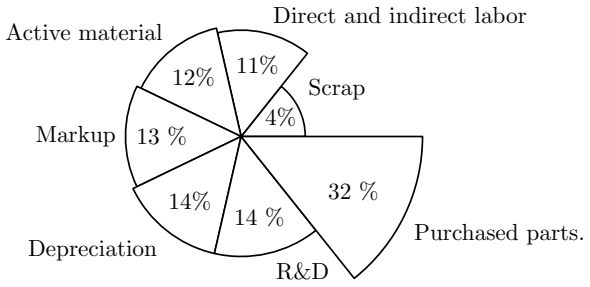

Figure 2.13: Battery system costs [9]

the developments in those two fields are complementary rather than diverging. For instance, a model presented in [10] proposes the use of recycled EVs batteries in microgrid applications. A survey, in which the cost structure depicted in Figure 2.13 is considered, presents the scenarios for Li-ion battery cost development shown in Table 2.4 [9].

	2009	2020	**Reduction** [%]
OEM	990-1200	360-440	36.6
Consumers	1400-1800	570-700	40

Table 2.4: Expected cost ($/kWh) reduction in Li-ion battery technologies [9]

Table 2.5 summarizes the range of parameters considered in the models presented in the following chapters. The DSE technology parameters are mainly focused on Li-ion batteries, which we assume to be the dominant, market leading technology. These values will be used in conjunction with the ones displayed in Table 2.3.

2.7 Bilevel Problems

The model presented in Chapter 5 is a hierarchical or bilevel optimization problem, from here onwards referred to as Bilevel Program (BLP). This section describes the basics of this formulation. A BLP is essentially an optimization problem constrained by other(s)

Description	Symbol	Range		Units
		From	to	
Cost per battery capacity unit	c_e^k	300	1200	€/kWh
Cost per battery power unit	c_p^k	$0.3 \cdot \lvert c_e^k \rvert$	$0.6 \cdot \lvert c_e^k \rvert$	€/kW
Battery maximum number of cycles	γ	5000	16250	cycle
Battery calendar life	τ_y	10	10	year
Cost per PV power unit	c_ϕ^k	800	1700	€/kW
PV calendar life	τ_ϕ	25	25	year
Discount rate	r	5	7	%
Maintenance rate	m	5	8	%

Table 2.5: Range of parameters considered in the models presented in the following chapters [1]

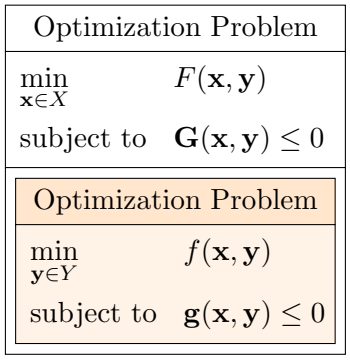

Figure 2.14: Bilevel problem structure

$$\begin{aligned} &\min_{\mathbf{x}\in X} && F(\mathbf{x},\mathbf{y}) \\ &\text{subject to} && \mathbf{G}(\mathbf{x},\mathbf{y}) \leq 0 \\ &&& \min_{\mathbf{y}\in Y} \quad f(\mathbf{x},\mathbf{y}) \\ &&& \text{subject to} \quad \mathbf{g}(\mathbf{x},\mathbf{y}) \leq 0 \end{aligned} \tag{2.8}$$

optimization problem(s). This situation is described in (2.8) and illustrated in Figure 2.14.

A BLP consists of one leader, or upper level player, and one or several followers, or low level players. The BLP can be viewed as a non-iterative version of the non-cooperative perfect-information Stackelberg game [6].

Decision makers at both levels can influence but not completely control decision makers at the other level [6]. The payoffs and actions at both levels are interdependent upon each other. In general, the objective functions at each level are a combination of variables controlled by that level and variables coming from the other level [6, 29]. The game's sequential dynamics are as follows:

1. The leader makes the first move. The leader tries to anticipate the followers' reactions and adjusts its controls in order to minimize its objective function.

2. The followers react to the leader's move, assuming that it is not going to readjust its controls.

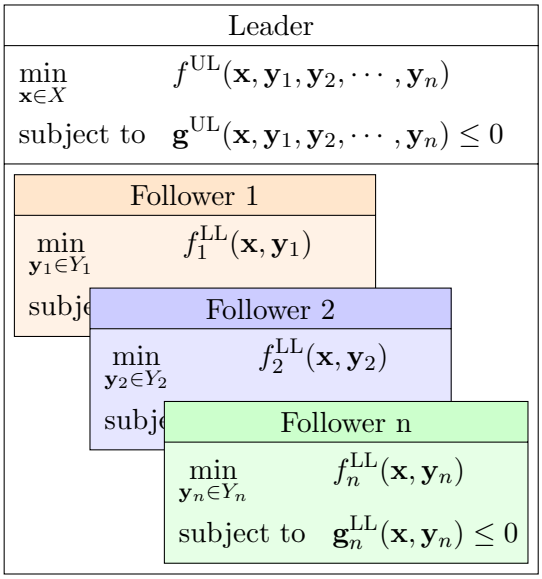

Figure 2.15: Bilevel problem structure with several followers

We use the superscript $^{\mathrm{UL}}$ for referring to variables pertaining to the upper level, i.e. to the leader, and the superscript $^{\mathrm{LL}}$ for variables pertaining to the lower level, i.e. to the follower(s). The resulting formulation is illustrated in Figure 2.15.

The traditional approach for solving a BLP consists in substituting the lower levels for their Karush-Kuhn-Tucker (KKT) conditions and solving the resulting Mixed Integer Program (MIP). The BLP is closely related to the concepts of Mathematical Problems with Equilibrium Constraints (MPEC) and Mathematical Problems with Complementarity Constraints (MPCC), mainly due to the complementary conditions arising when the lower levels are replaced by their KKT conditions. A complementarity problem for a function $F : \mathbb{R}^n \to \mathbb{R}^n$ is defined as $0 \leq F(x) \perp x \leq 0$ [29]. Solving the resulting MIP often requires the use of decomposition techniques [7,29,35,36]. An alternative approach consists in substituting the followers for their strong duality conditions [29], which results in a Nonlinear Program (NLP). The latter approach is implemented in Chapter 5.

2.8 Time Resolution

A resolution of 1h is adopted for all the models and analyses introduced in this thesis. This value is a compromise between granularity and problem tractability, and captures both the daily and seasonal variations. This value is as well in line with the majority of simulation software, the analysed spot market and load levels data (2007-2012), and the national standards [62–64].

Our analysis is based on time series. These time series are vectors with domains defined

Set	Definition	Description
D	$\{d_1, \ldots, d_v, \ldots, d_{\tau_d}\}$	Days in the analysis period
H	$\{h_1, \ldots, h_j, \ldots, h_{24}\}$	Hours in each day
$\Omega = D \times H$	$\{d_1h_1, d_1h_2, \ldots, d_vh_{24}, d_{v+1}h_1, \ldots, d_{\tau_d}h_{24}\}$	All hours in all days considered
Ω^0	$\{d_1h_1, d_1h_2\}$	The first 2 periods
$\Omega^{\bar{0}} = \Omega - \Omega^0$	$\{d_1h_3, d_1h_4, \ldots, d_vh_{24}, d_{v+1}h_1, \ldots, d_{\tau_d}h_{24}\}$	All hours except the first 2 periods
Ω^{+1}	$\{d_1h_2, d_1h_3, \ldots, d_vh_{24}, d_{v+1}h_1, \ldots, d_{\tau_d}h_{24}\}$	All hours except the first period

Table 2.6: Sets used in the models formulation

in Table 2.6. The analysis period encompasses τ_d days, e.g., 365 days of 24h each. Sets D and H correspond to the total number of days and hours within each day, respectively. The total number of hours in the analysis period is defined as the Cartesian product of the sets D and H, $\Omega = D \times H$. We used the simplified index notation $a(d_v, h_j) = a_{d_v,h_j} = a_i$ for denoting elements in vectors that are a mapping from Ω into $\mathbb{R}$. Finally, Ω^0, $\Omega^{\bar{0}}$, $\Omega^{+1} \subset \Omega$.

2.9 Summary of Assumptions

This section summarizes the underlying assumptions upon which the following chapters build. Some assumptions omitted in this chapter are included in this list for the sake of completeness.

1. The most important assumption is that the retailer has an economic incentive, or perceives a profit, resulting from the ability to control the load that is greater or equal to the incentive it offers to the final electricity consumers to implement PV and DSEs.

2. Each building is assumed to comply, completely or partially, with the principles dictated by the 2*Sol* system. Buildings are assumed to implement electrified space-conditioning and DHW-production systems. The building's total electricity profile consists of the electricity due to lighting, appliances, and the HPs consumption, as illustrated in Chapter 3.

3. Each building is assumed to implement two HPs, one for space conditioning and one for DHW production.

4. The seasonal COPs are assumed constant for each building. Each building features a constant COP during the whole year. The assumed COP encompasses both the Carnot and the machine efficiency.

5. All DR objectives have to be implemented without diminishing users' comfort. The resulting electricity profile is assumed to be closely linked to comfort.

6. Buildings are assumed to have an economic relation with a retailer and not with the wholesale market directly. This relation is depicted in Figure 2.5.

7. We assume a price structure explicitly addressing the integral energy consumption and the maximum daily power, as elaborated in Section 2.5.2.

8. Decentralized storage is assumed, as explicitly stated in the term DSE.

9. Batteries are modelled on a high, systemic level. We consider electrochemical batteries only, and among them Li-ion batteries mainly.

10. Electricity is assumed to flow in the direction of the building only.

11. Neither subsidies nor feed-in tariffs are considered.

12. The electricity grid is not explicitly modelled, mainly due to the time dependence in the nodal analysis. Traditional OPF is static.

13. We assume that users behave rationally, in the economic sense, and will try to reduce costs or, equivalently, to maximize their profits.

14. We assume that users pursue an economic incentive only, as non-economic incentives are difficult to quantify. The economic incentive constitutes a lower bound or conservative approach.

15. We assume that the IT infrastructure necessary for transmitting data is available and do not consider its costs. The underlying assumption is that electricity utilities are horizontally integrated with IT services and that the so-called smart-grid programs will converge to a ubiquitous AMI.

16. All the models and time series have a time resolution of 1 h.

Chapter 3

Load Generator

Models are representations, simplifications, or abstractions of reality. This chapter is devoted to the development of a model encapsulating the most relevant and characteristic aspects of the electricity profile that a *lowEx* community will exhibit.

The objective of this module is not to accurately model the uniqueness of each building's thermal and electrical dynamics, but to create plausible electricity profiles, representative of both the heterogeneity displayed by electrical loads in individual households, and of the resulting aggregate consumption pattern. Even if some buildings display atypical consumption patterns, the aggregate consumption converges to well-known and, to great extent, predictable profiles. *LowEx* communities will exhibit different electricity profiles than other agglomerations of buildings featuring traditional heating and cooling systems. In these communities, the electricity required for thermal conditioning is not necessarily the dominant component.

The aim of the load generator developed in this chapter is to obtain realistic electricity profiles using a configurable, scalable, and computationally efficient procedure. The requirement of simultaneously accounting for both the individual profiles and the aggregate levels is approached by combining the bottom-up methodology implemented by SIA norms [62–64] with a top-down strategy that allows designing the aggregate figures. The load generator constitutes then a design or synthesis tool, rather than mere analysis software. Given a set of objective figures, for instance, the national statistics, it is possible to find a distribution of parameters that on the aggregate level converges to the design objectives.

Section 3.1 describes the load generator's structure. Section 3.2 deals with the building thermal modelling. Section 3.3 is dedicated to the occupancy modelling. The dispatch of the HP, presented in Section 3.4, is an attempt to model some aspects of the control. Section 3.5 describes the composition of the aggregate load that will be used in the price modelling in the subsequent chapters. This chapter concludes with a brief enumeration of the computational issues in Section 3.6, and a general summary in Section 3.7.

	Unit	Room			Kitchen		
Scenario		0	1	2	0	1	2
s_{ap}	W/m^2	2	1	3	40	30	50
s_{li}	W/m^2	6.3	3	10	12	6	18
s_{dhw}	l/(P day)	40	30	50	30	10	50

Table 3.1: Scenarios employed in the building simulation. The appliances s_{ap} and DHW s_{dhw} scenarios are as defined in [63]. The lighting scenario values s_{li} are modified in order to account for LED lighting.

3.1 Model's Structure

The load generator mainly focuses on residential buildings. The different calculations are based on the profiles and scenarios defined in the SIA norms [62–64]. Office buildings are as well taken into account for the construction of the aggregate electricity profile, described later in Section 3.5. However, office buildings are loosely modelled, without considering multiple thermal zones nor the intricate mobility patterns and occupancy regimes that are characteristic in non-residential buildings. We simulate office buildings in a deterministic way, using the profiles and scenarios as defined in [63]. Hereinafter, unless otherwise clarified, we refer to residential buildings only.

Our calculations are based on the scenarios presented in Table 3.1, and on the normalized profiles displayed in Figures 3.1 and 3.2. The appliances s_{ap} and DHW s_{dhw} scenarios are as defined in [63]. The lighting scenario s_{li} is modified to account for state-of-the-art, more efficient technologies; namely, LED lighting. We use the occupancy profile as a probability rather than as a deterministic value. Therefore, the evening values are modified in order to reflect a non-deterministic, though high probability of presence ($p_t < 1$).

The lighting and appliances profiles are modulated with the occupancy profile. In addition, the daylight hours, illustrated in Figure 3.3, are superimposed to the final lighting schedule.

The load generator's structure is depicted in the block diagram in Figure 3.4. The scalars and configuration parameters involved in the calculations are listed in Tables 3.2 and 3.3, respectively. Correspondingly, the vectors are presented in Table 3.4, with sets defined in Table 2.6 on page 34. The most important blocks are the "Random Occupancy" block, described in Section 3.3, and the "HP scheduler" block, described in Section 3.4.

3.2 Thermal Modelling

There exists a very high correlation between HDDs and the energy required for heating [54]; Figure 1.4b on page 8 confirms this observation. In addition, due to the expected high COP featured by HPs implemented in *lowEx* communities, heating and cooling are not the dominant component in the total electricity shares. Based on these facts, we formulate a

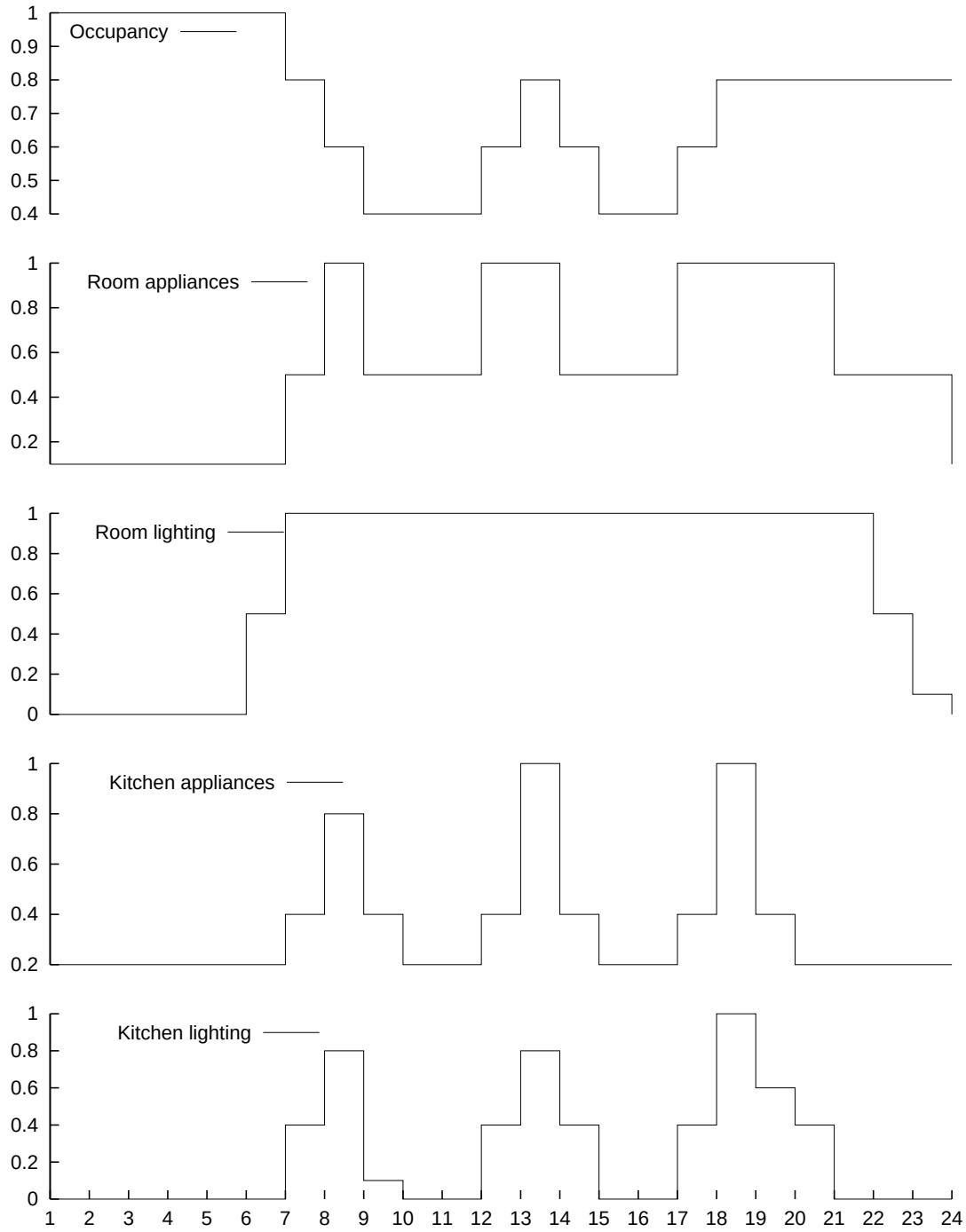

Figure 3.1: Modified, normalized SIA occupancy profiles [63]. The room lighting and the occupancy profiles are modified versions.

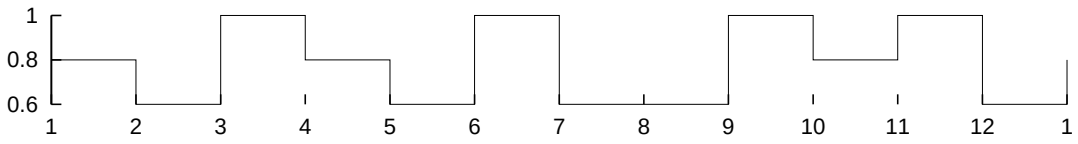

Figure 3.2: SIA monthly occupancy profile [63]

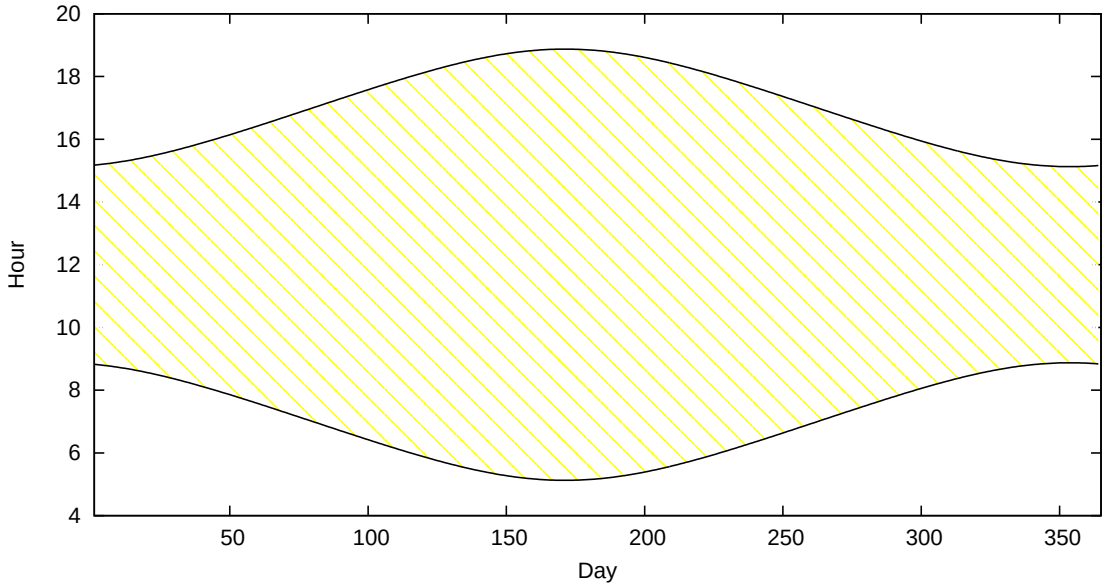

Figure 3.3: Daylight hours for Zurich, Switzerland

Description	**Symbol**	**Units**
Number of persons	P	P
Constructed area	A_s	m^2
Facade area	A_f	m^2
Glazing area	A_w	m^2
Shape factor	H	—
U-value	U	$\mathrm{kW_{th}}/(\mathrm{m}^2\,\mathrm{K})$
Room area	A_s^r	%
Kitchen area	A_s^k	%
HP electrical power	hp	kW
DHW HP electrical power	$\mathrm{hp_{dhw}}$	kW
COP	cop	—
Thermal capacity	C	$\mathrm{kWh_{th}/K}$

Table 3.2: Scalars involved in the definition of the load generator depicted in Figure 3.4

Description	Symbol
Building type	btype $\in$ {residential,office}
Location	loc
Markov type	markov $\in$ {deterministic,random}
Mechanical shading factor	$\mathrm{sd}_{\mathrm{mec}} \in [0, 1]$
Shading factor for the shade polygon	$\mathrm{sd}_{\mathrm{pol}} \in [0, 1]$
Equivalent orientation and solar transmission	$g_{\mathrm{eq}} \in [0, 0.25]$
DHW consumption scenario	$s_{\mathrm{dhw}} \in \{0, 1, 2\}$, see Table 3.1
Lighting scenario	$s_{\mathrm{li}} \in \{0, 1, 2\}$, see Table 3.1
Room appliances scenario	$s^r_{\mathrm{ap}} \in \{0, 1, 2\}$, see Table 3.1
Kitchen appliances scenario	$s^k_{\mathrm{ap}} \in \{0, 1, 2\}$, see Table 3.1

Table 3.3: Additional configuration parameters involved in the definition of the load generator depicted in Figure 3.4

Description	Symbol	Set	$\{\cdot\}$	Units
Ambient temperature	$\mathbf{T}_{\mathrm{amb}}$	Ω	T_{amb_i}	°C
Indoor temperature	$\mathbf{T}_{\mathrm{ind}}$	Ω	T_{ind_i}	°C
CDDs	**cdd**	Ω	cdd_i	°C day
HDDs	**hdd**	Ω	hdd_i	°C day
Normalized occupancy	**p**	Ω	p_i	—
Infiltration losses	$\mathbf{Q}_{\mathrm{infl}}$	Ω	Q_{infl_i}	$\mathrm{kWh_{th}}$
Internal gains due to appliances and lighting	$\mathbf{Q}_{\mathrm{ap+li}}$	Ω	$Q_{\mathrm{ap+li}_i}$	$\mathrm{kWh_{th}}$
Internal gains due to persons	$\mathbf{Q}_{\mathrm{per}}$	Ω	Q_{per_i}	$\mathrm{kWh_{th}}$
Transmission losses	$\mathbf{Q}_{\mathrm{trans}}$	Ω	Q_{trans_i}	$\mathrm{kWh_{th}}$
Ventilation losses	$\mathbf{Q}_{\mathrm{vent}}$	Ω	Q_{vent_i}	$\mathrm{kWh_{th}}$
Normalized solar radiation on a vertical surface	$\mathbf{Q}'_{\mathrm{sol}}$	Ω	Q'_{sol_i}	$\mathrm{kWh_{th}/m^2}$
Equivalent total solar gains	$\mathbf{Q}_{\mathrm{sol}}$	Ω	Q_{sol_i}	$\mathrm{kWh_{th}}$
Normalized solar irradiance on a horizontal plane	$\mathbf{E}'_e$	Ω	E'_{e_i}	$\mathrm{kWh/m^2}$
Normalized corrected solar irradiance	$\mathbf{E}_e$	Ω	E_{e_i}	$\mathrm{kWh/m^2}$
Normalized shades	**sd**	Ω	sd_i	—
HP electricity consumption	$\mathbf{x}_{\mathrm{hp}}$	Ω	x_{hp_i}	kWh
DHW HP electricity consumption	$\mathbf{x}_{\mathrm{hp,dhw}}$	Ω	$x_{\mathrm{hp,dhw}_i}$	kWh
Appliances and lighting consumption	$\mathbf{x}_{\mathrm{ap+li}}$	Ω	$x_{\mathrm{ap+li}_i}$	kWh
Appliances electricity consumption (rooms)	$\mathbf{x}^r_{\mathrm{ap}}$	Ω	$x^r_{\mathrm{ap}_i}$	kWh
Appliances electricity consumption (kitchen)	$\mathbf{x}^k_{\mathrm{ap}}$	Ω	$x^k_{\mathrm{ap}_i}$	kWh
Lighting electricity consumption (rooms)	$\mathbf{x}^r_{\mathrm{li}}$	Ω	$x^r_{\mathrm{li}_i}$	kWh
Lighting electricity consumption (kitchen)	$\mathbf{x}^k_{\mathrm{li}}$	Ω	$x^k_{\mathrm{li}_i}$	kWh
DHW daily consumption	**dhw**	D	dhw_d	$\mathrm{kWh_{th}}$
Daylight hours (from,to)	**dl**	D	dl_d	h

Table 3.4: Vectors involved in the definition of the load generator depicted in Figure 3.4

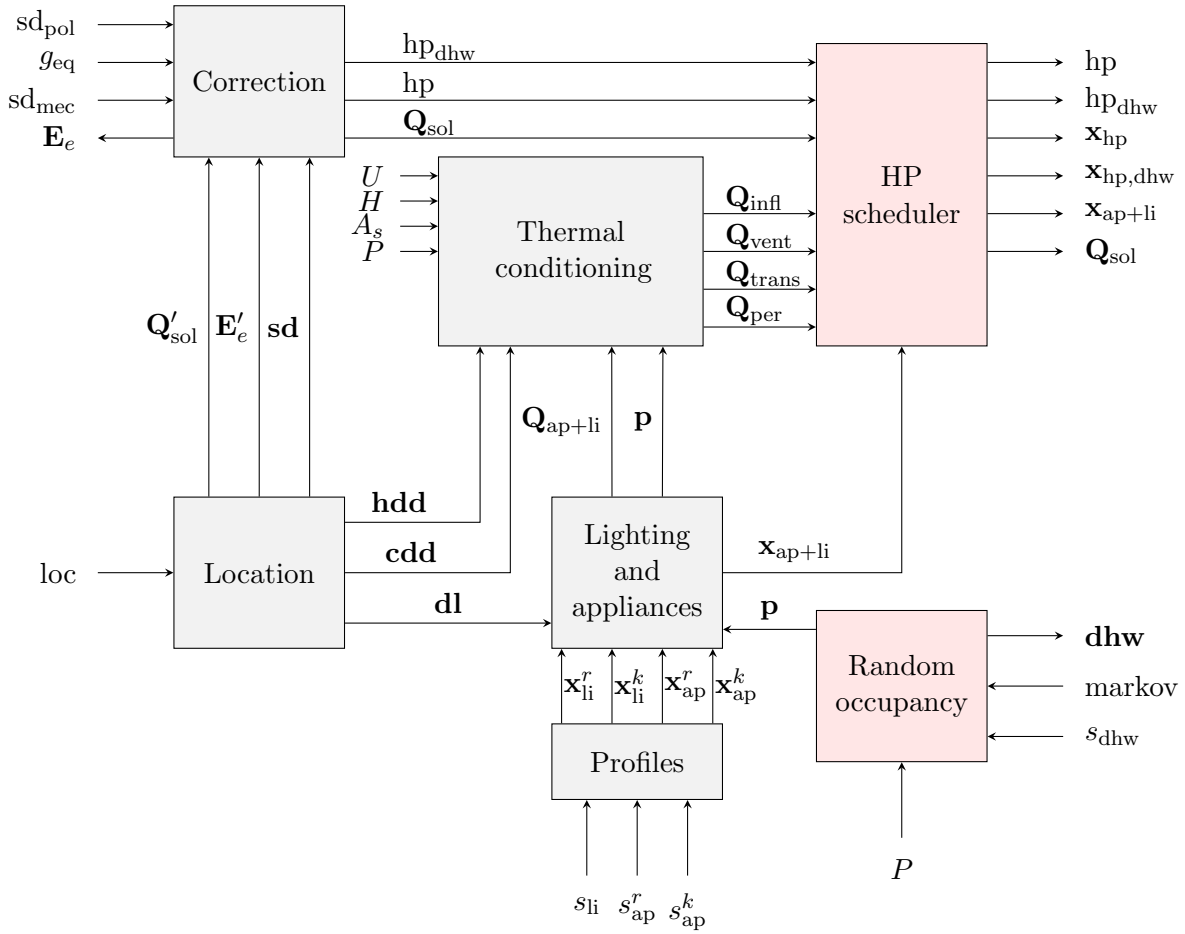

Figure 3.4: Load generator block diagram. All the variables and configuration parameters are defined in Tables 3.2, 3.3, and 3.4.

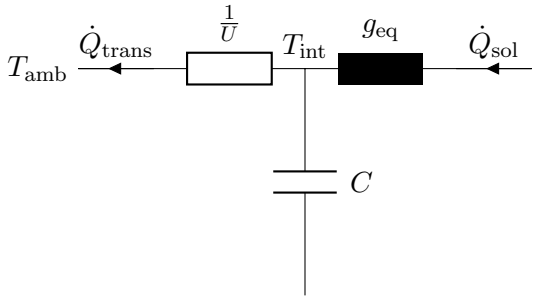

Figure 3.5: Lumped elements model used in the thermal simulation

simplified thermal model with the structure depicted in Figure 3.5. There is a broad range of software, e.g., ESP-r [69], that can be used to calculate the buildings' thermal loads. We

opted for a simplified model, for we are not interested in accurately modelling the thermal load of a particular object, but in profiling the thermal load of a group of buildings in a fast and computationally efficient way. The calculations of the thermal conditioning module are further described in Appendix A.

When modelling a building's thermal behavior, the main source of uncertainty is the weather. A common practice is to use a Typical Reference Year (TRY), which encapsulates the features and patterns found in multi-year datasets. There exist many libraries providing TRYs for different locations. If these libraries are not available, a statistical year can be generated from a given set of weather records (See Appendix on [58]).

In contrast to the thermal behavior, the modelling of the electricity consumption resulting from the users' interaction is less standardized. Some simulation platforms approach this problem by using diversity profiles [52]. This methodology, however, does not capture the stochastic nature of occupancy. The following section describes our approach for modelling uncertainty in the occupancy.

3.3 Occupancy Modelling

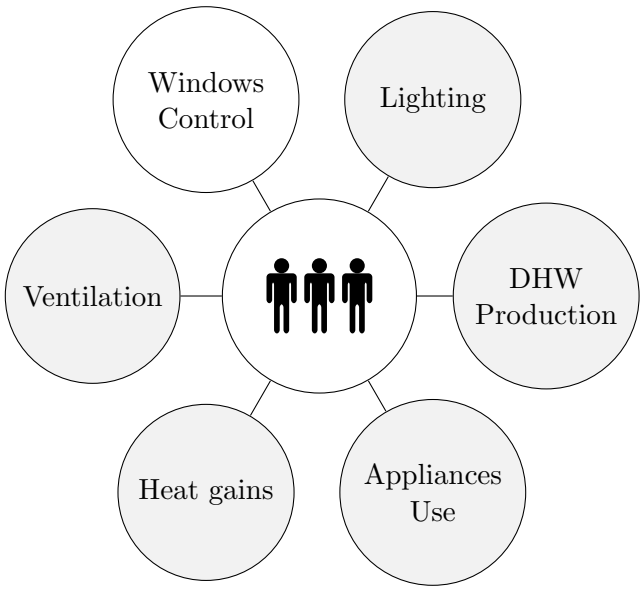

Figure 3.6: Occupants' interaction with the building

Occupants interact with the building producing heat gains, consuming resources, emitting pollutants, and carrying out control actions, among others [52]. As sketched in Figure 3.6, we consider the interaction between occupants and the building regarding ventilation, heat gains, lighting, appliances, DHW consumption, but not control actions, such as window-opening.

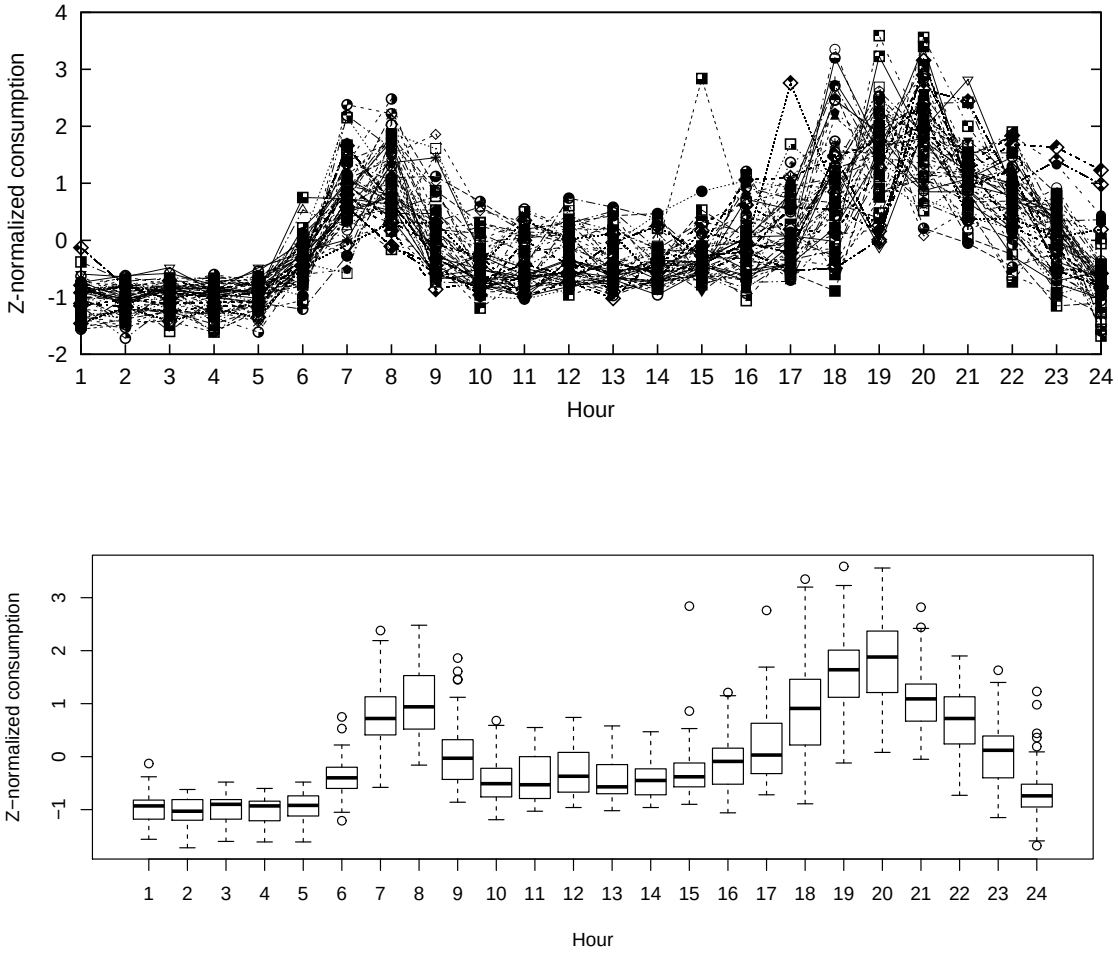

Figure 3.7: Electricity consumption for a reference household. A period of 50-day was considered. The upper figure is the overlapping of the z-normalized hourly time series, and the bottom one are the boxplots for the same set. Data source: [23].

As mentioned in the introduction of this chapter, despite the fact that the aggregate consumption pattern is quasi-deterministic, the electricity consumption that individual residential buildings exhibit can be highly heterogeneous. We analysed the electricity consumption data of 30 households located in Switzerland and South Germany, provided by a home automation company [23], and a set of 6 houses with very high time resolution, located in Boston, which are part of an electricity disaggregation project [39]. Figure 3.7 shows that it is possible to identify daily consumption patterns within a particular household. However, as depicted in Figure 3.8, these patterns can greatly vary among different households.

In order to represent the randomness inherent to occupants' mobility and presence,

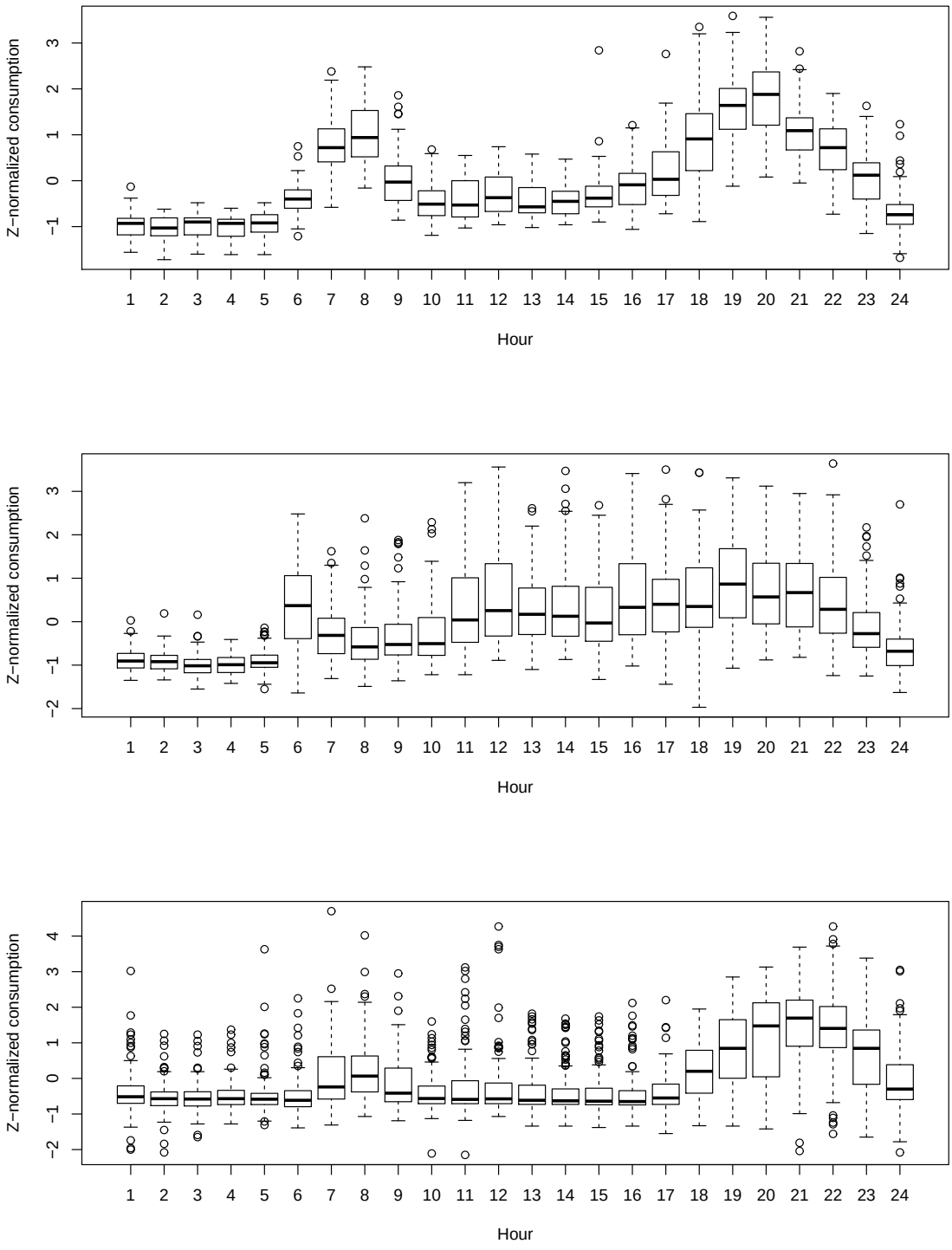

Figure 3.8: Daily electricity consumption pattern displayed by 3 different households. Data Source: [23].

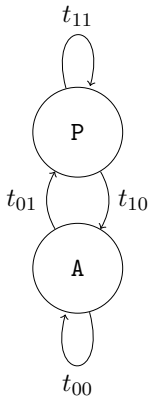

Figure 3.9: Two-state DTMC used to model occupancy, with probability matrix given by (3.1).

$$P_{\mathrm{B}} = \begin{bmatrix} t_{11} & t_{10} \\ t_{01} & t_{00} \end{bmatrix} = \begin{bmatrix} t_{11} & 1 - t_{11} \\ t_{01} & 1 - t_{01} \end{bmatrix} \tag{3.1}$$

$$\mu = \frac{t_{01} + t_{10}}{t_{00} + t_{11}} \tag{3.2a}$$

$$t_{01} = \min\left\{1, \frac{\mu - 1}{\mu + 1} p_t + p_{t+1}\right\} \tag{3.2b}$$

$$t_{11} = \min\left\{1, \frac{p_t - 1}{p_t}\left(\frac{\mu - 1}{\mu + 1} p_t + p_{t+1}\right) + \frac{p_{t+1}}{p_t}\right\} \tag{3.2c}$$

we model each occupant by means of a two-state Discrete Time Markov Chain (DTMC), using the methodology proposed in [52]. The DTMC is illustrated in Figure 3.9, where the two states are Presence (`P`) and Absence (`A`), respectively. The transition probabilities are given by the Bernoulli distribution in (3.1) [4,52]. t_{10} is the probability of going from `P` to `A`, i.e. the probability that an occupant who is present leaves home, t_{11} is the probability of staying at home, t_{01} is the probability that an occupant who is absent arrives home, and t_{00} is the probability of staying away.

The probability of an occupant being present at one particular hour is given by p_t. The probability that she is present at the immediately consecutive time step is denoted by p_{t+1}. These probabilities correspond to the occupancy profile values depicted in Figure 3.1. In [52], the probabilities are expressed in terms of a mobility parameter μ, defined in (3.2a). A value $\mu < 1$ means that the probability of transition from `A` to `P` t_{01} is less or equal than the probability of being present at the next time step: $t_{01} \leq p_{t+1}$. We calculate t_{01} and t_{11} as in (3.2b) and (3.2c), respectively. The normalized occupancy profile used in the calculations is the average of all individual random profiles.

3.4 Heat Pump Schedule

We consider some elements of the control without explicitly modelling it. For instance, we assume a constant shading factor during the heating period, specified by the $0 \leq \mathrm{sd}_{\mathrm{mec}} \leq 1$ parameter. The HP scheduler block is another attempt to account for such control element.

If final consumers behave rationally, in the economic sense, they will orient their investments and actions to reducing costs. Following this reasoning, and recalling that final consumers pay an electricity tariff that explicitly penalizes the maximum daily peak, it is

possible to infer that the building administrator, or the automatic building control, has an incentive to dispatch the HPs in a way that does not contribute to an increase in the daily peak.

For the sake of simplicity, we assume that the HP is operated in cycling mode.[1] We assume as well that the building can be modelled as a volume with a thermal capacity C. The building control can use this thermal capacity as a thermal battery, and dispatch the HP avoiding the coincidence with the electricity peaks due to lighting and appliances. The HP schedule constitutes thus a decision variable than can be controlled to reduce the overall electricity costs. However, as we are not considering the HP investment costs, we assume this dispatch to be part of a pre-optimization step, rather than including it among the decision variables in the models developed later in this dissertation. The output of the HP scheduler constitutes the starting point for the models presented in the subsequent chapters.

It is possible to store heat in the building by increasing the temperature of its thermal mass. We impose the restriction $|\Delta T| \leq 3°\text{C}$. The stored heat Q_{sto} is related to C as in (3.3a). By increasing the temperature of the thermal mass, additional thermal losses $Q^{\text{add}}_{\text{trans}}$, given by (3.3b), are incurred.

$$Q_{\text{sto}} = C\Delta T = C\left(T_{\text{int}} - T_{\text{amb}}\right) \tag{3.3a}$$

$$Q^{\text{add}}_{\text{trans}} = UHA_s\Delta T = UHA_s\frac{Q_{\text{sto}}}{C} \tag{3.3b}$$

The two HPs (space conditioning and DHW production) are modelled as binary variables. The MIP used to obtain the HPs schedules is described in Section A.1. The output of this module are the HP schedules, $\mathbf{x}_{\text{hp}}$ and $\mathbf{x}_{\text{hp,dhw}}$, respectively. These two time series, together with the electricity profile corresponding to lighting and appliances $\mathbf{x}_{\text{ap+li}}$, thoroughly define the building electricity consumption profile.

3.5 Load Aggregation

The price structure defined in Section 2.5.2 is a function of the aggregate load level. This section is devoted to the construction of a *lowEx* community and of the corresponding aggregate electricity consumption profile. The total electricity profile has to be representative of the distribution of physical and operational parameters, and has to converge to the intended design figures. This process comprises the definition of all buildings constituting the target *lowEx* community, the simulation of each building in order to obtain the individual electricity profiles, and the aggregation of the total load. Based on the total load, we obtain the electricity prices that will be used in the subsequent chapters.

[1] Two states: off and maximum power.

The distribution of parameters that are used to construct the aggregate load responds to a twofold objective. On one hand, we are interested in defining characteristics of existing buildings, such as area distribution, area per occupant, ratio between single family houses and apartment blocks, or characteristics that *lowEx* communities will —or are likely to— implement, such as high COPs, relatively high U-values, particular lighting technologies, among others. On the other hand, the resulting total electricity profile has to exhibit the desired shape and composition specified by the design parameters. Besides emulating the consumption patterns that can be identified in the aggregate national load levels [49], we are interested in reproducing realistic energy and electricity shares, and ratios between shares, such as appliances to lighting, or heating to DHW energy ratios.

We approach this twofold objective by following an iterative heuristic procedure. The deterministic equivalent of each building can be represented in terms of linear equations. By using these equations, it is possible to choose parameters that in the aggregate view converge to the target design figures.

The distribution of parameters is based on our own assumptions and on general European statistics [13]. Some parameters are coupled, e.g., the glazing area A_w and the U-values U, or the constructed area A_s and the shape factor H. A particularly important parameter is the COP. The $2Sol$ methodology strives to achieve a high COP (COP = 10); however, as we only consider an average seasonal COP, we define it as a normal distribution centered at 6, which is a more conservative and realistic value for the average. Figure 3.10 depicts some of the distributions used to obtain a *lowEx* community of 3000 buildings.

We simulate 3000 buildings, which is a number large enough to converge to the figures observed in the aggregate load levels. On top of these buildings, and in order to account for the share of non-residential buildings in the aggregate profile,[2] we add a number of office buildings, simulated with deterministic profiles according to [63]. The resulting duration curves are shown in Figure 3.11.

3.6 Computational Details

All simulations and optimizations ran on an 8-core Intel(R) Core(TM) i7-3720QM computer. Each processor core clocks at 2.60GHz. The system has 8Gb of RAM and runs on the GNU/Linux (kernel 3.x.) operating system.

The building simulations were implemented using a combination of python [55] and shell scripts. The MIP used to obtain the HP dispatch, described in Section A.1, was implemented in GAMS [15].

The generation of each building (before the HP dispatch) takes approximately 1.7s. The building generator includes, additionally, an initialization time for the generation of the weather and location-related files. Depending on the resolution of the weather files,

[2] See Figure 1.2b on page 6.

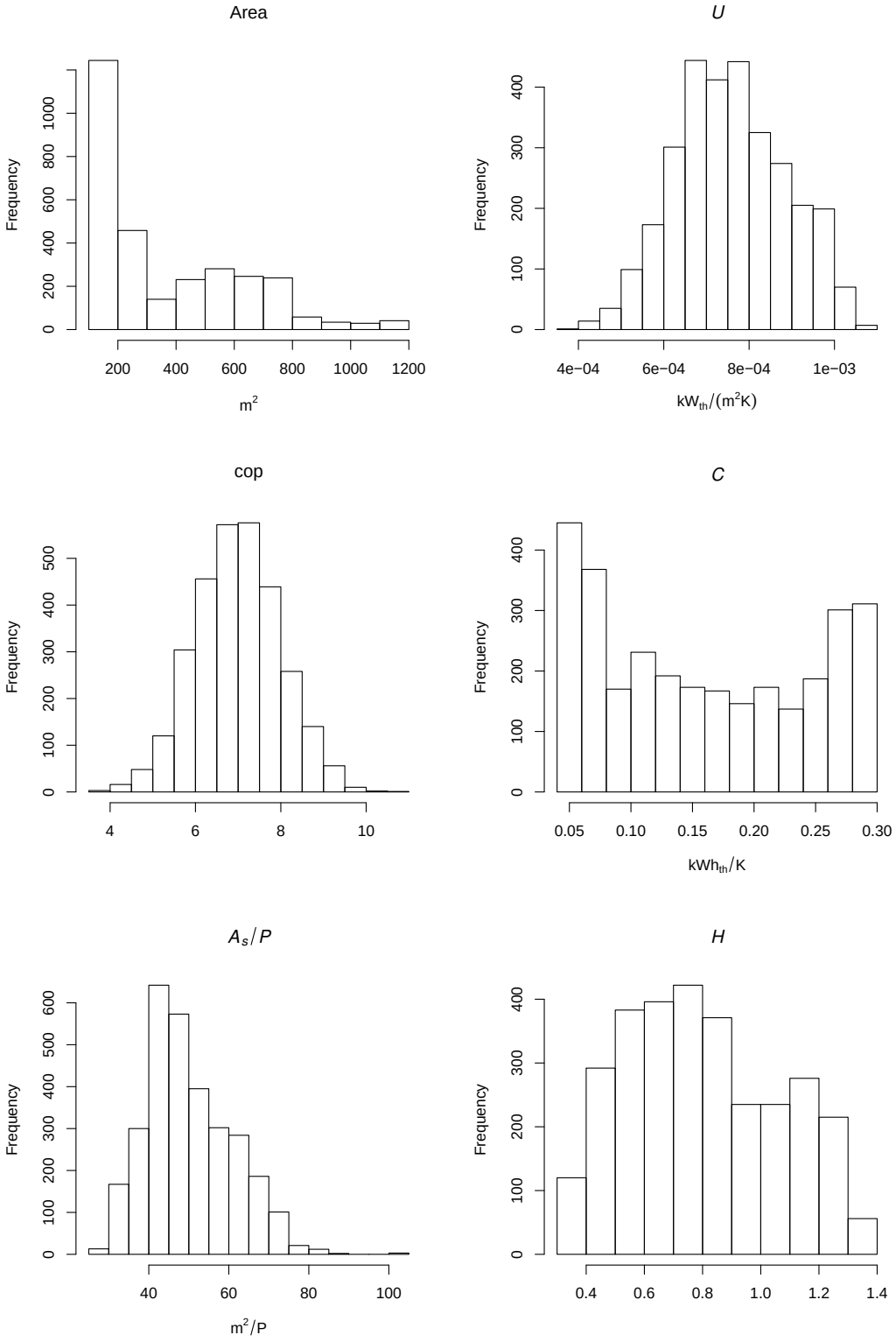

Figure 3.10: Distribution of parameters used for the generation of a *lowEx* community of 3000 buildings

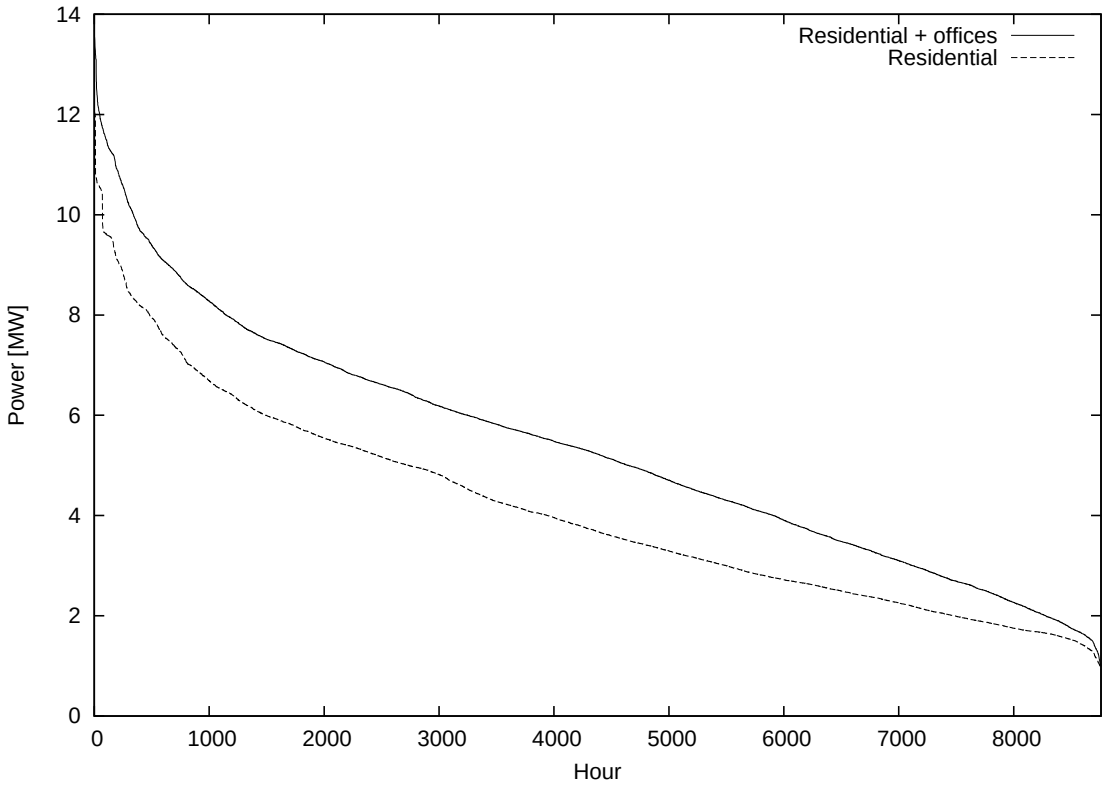

Figure 3.11: Duration curve $d(h_y)$ for an aggregation of 3000 buildings

the elapsed time can be between 10s and 50s per location.

The MIP takes approximately 10s per building, with times ranging between 4s and several minutes. The optimization time was in general found to be longer for buildings with high UH products, e.g., $UH > 1.5$.

3.7 Summary

This chapter presented a methodology aimed at simulating the aggregate electrical load of a *lowEx* community and, correspondingly, at providing the inputs for the demand-based price calculation. The total load is obtained on the basis of a distribution of parameters that are representative of the characteristics that a *lowEx* community will —or is expected to— implement. The load generator is a design tool that combines bottom-up and top-down approaches to achieve a dual objective. On one side, it is able to realistically represent the heterogeneity and randomness found in individual buildings' consumption profiles. On the other side, the sum of all loads produced by the load generator (3000 buildings in this particular case) converge to a pattern, whose shape and composition can be partially influenced by the design objectives. In other words, the total aggregate load can be designed

to resemble certain pattern or to have a predetermined structure.

The load generator presented in this chapter allows for the profiling of several buildings in a computationally efficient way. It follows a statistical rather than physical approach. The model focuses on generating plausible and credible electricity profiles, instead of accurately modelling a particular building or group of buildings.

In general, it is possible to accurately simulate a building's thermal response, and there exists a wide range of software for this purpose. On the other hand, modelling the final electricity consumption greatly depends on how accurately occupancy is modelled. Modelling occupancy by using only diversity profiles, e.g., daily profiles that are repeated every day, might be a good approach for simulating individual buildings, but not when the objective is to simulate a plurality of buildings and their aggregate behavior, as those diversity profiles do not necessarily take into account top-down considerations.

The main focus of our simulations is on residential buildings, but office buildings are also included in the construction of the total electricity profile. Office buildings are, however, modelled in a deterministic way without considering multiple zones nor random occupancy regimes. The office buildings are inserted to account for characteristic office patterns. These additional patterns result in a reduced standard deviation in the total consumption, and introduce a differentiation between weekdays and weekends.

The load generator is implemented as a collection of software libraries, each one corresponding to one of the blocks in Figure 3.4. Traditional simulation software focuses mainly on thermal modelling. Given the energy and electricity shares exhibited by *lowEx* buildings, thermal modelling is not the most important component in our analysis. Other factors contribute more significantly to the final consumption's shape and composition. The main driving factor defining each building's electricity consumption profile is occupancy. In order to realistically represent the randomness associated with occupancy schedules, each occupant is modelled as a two-state DTMC. The final occupancy profile is the average of all random realizations. This strategy results in an aggregate consumption that converges to the quasi-deterministic pattern observed in real profiles. The random occupancy generator is additionally used to generate different occupancy scenarios for each building.

Another important element in the analysis is the HP operation. The HPs' schedules are modelled as an MIP. The objective of this block is to emulate an element of the control, namely the user's reaction to an electricity tariff that explicitly penalizes the daily peak. Under such tariff, users have an incentive to dispatch the HPs in a way that does not contribute to an increase in the daily peaks. The HP schedule block models the building as a thermal battery with capacity C. The output of this block completely defines the building's electricity profile, which is formed by the electricity due to lighting and appliances, and the HPs schedules.

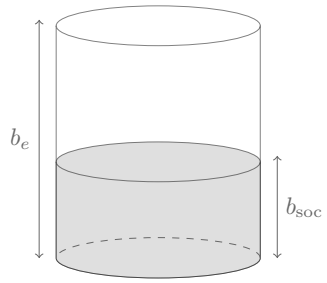

Chapter 4

Battery and PV Selection Model, the User's Perspective

The determination of the optimal battery and PV installation size depends upon the intended application and operative objectives. "*What is the optimal battery and PV capacity that a user is willing to install?*" is, naturally, an incomplete question if the intended objectives, conditions, and constraints are not enunciated. As discussed in Chapter 2, we assume that users have, primarily, an economic incentive. If consumers behave rationally, in the economic sense, and face an electricity tariff with the structure proposed in Section 2.5.2, then they are encouraged to time-shift their consumption, reduce their maximum daily peak and, in general, become responsive to demand-based prices.

This chapter approaches the question of optimal battery and PV selection from the individual user's perspective. The proposed strategy builds on the data and model obtained in Chapter 3.

Our intuition is that in the presence of a demand-based tariff, which splits the electricity price into hourly and daily peak components, final electricity consumers have an economic incentive to reshape their electricity profile. The final electricity consumption pattern is assumed to be mainly linked to comfort. Our premise is that users value comfort very highly and do not want to deviate from their comfort levels. In this scenario, a battery provides a mechanism to accommodate the electricity profile without deviating from the comfort objectives.

The energy generated on-site with a PV installation increases the profit possibilities when the PV is operated in conjunction with a DSE, at least, during the months when solar radiation is relatively abundant. A DSE offers on its own the possibility for time-shifting energy and consequently profiting from the demand-based tariff. As we are interested in exploring the interplay between battery and PV, a model aiming to size these two elements has to consider them simultaneously in the context of the building's electricity profile and the price dynamics.

We formulate the problem of sizing the battery and PV elements as a stochastic linear optimization model. The resulting stochastic Linear Program (LP) is an arbitration model, in which the user's objective is to minimize costs. This model is presented in Section 4.1. Section 4.2 describes how to account for uncertainty. Section 4.3 is devoted to a detailed

analysis of the results, including the sensitivity analysis and the evaluation of different costs-development scenarios. Section 4.4 is a brief compendium of the computational issues. This chapter concludes with a comprehensive summary and conclusions in Section 4.5.

4.1 Optimal Battery Selection Model

Description	Symbol	Type	Units
Power conversion factor	ξ	Exogenous	kW/kWh
Length of the analysis period	τ_d	Exogenous	day
Minimum SOC	$b_{\text{soc}}^{\min}$	Exogenous	%
Battery energy capacity	b_e	Endogenous	kWh
Battery input power	b_p^{in}	Endogenous	kW
Battery output power	b_p^{out}	Endogenous	kW
PV peak power	ϕ_p	Endogenous	kW
PV effective area and efficiency	ϕ_a	Endogenous	m^2
Battery marginal cost	$c_{b_e}^m$	Exogenous	€/kWh
Daily per-unit battery energy fixed cost	$c_{b_e}^f$	Exogenous	€/kWh day
Daily per-unit battery power fixed cost	$c_{b_p}^f$	Exogenous	€/kW day
Daily per-unit PV power fixed cost	c_{ϕ}^f	Exogenous	€/kW day

Table 4.1: Scalars involved in the definition of model (4.1). Exogenous variables affect the model but are not in turn affected by the model. Endogenous variables are created within the model.

Table 4.1 introduces the scalar quantities involved in the model calculations. Exogenous variables are parameters affecting the model without being in turn modified, while endogenous variables are produced by the model.

Reshaping the electricity consumption pattern by means of a DSE has inherently a time-dependent nature. The user is interested in the overall cost reduction during the entire analysis period spanning τ_d days. This time dependence supposes the use of time series, hereinafter also and indistinctly referred to as vectors, whose domains are given by the sets defined in Table 2.6 on page 34.

The different vectors involved in the model calculations are summarized in Table 4.2. For each instance of the model, and only for that particular instance, each one of the vectors is a $\mathbb{R}$-valued function, whose domain is the associated set in Table 4.2. For instance, the electricity withdrawn from the grid $\mathbf{x}_g$ is defined as a function:

$$\begin{array}{rccc} f: & \Omega & \to & \mathbb{R} \\ & d,h & \mapsto & \mathbf{x}_g(d,h) = x_{g_{d,h}} = x_{g_i} \end{array}$$

The price structure imposes the requirement that the model be traversed on a daily basis, which is equivalent to having τ_d different optimization problems of length 24. On the other hand, the conservation equations describing the energy balance in the battery constitute a continuous system with memory. This system requires that the model be navigated as a linear space and not on a daily basis. Vectors defined with domain set Ω can be navigated either as a linear space or as matrix in $\mathbb{R}^{\tau_d \times 24}$. The following elements are identical $\mathbf{x}_g(d,h) = \mathbf{x}_g(dh) = x_{g_{d,h}} = x_{g_i}$. Superscripts ^{0},$^{\bar{0}}$, or $^{+1}$ indicate that the vectors are defined for the domains Ω^0, $\Omega^{\bar{0}}$, and Ω^{+1}, respectively. For instance,

$$\mathbf{b}_{\text{soc}}^{\bar{0}} = \{\mathbf{b}_{\text{soc}}(d_1 h_3), \mathbf{b}_{\text{soc}}(d_1 h_4), \ldots, b_{\text{soc}_i}, \ldots, \mathbf{b}_{\text{soc}}(d_{\tau_d} h_{24})\}$$

Description	**Symbol**	**Type**	**Set**	$\{\cdot\}$	**Units**
Electrical load	$\mathbf{x}_l$	Exogenous	Ω	x_{l_i}	kWh
Stochastic version of the electrical load	$\tilde{\mathbf{x}}_l$	Exogenous	Ω	$\tilde{x}_{l_i}$	kWh
Electricity withdrawn from the grid	$\mathbf{x}_g$	Endogenous	Ω	x_{g_i}	kWh
Electricity flowing into the battery	$\mathbf{x}_b^{\text{in}}$	Endogenous	Ω	$x_{b_i}^{\text{in}}$	kWh
Electricity flowing out of the battery	$\mathbf{x}_b^{\text{out}}$	Endogenous	Ω	$x_{b_i}^{\text{out}}$	kWh
Normalized corrected solar irradiance	$\mathbf{E}_e$	Exogenous	Ω	E_{e_i}	kWh/m^2
Battery State of Charge (SOC)	$\mathbf{b}_{\text{soc}}$	Endogenous	Ω	b_{soc_i}	kWh
Electricity prices (energy component)	$\mathbf{c}_g$	Exogenous	Ω	c_{g_i}	€/kWh
Daily peak prices (power component)	$\mathbf{c}_g^{\max}$	Exogenous	D	$c_{g_d}^{\max}$	€/kW
Electricity withdrawn from the grid per days	$\mathbf{x}_g^{\Delta}$	Endogenous	D	$\mathbf{x}_g^d$	kWh
Electricity withdrawn from the grid for day d	$\mathbf{x}_g^d$	Endogenous	H	$x_{g_j}^d$	kWh
Electricity prices (energy component) per days	$\mathbf{c}_g^{\Delta}$	Exogenous	D	$\mathbf{c}_g^d$	€/kWh
Electricity prices (energy component) for day d	$\mathbf{c}_g^d$	Exogenous	H	$c_{g_j}^d$	€/kWh
Maximum daily peaks	$\mathbf{k}_g^{\Delta}$	Endogenous	D	κ_g^d	kW

Table 4.2: Vectors involved in the definition of model (4.1). Exogenous variables affect the model, but are not in turn affected by the model. Endogenous variables are created within the model.

Vector $\mathbf{x}_g^{\Delta}$ in Table 4.2 contains the clustered-by-day subsets of electricity values withdrawn from the grid: $\mathbf{x}_g^{\Delta} \subseteq \mathbf{x}_g$. All the elements in $\mathbf{x}_g^{\Delta}$ are of length 24. Each of the 24h-vectors in $\mathbf{x}_g^{\Delta}$ is denoted $\mathbf{x}_g^d$, where the superscript ^{d} indicates the corresponding day. For instance, $\mathbf{x}_g^{d_3}$ is the vector of grid electricity values containing the 24 values in day d_3. The same applies to the clustered-by-day electricity prices $\mathbf{c}_g^{\Delta}$.

The battery and PV selection model is given by (4.1).

$$\min_{\chi^*} \sum_{d=d_1}^{d_{\tau_d}} \sum_{h=h_1}^{h_{24}} c_{g_i} x_{g_i} \tag{4.1a}$$
$$+ \sum_{d=d_1}^{d_{\tau_d}} c_{g_d}^{\max} \cdot \kappa_g^d$$
$$+ \frac{1}{2} c_{b_e}^m \sum_{d=d_1}^{d_{\tau_d}} \sum_{h=h_1}^{h_{24}} (x_{b_i}^{\text{in}} + x_{b_i}^{\text{out}})$$
$$+ \tau_d \big(c_{b_e}^f b_e + c_{b_p}^f b_p^{\text{in}} + c_{b_p}^f b_p^{\text{out}} \big)$$
$$+ \tau_d \cdot c_\phi^f \cdot \phi_p,$$

subject to

$$b_e - b_{\text{soc}_i} \geq 0, \quad \forall b_{\text{soc}_i} \in \mathbf{b}_{\text{soc}} \tag{4.1b}$$
$$b_{\text{soc}_i} - b_{\text{soc}}^{\min} \cdot b_e \geq 0, \quad \forall b_{\text{soc}_i} \in \mathbf{b}_{\text{soc}}^{\bar{0}} \tag{4.1c}$$
$$b_{\text{soc}_i} - b_{\text{soc}}^{\min} \cdot b_e = 0, \quad \forall b_{\text{soc}_i} \in \mathbf{b}_{\text{soc}}^{0} \tag{4.1d}$$
$$x_{b_i}^{\text{out}} = 0, \quad \forall x_{b_i}^{\text{out}} \in \mathbf{x}_b^{\text{out}^0} \tag{4.1e}$$
$$b_p^{\text{in}} - \xi x_{b_i}^{\text{in}} \geq 0, \quad \forall x_{b_i}^{\text{in}} \in \mathbf{x}_b^{\text{in}} \tag{4.1f}$$
$$b_p^{\text{out}} - \xi x_{b_i}^{\text{out}} \geq 0, \quad \forall x_{b_i}^{\text{out}} \in \mathbf{x}_b^{\text{out}} \tag{4.1g}$$
$$x_{b_i}^{\text{out}} + \phi_a E_{e_i} + x_{g_i} - x_{b_i}^{\text{in}} - \tilde{x}_{l_i} \geq 0, \quad \forall x_{g_i} \in \mathbf{x}_g, \forall x_{b_i}^{\text{in}} \in \mathbf{x}_b^{\text{in}}, \forall x_{b_i}^{\text{out}} \in \mathbf{x}_b^{\text{out}}, \quad \forall \tilde{x}_{l_i} \in \tilde{\mathbf{x}}_l, \forall E_{e_i} \in \mathbf{E}_e \tag{4.1h}$$
$$\Delta b_{\text{soc}_i} - b_{\eta_c} x_{b_i}^{\text{in}} + \frac{1}{b_{\eta_d}} x_{b_i}^{\text{out}} = 0, \quad \forall b_{\text{soc}_i} \in \mathbf{b}_{\text{soc}}^{+1}, \forall x_{b_i}^{\text{in}} \in \mathbf{x}_b^{\text{in}^{+1}}, \forall x_{b_i}^{\text{out}} \in \mathbf{x}_b^{\text{out}^{+1}} \tag{4.1i}$$
$$\phi_p - \xi \phi_a E_{e_i} \geq 0, \quad \forall E_{e_i} \in \mathbf{E}_e \tag{4.1j}$$
$$\kappa_g^d - \xi x_{g_j}^d \geq 0, \quad \forall \kappa_g^d \in \mathbf{k}_g^\Delta, \forall x_{g_j}^d \in \mathbf{x}_g^d, \forall \mathbf{x}_g^d \in \mathbf{x}_g^\Delta \tag{4.1k}$$
$$b_e \geq 0, \quad b_p^{\text{in}} \geq 0, \quad b_p^{\text{out}} \geq 0, \quad \phi_a \geq 0, \quad \phi_p \geq 0 \tag{4.1l}$$
$$x_{b_i}^{\text{out}} \geq 0, \quad \forall x_{b_i}^{\text{out}} \in \mathbf{x}_b^{\text{out}^{\bar{0}}}; \quad x_{b_i}^{\text{in}} \geq 0, \quad \forall x_{b_i}^{\text{in}} \in \mathbf{x}_b^{\text{in}}; \quad x_{g_i} \geq 0, \quad \forall x_{g_i} \in \mathbf{x}_g \tag{4.1m}$$

The objective function is defined in (4.1a), with controls given by:

$$\chi^* = \{\mathbf{x}_g, \mathbf{x}_b^{\text{in}}, \mathbf{x}_b^{\text{out}}, \mathbf{k}_g^\Delta, \mathbf{b}_{\text{soc}}, b_e, b_p^{\text{out}}, b_p^{\text{in}}, \phi_a, \phi_p\}$$

The first two terms in the objective function (4.1a) represent the total electricity fee under the demand-based tariff described in Section 2.5.2. The first term is the cost of the integral energy consumption, while the second term addresses the daily peaks cost.

The second term in (4.1a), in combination with (4.1k), is the linear recast of the non-

linear term

$$\xi \sum_{d=d_1}^{d_{\tau_d}} c_{g_d}^{\max} \cdot \max \mathbf{x}_g^d$$

The quantity ξ is used as a power conversion factor. All the models presented in this thesis have a time resolution of 1h; therefore, $\xi = 1\text{kW/kWh}$. If the time resolution is 15-min, $\xi = 4\text{kW/kWh}$.

The third term in the objective function (4.1a) penalizes the battery cycling life. The fourth term represents the cost of the selected battery energy and power. The last term accounts for the PV cost.

Constraints (4.1b) and (4.1c) impose upper and lower limits for the State of Charge (SOC),[1] while constraints (4.1d) and (4.1e) define the battery's initial conditions. Constraints (4.1f) and (4.1g) indicate that the energy flowing into and out of the battery cannot be greater than the respective input and output powers. Constraint (4.1h) is the building's balance equation. Constraint (4.1i) is the differential equation modelling the battery SOC. The term Δb_{soc_i} represents the change in the SOC with respect to the previous time step. Finally, (4.1j) indicates than the generated PV electricity must be less or equal than the selected PV capacity.

4.2 Accounting for Uncertainty

The model formulated in the previous section can be regarded as a strategic tool that a final electricity consumer, facing a demand-based electricity tariff, can use to decide whether or not to invest in a DSE and PV. For a user confronted with this strategic decision, the electricity consumption connected to occupancy is the only uncertain variable. As mentioned in Section 3.2, the weather uncertainty is accounted for by using a TRY or a statistical year. Given that the electricity prices, and the PV and battery costs are known beforehand, the only remaining source of uncertainty is the occupancy.

In order to account for this uncertainty, the electrical load vector $\mathbf{x}_l$ is modelled as a random variable, denoted $\tilde{\mathbf{x}}_l$, with elements $\tilde{x}_{l_i}$. Model (4.1) is a stochastic LP, in which the $\tilde{\mathbf{x}}_l$ vector assumes the form of a discrete distribution with 10 different scenarios, each with probability $p_s = 1/10$. These realizations, or scenarios, correspond in turn to 10 realizations of the random DTMC documented in Section 3.3.

A stochastic LP can be modelled as a 2-stage program [45]. At the first stage, without knowing the future, "here and now" decisions are made. Afterwards, when the random variables unfold, "wait and see" decisions react to compensate the effect of the random variables outcome. The reaction of the decision maker to this outcome is referred to as recourse [45, 57, 59]. The new objective function is the expected value of the cost.

[1] SOC = b_e − DOD. Minimum SOC = Maximum DOD

In our model, as all the costs are known beforehand, the battery-dimension variables: b_e, b_p^{out}, and b_p^{in}, as well as the PV size —ϕ_p and ϕ_a— are first stage variables, i.e. they are determined before the random variables become known. On the other hand, the vectors $\mathbf{b}_{\text{soc}}, \mathbf{k}_g^{\Delta}, \mathbf{x}_b^{\text{in}}, \mathbf{x}_b^{\text{out}}$, and $\mathbf{x}_g$, as well as their associated equations, are second stage or recourse variables. The number of scenarios was chosen to be 10 as a compromise between accuracy and tractability.

4.3 Experiments and Results

This section is dedicated to the analysis of the battery and PV selection model introduced in Sections 4.1 and 4.2. The different analyses are conducted by defining a case study and establishing a parallel between two different electricity tariffs.

The price structure discussed in Section 2.5.2 explicitly addresses the total electricity consumption and the maximum peak on a daily basis. Both the energy and the power components are normalized to a value of 0.2€/kWh, resp. 0.2€/kW, which is the reference value used in the definition of the costs summarized in Table 2.3 on page 31. The daily peak components are directly derived from the aggregate load levels obtained in Section 3.5.

The two tariffs feature the same power components $\mathbf{c}_g^{\max}$, but different energy components $\mathbf{c}_g$. We consider a constant tariff, denoted p1, and a 4-level tariff, denoted p4. Both tariffs are normalized to a mean value of 0.2€/kWh; consequently, in p1 $c_{g_i} = 0.2$€/kWh, $\forall c_{g_i} \in \mathbf{c}_g$. p4 is defined as a function of the duration curve $d(h_y)$ depicted in Figure 3.11 on page 50, including office buildings. Each element $x_{l_i}^{\text{total}}$ of the aggregate load $\mathbf{x}_l^{\text{total}}$ is mapped to a price element c_{g_i} using the function $d(h_y)$ as follows: $c_{g_i} = \text{p4}_1$ if $x_{l_i}^{\text{total}} < d(4000)$, or $c_{g_i} = \text{p4}_2$ if $d(4000) \leq x_{l_i}^{\text{total}} < d(1500)$, or $c_{g_i} = \text{p4}_3$ if $d(1500) \leq x_{l_i}^{\text{total}} < d(330)$, or $c_{g_i} = \text{p4}_4$ if $x_{l_i}^{\text{total}} \geq d(330)$. Consequently, $c_{g_i} \in \{\text{p4}_1, \text{p4}_2, \text{p4}_3, \text{p4}_4\}$, $\forall c_{g_i} \in \mathbf{c}_g$.

The profit that users can obtain is, as can be easily inferred, proportional to the standard deviation of p4.[2] We select values for the p4_{1-4} levels that result in a standard deviation $\sigma = 0.6$.[3] The selected values are $\text{p4}_1 = 0.5$, $\text{p4}_2 = 1.0$, $\text{p4}_3 = 1.5$, and $\text{p4}_4 = 2.5$. Values are normalized to 0.2€/kWh by dividing them by their average and multiplying by 0.2.

The results presented within the following sections are alternately discussed for the two tariffs p1 and p4.

bytpe=residential
A_s=700.0
A_s^r=0.7
A_w=0.3
loc=Zurich
cop=6.0
$U = 5.6 \times 10^{-4}$
H=0.9
C=105
P=18
ori=0.1
sd_{pol}=0.4
sd_{mec}=0.8
s_{li}=1
s_{ap}^r=0
s_{ap}^k=0
s_{dhw}=0

Figure 4.1: Reference building b0's input parameters for the load generator

Parameter	Value	Units
hp	3.1	kW
hp_{dhw}	3	kW
HDDs	3695	°C day
CDDs	83	°C day
Thermal losses	48.4	$\text{kWh}_{\text{th}}/\text{m}^2$ year
Heating energy	33.0	$\text{kWh}_{\text{th}}/\text{m}^2$ year
Cooling energy	10.5	$\text{kWh}_{\text{th}}/\text{m}^2$ year
Solar gains	12.4	$\text{kWh}_{\text{th}}/\text{m}^2$ year
DHW energy	20.9	$\text{kWh}_{\text{th}}/\text{m}^2$ year
f_{load}	0.23	—

Table 4.3: Reference building b0's statistics. Figures are the expected values of the 10 stochastic realizations.

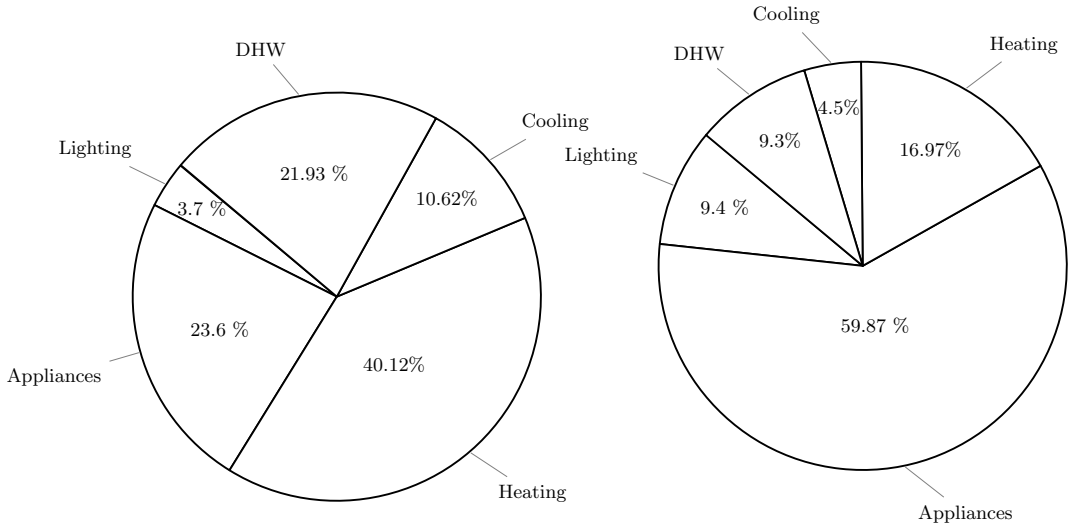

(a) Energy (b) Electricity

Figure 4.2: Building b0's electricity and energy shares. Figures are the expected values of 10 stochastic realizations.

4.3.1 Case Study

The results and sensitivity analyses presented in the following sections refer to the test building "b0", whose parameters are given in Figure 4.1 and statistics in Table 4.3. The vectors defining this building's electricity profile are in reality 10 sets of time series, each representing a different realization of the stochastic occupancy. The energy and electricity shares for the test building are depicted in Figure 4.2, these shares correspond to the expected value of all stochastic realizations.

We introduce here an important metric used in the following discussions. The load factor f_{load} (4.2) is the quotient between the average and the maximum electricity withdrawn from the grid.

$$f_{\text{load}} = \frac{\overline{\mathbf{x}}_g}{\max \mathbf{x}_g} \tag{4.2}$$

4.3.2 Sensitivity to the Model's Parameters

In this section, the model's sensitivity to economic and technical —not building-related— parameters is measured. The sensitivity analysis can be carried out using the One at a Time (OAT) methodology because the model is linear. An additional consequence of the model's linearity is the fact that changing the costs is equivalent to changing the electricity prices, as long as the ratio between costs and prices remains constant. In our analysis, the mean value of the electricity prices is kept constant.

The sensitivity analyses are displayed in the form of "tornado plots" in Figures 4.3 and 4.4, corresponding to tariffs p1 and p4, respectively. Each tornado plot illustrates the sensitivity of one particular endogenous parameter, e.g., the battery energy capacity b_e, to the OAT variation of some selected exogenous parameters. The bars indicate how much the endogenous parameter changes, when the exogenous parameter associated with each bar changes by $\pm 10\%$.

Factors such as α and the battery efficiency —b_{η_c} and b_{η_d}— are referred to as non-economic, as they are not subject to a direct economic penalization or cost. The smaller the α component, the bigger the daily peak component, and smaller the energy contribution (See Figure 2.9 on page 27). The following observations are derived from the inspection of Figures 4.3 and 4.4.

The most sensitive variable is the PV peak power ϕ_p and the least sensitive is the battery output power b_p^{out}.

Following an overall inspection of Figures 4.3, it can be conjectured that the selection of the battery components is associated with the goal of reducing the daily peaks, while

[2]This fact was corroborated by running the model under different combinations resulting in the same standard deviation values.

[3]The ratio between the dual tariff's high and low values in the Zurich area in 2013 was between 1.5 and 2.0. Source: EWZ.

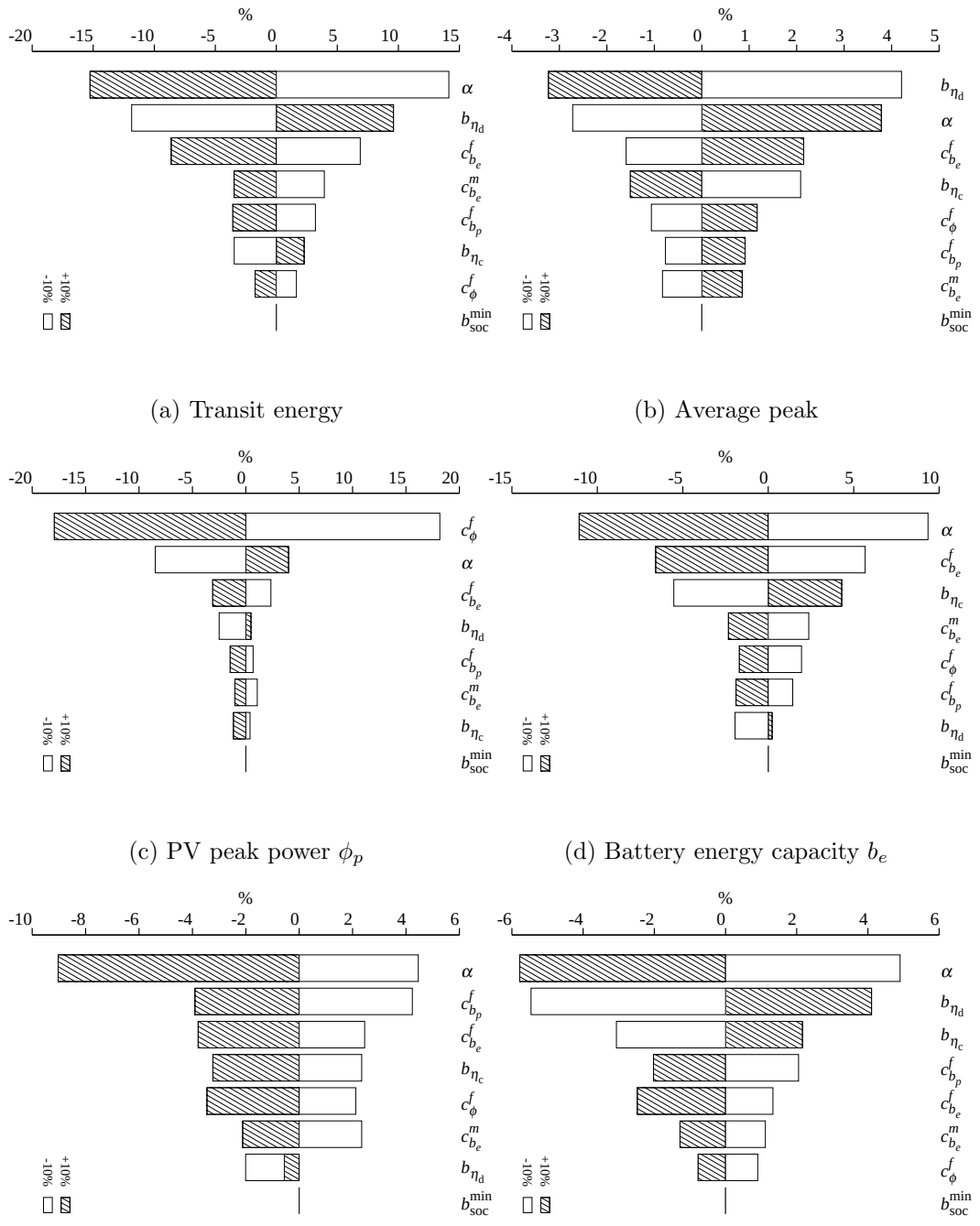

(a) Transit energy

(b) Average peak

(c) PV peak power ϕ_p

(d) Battery energy capacity b_e

(e) Battery input power b_p^{in}

(f) Battery output power b_p^{out}

Figure 4.3: Sensitivity to the model's parameters for building b0 under tariff p1

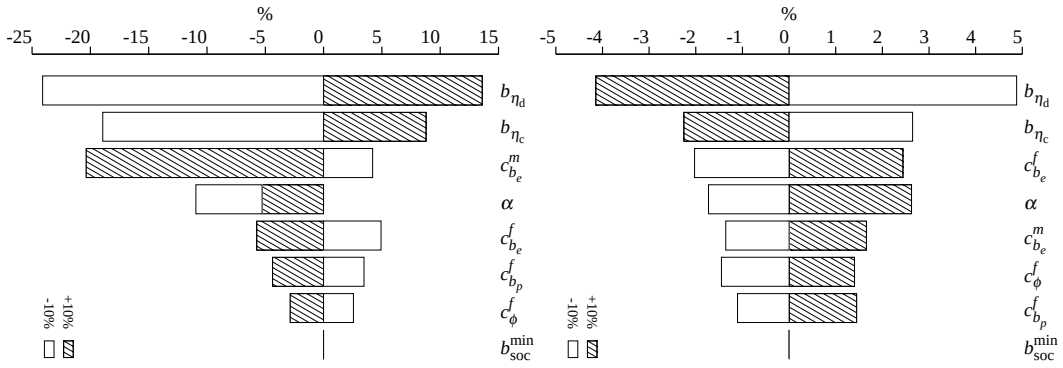

(a) Transit energy

(b) Average peak

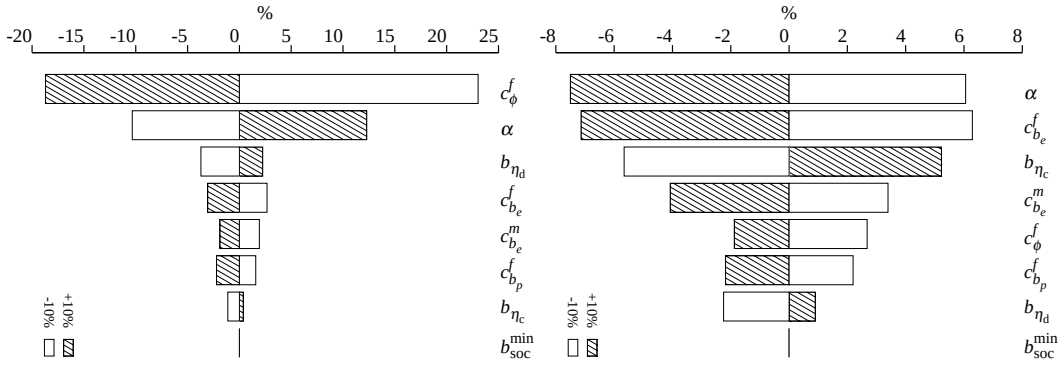

(c) PV peak power ϕ_p

(d) Battery energy capacity b_e

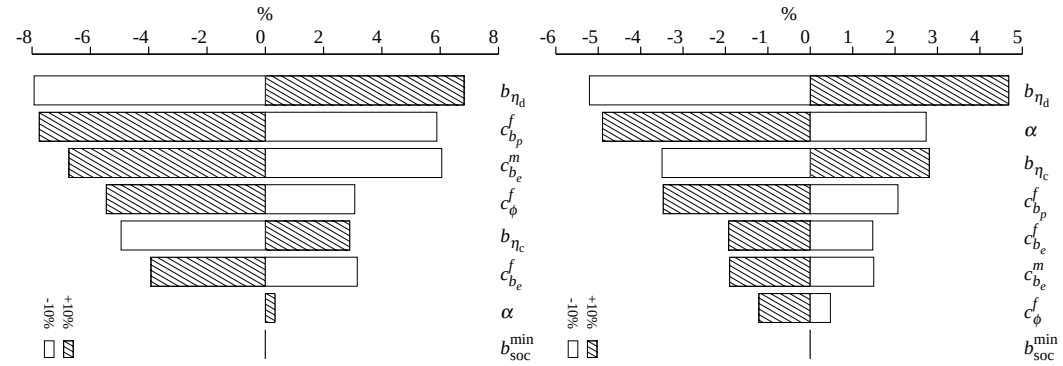

(e) Battery input power b_p^{in}

(f) Battery output power b_p^{out}

Figure 4.4: Sensitivity to the model's parameters for building b0 under tariff p4

the dimension of the PV element is associated with the goal of reducing the energy fee. The size of the battery components is inversely proportional to α, while the size of the PV element is in direct proportion with it. When α increases, i.e. when the peak element becomes less important, the PV element increases as well.

The situation is similar under tariff p4 (Figures 4.4), except that the influence of α on the battery input power b_p^{in} is almost negligible. This fact, together with the comparatively larger influence of the PV cost c_ϕ^k on b_p^{in}, suggests a coupling between ϕ_p and b_p^{in}. In fact, the results for the 4-level tariff p4 in Figures 4.4 reveal that ϕ_p and b_p^{in} are coupled and relate to the goal of reducing the energy fee. Analogously, it can be inferred that b_e and b_p^{out} are related to the goal of reducing the peak component fee.

The battery capacity costs —$c_{b_e}^f$ and $c_{b_e}^m$— affect not only b_e, but b_p^{in}, and to a lesser extent b_p^{out}. The particularly large sensitivity of b_p^{in} to $c_{b_e}^m$ (Figure 4.4e) confirms the existence of a link between b_p^{in} and the goal of reducing the energy component fee. The battery power costs $c_{b_p}^f$ have a lower impact on the battery capacity selection.

The sensitivity analyses depicted in Figures 4.3 reflect a scenario in which the only cost reduction possibility is the manipulation of the daily peaks. In this scenario, all battery components exhibit the largest sensitivity to changes in α. The dynamic tariff p4 introduces an additional cost reduction possibility. In the sensitivity analyses depicted in Figure 4.4, α is not any longer the dominant component. It is still the case for b_e, but not for b_p^{in} or b_p^{out}. This fact indicates that the peak and energy components come closer in importance. In general, the battery components are less sensitivity to changes in the parameters under tariff p4 than under the constant tariff p1.

4.3.3 Sensitivity to the Building's Parameters

This section explores the model's sensitivity to building parameters. The configuration parameters defining building b0 are summarized in Figure 4.1. The tornado plots in Figures 4.5 and 4.6 illustrate the model's sensitivity to some selected building's parameters under tariffs p1 and p4, respectively. The results presented in this section are to be read carefully, as some parameters have non-linear relations with quantities such as the thermal energy or the solar gains.

In general, the model is less sensitive to the building's parameters than it is to the exogenous parameters described in the previous section. The quantity UH, which is linearly related to the thermal energy and to the electricity consumption, has a larger impact on the PV size ϕ_p and on the battery input power b_p^{in}, both of them regarded as energy variables in the previous section. The energy variables and the transit energy are anti-correlated with the COP. On the other hand, the power variables, i.e. the battery capacity b_e and the battery output power b_p^{out}, are correlated with the COP.

Under tariff p4, most building parameters provoke positive changes on b_e, b_p^{in}, and ϕ_p, but negative changes on b_p^{out}. This fact indicates that the energy component acquires

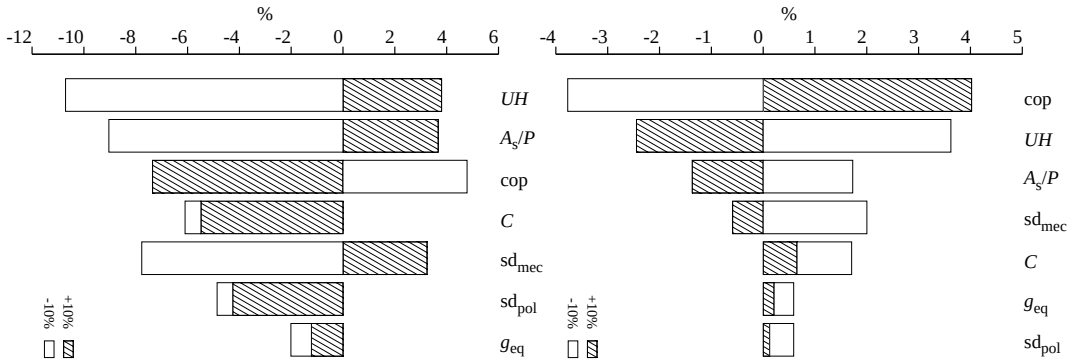

(a) Transit energy

(b) Average peak

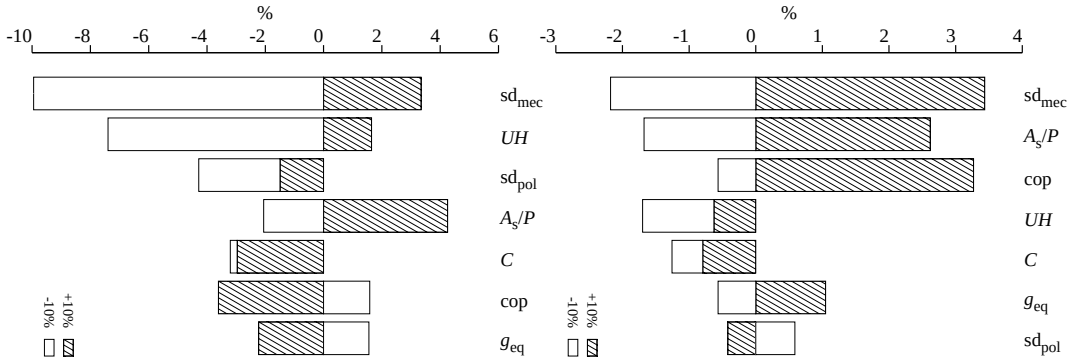

(c) PV peak power ϕ_p

(d) Battery energy capacity b_e

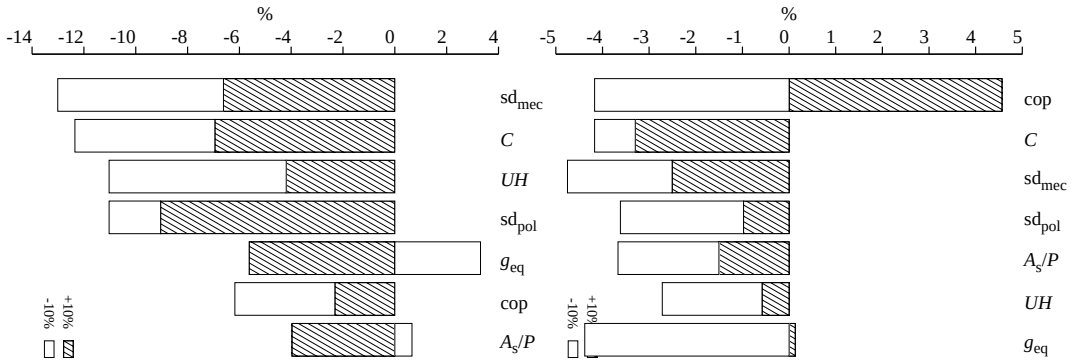

(e) Battery input power b_p^{in}

(f) Battery output power b_p^{out}

Figure 4.5: Sensitivity to the building's parameters for building b0 under tariff p1

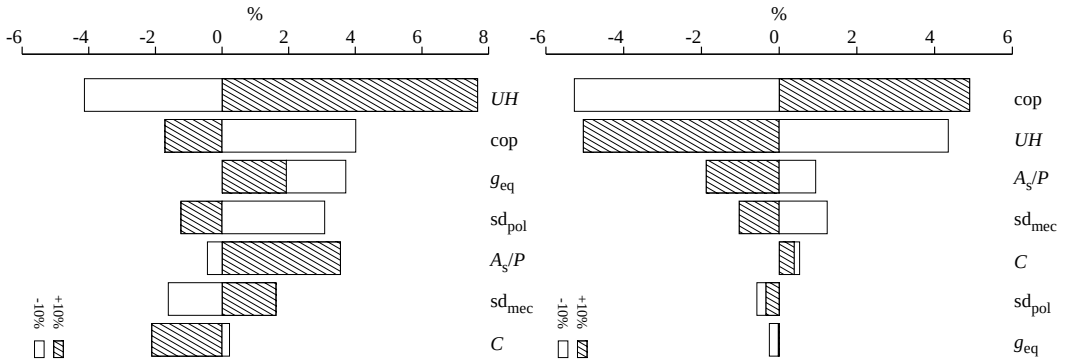

(a) Transit Energy

(b) Average peak

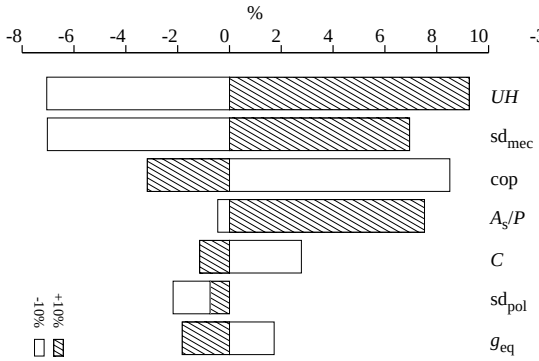

(c) PV peak power ϕ_p

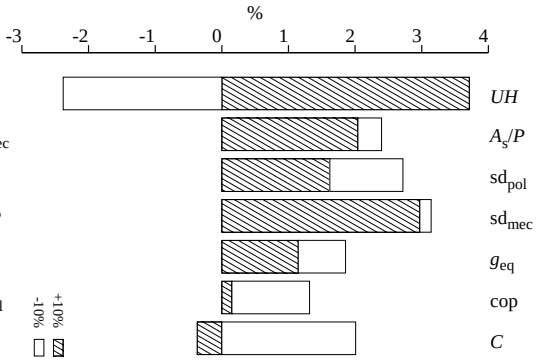

(d) Battery energy capacity b_e

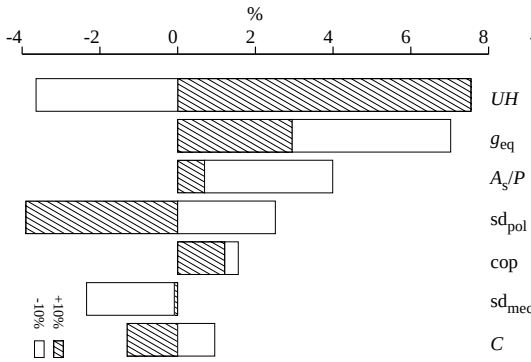

(e) Battery input power b_p^{in}

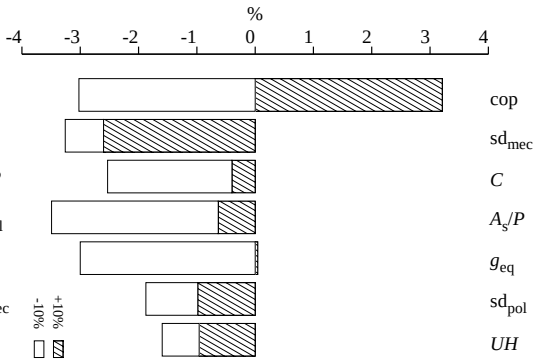

(f) Battery output power b_p^{out}

Figure 4.6: Sensitivity to the building's parameters for building b0 under tariff p4

relevance upon the peak component. This observation is corroborated by comparing the transit energy's sensitivities under both tariffs in Figures 4.3a and 4.4a, respectively.

Finally, Tables 4.4 and 4.5 provide extended results for different scenarios in which the building's parameters are varied with respect to the reference initial values summarized in Figure 4.1. The reference values and the corresponding results are highlighted at the tables' left and top, respectively. Two additional scenarios are included per each reference value. Each cell displays the relative variation between the corresponding scenario and the reference results.

	Ref	**Value**	b_e	b_p^{in}	b_p^{out}	ϕ_p	C	C_g	$C_g^{\max}$	**Trs**	$\overline{\textbf{peak}}$	f_{load}
Ref		—	4.9	0.9	3.7	3.5	6145.2	2319.1	2588.1	1483.9	4.7	0.4
cop	6	3.2	-28.6	-22.9	-20.5	-15.2	19.7	22.0	30.0	-65.8	31.8	13.8
		10	0.9	-11.2	0.5	-6.4	-12.5	-14.3	-17.5	11.4	-17.7	-9.0
U	5.6E-4	4.4E-4	-2.7	-7.2	-5.6	-7.3	-2.9	-2.4	-2.7	4.3	-2.3	-5.0
		8E-4	3.3	1.1	12.7	-9.4	6.8	6.7	9.2	-5.1	9.0	-1.9
loc	Zurich	Kloten	-4.8	-8.9	-4.1	-17.2	0.3	2.0	2.6	-9.0	2.9	0.3
A_s/P	40	30	4.0	2.6	5.9	1.5	3.4	3.8	3.1	-2.6	2.9	0.8
		50	-3.3	-5.5	3.0	-0.9	-2.0	-3.2	-1.5	-0.4	-1.4	-3.6
C	105	94.5	0.2	0.0	-1.8	-5.2	0.5	0.9	1.2	-0.1	1.5	2.3
		115.5	-1.0	-5.0	-3.4	-6.5	0.3	0.8	1.7	-6.2	1.8	0.3
sd_{pol}	0.4	0.6	-0.6	-11.3	-2.5	-5.8	0.4	1.1	1.4	-0.8	1.3	-7.8
		1.0	-0.4	-1.6	-0.3	-6.8	0.9	1.7	1.7	-1.8	1.6	0.5
sd_{mec}	0.8	0.6	2.8	-5.7	1.9	12.2	0.8	-0.5	-0.4	6.3	-0.8	-9.3
		0.1	-1.2	-12.7	-2.7	-17.7	-0.5	0.6	1.3	-7.0	1.7	1.8
g_{eq}	0.1	0.15	3.3	-0.3	0.5	9.2	-1.5	-4.1	-2.4	8.0	-3.0	-5.3
		0.2	0.3	2.4	1.4	17.0	-3.1	-7.5	-4.7	9.2	-5.5	-6.8
s_{dhw}	0	1	-6.4	-19.1	-4.5	-9.3	-4.3	-4.5	-2.6	-8.4	-2.6	-9.6
		2	4.5	13.6	7.6	5.8	3.7	3.5	3.0	0.5	3.2	1.3
s_{li}	1	0	10.5	-12.8	9.3	-19.7	11.3	11.9	14.9	4.1	15.2	-17.6
		2	25.3	-12.1	23.2	-28.4	22.0	20.9	27.1	13.3	27.2	-29.8
s_{ap}^{r}	0	1	-5.6	-14.4	-4.2	-17.3	-4.3	-3.1	-3.0	-9.5	-3.0	0.8
		2	5.2	-1.2	3.3	5.9	4.1	3.9	4.0	8.2	4.0	-3.3
s_{ap}^{k}	0	1	-20.9	-17.1	-9.4	-30.7	-15.2	-13.4	-13.8	-38.5	-13.2	7.4
		2	13.1	14.7	15.7	19.3	11.4	10.3	9.8	21.5	10.0	-13.3

Table 4.4: Per cent variation on the model's outcome for different building b0 parameter scenarios under tariff p1. C is the total cost, C_g is the energy component fee, $C_g^{\max}$ is the peak component fee, Trs is the transit energy, $\overline{\text{peak}}$ is the average peak, and f_{load} is the load factor. Highlighted values on the left are the reference parameters, and highlighted values on top are the model results under the reference parameters. All other values are percentages. Location Kloten has values hdd=3678 and cdd=98.

	Ref	**Value**	b_e	b_p^{in}	b_p^{out}	ϕ_p	C	C_g	C_g^{max}	**Trs**	$\overline{\textbf{peak}}$	f_{load}
Ref		—	6.0	1.2	4.2	4.0	6525.1	2539.9	2401.5	3063.5	4.3	0.4
cop	6	3.2	-34.1	-15.1	-22.4	-11.2	18.3	19.2	32.6	-32.0	34.6	0.5
		10	5.2	-1.6	4.0	-4.9	-12.6	-14.9	-22.7	7.9	-23.2	-6.9
U	5.6E-4	4.4E-4	0.9	0.8	-2.7	1.1	-2.7	-3.1	-4.9	4.7	-4.6	-8.0
		8E-4	0.8	8.8	11.7	-6.8	6.3	5.2	9.8	2.4	9.5	-4.1
loc	Zurich	Kloten	-3.8	-5.7	-3.0	-14.2	0.4	2.2	2.6	-5.4	2.9	2.2
A_s/P	40	30	2.5	7.8	4.7	3.9	2.9	2.0	3.2	3.1	3.1	-1.3
		50	2.3	4.6	7.7	6.2	-1.7	-3.5	-4.6	5.4	-4.9	-6.6
C	105	94.5	2.1	7.3	-0.6	-0.1	0.3	-0.5	0.1	4.2	0.3	0.7
		115.5	0.0	-3.5	-2.7	-2.7	0.4	0.9	1.5	-2.8	1.4	-1.3
sd_{pol}	0.4	0.6	-0.6	-0.9	-1.5	-2.0	0.7	1.3	1.1	-0.3	0.9	-6.1
		1.0	1.0	1.5	0.9	-3.3	1.0	1.7	1.0	0.4	0.8	-5.8
sd_{mec}	0.8	0.6	4.6	3.5	3.0	19.5	1.0	-1.3	-2.1	5.6	-2.8	-16.1
		0.1	-2.6	-4.6	-4.1	-15.9	-0.7	0.4	1.8	-4.8	2.3	0.5
g_{eq}	0.1	0.15	7.4	6.2	2.0	17.0	-1.0	-4.5	-5.3	8.7	-6.5	-4.4
		0.2	6.2	7.2	5.3	22.5	-2.7	-8.2	-8.6	10.8	-10.0	-6.1
s_{dhw}	0	1	1.8	-0.4	1.2	2.8	-3.6	-4.8	-6.3	2.4	-6.9	-7.5
		2	1.2	11.6	4.0	7.8	3.0	1.2	4.0	2.7	4.4	-6.6
s_{li}	1	0	15.3	3.1	12.9	-8.0	11.6	11.9	13.3	12.1	13.6	-10.4
		2	30.5	10.0	27.8	-10.9	22.5	21.4	25.0	23.5	25.1	-21.8
s_{ap}^{r}	0	1	-7.0	-9.4	-3.9	-14.2	-4.4	-3.7	-2.7	-8.8	-2.7	-2.0
		2	5.3	2.9	3.3	11.6	4.5	3.9	3.5	6.8	3.3	-4.4
s_{ap}^{k}	0	1	-25.7	-17.2	-12.4	-31.7	-16.1	-15.3	-12.0	-27.4	-11.3	0.2
		2	17.1	20.5	17.1	22.9	11.5	9.6	7.4	21.7	7.2	-3.1

Table 4.5: Per cent variation on the model's outcome for different building b0 parameter scenarios under tariff p4. C is the total cost, C_g is the energy component fee, C_g^{max} is the peak component fee, Trs is the transit energy, $\overline{\text{peak}}$ is the average peak, and f_{load} is the load factor. Highlighted values on the left are the reference parameters, and highlighted values on top are the model results under the reference parameters. All other values are percentages. Location Kloten has values hdd=3678 and cdd=98.

4.3.4 Battery and PV Cost Scenarios

In order to study the model's response to the developments in the battery and PV costs, we formulate 5 PV and 28 battery cost scenarios. The 28 battery cost scenarios correspond to the combinations between 7 battery capacity and 4 battery power scenarios. The battery power cost c_p^k is assumed to be a percentage of the battery energy cost c_e^k as follows: $c_p^k \in \{0.3, 0.4, 0.5, 0.6\} \cdot \xi \cdot c_e^k\,[€/\text{kW}]$. These costs are based on the values presented in Table 2.3 on page 31. This section is concerned with the description of the technical results, while Section 4.3.5 is dedicated to describe the different investment shares.

For Li-ion batteries, the efficiency —b_{η_c} and b_{η_d}— and the maximum number of cycles γ are assumed to increase linearly as a function of the cost, i.e. the higher the cost, the closer the efficiency to 1.0 and the higher γ. The assumed functions are $b_{\eta_c} = b_{\eta_d} = 7.5 \times 10^{-5} c_e^k + 0.88$ and $\gamma = 12.5 c_e^k + 1250$, respectively.

Figures 4.7 and 4.8 summarize the results for the scenarios with variable battery c_e^k and constant PV c_ϕ^k costs under tariffs p1 and p4, respectively. The different lines represent the power cost scenarios. As expected, the PV size ϕ_p and the battery capacity b_e increase with decreasing c_e^k. However, it is interesting to notice that the ratio ϕ_p/b_e decreases with decreasing c_e^k. The same occurs for the ratio between the battery output power and energy capacity b_p^{out}/b_e. These two ratios are approximately equal, and decrease in favor of the ratio between the battery input power and energy capacity b_p^{in}/b_e. The latter ratio moderately increases with decreasing c_e^k. The cost of the peripherals c_p^k seems to have only a marginal impact on those ratios. The quotients ϕ_p/b_e and b_p^{out}/b_e are larger under tariff p1, and b_p^{in}/b_e is larger under tariff p4.

The transit energy per kWh of installed capacity is more than double under the p4 than under the p1 tariff, except for the lowest c_e^k values. These results clearly indicate that the energy component acquires importance with respect to the peak component, i.e. that besides the peak reduction, it is also possible to attain a profit by shifting energy between regions of high and low prices. The transit energy increases linearly with increasing c_e^k in the p1 case, and has a concave form in the p4 case.

Figure 4.9 illustrate the results for the scenarios with constant battery —c_e^k and c_p^k— and variable PV c_ϕ^k costs under tariffs p1 and p4. The b_e/ϕ_p, b_p^{out}/ϕ_p, and b_p^{in}/ϕ_p ratios decrease with decreasing c_ϕ^k, though the decrease in b_p^{in}/ϕ_p is comparatively smaller. This behavior is analogous to the one observed for ratios ϕ_p/b_e, b_p^{out}/b_e, and b_p^{in}/b_e in the experiments with variable battery costs.

Finally, Figure 4.10 depicts the load factors f_{load} for the different battery and PV cost scenarios. The increment in f_{load} is larger under tariff p4, in part due to the larger peak reduction, but also due to the increasing importance of the energy component. On the other hand, f_{load} factors decrease with decreasing PV cost. This fact indicates that despite the average peak reduction, the standard deviation in the consumption increases, i.e. the difference between the mean and maximum values grows larger.

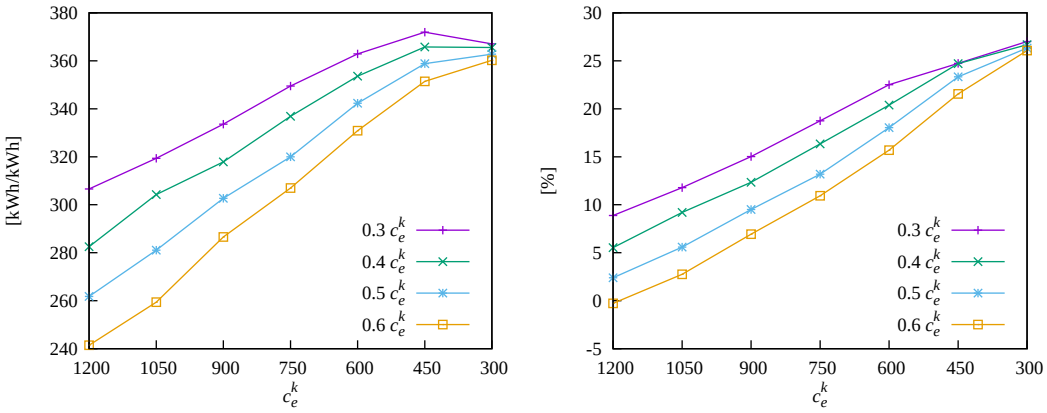

(a) Transit energy/b_e

(b) Peak reduction

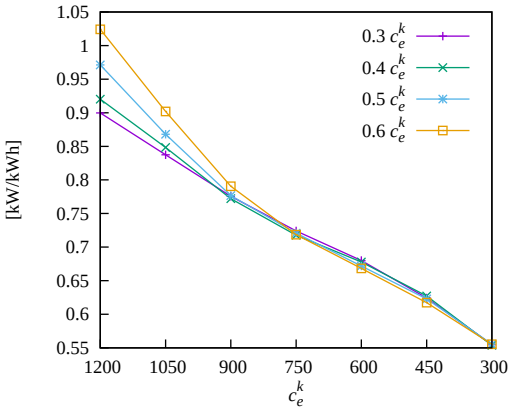

(c) PV peak power ϕ_p/b_e

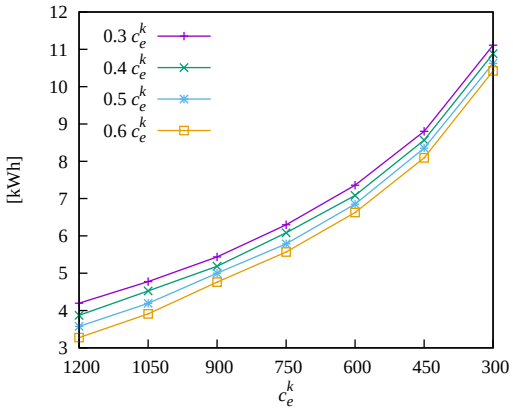

(d) Battery energy capacity b_e

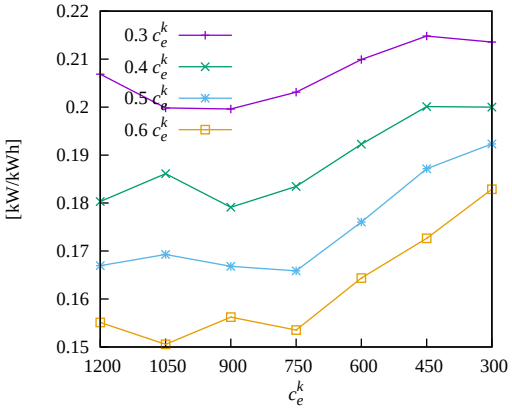

(e) Battery input power b_p^{in}/b_e

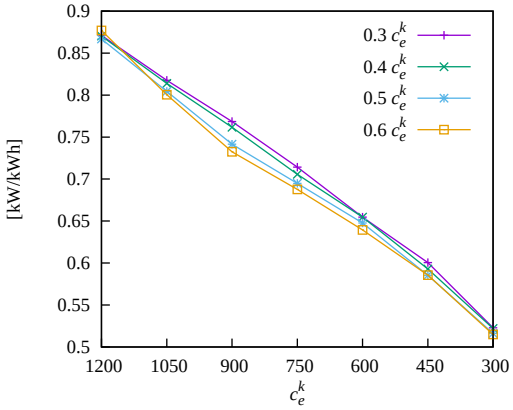

(f) Battery output power b_p^{out}/b_e

Figure 4.7: Battery cost (c_e^k) scenarios for building b0 under tariff p1. Each line represent a power cost (c_p^k) scenario, assumed proportional to c_e^k. Some quantities are normalized to the battery capacity b_e and expressed in kW/kWh or kWh/kWh. PV costs are kept constant, $c_\phi^k = 1400$ €/kW.

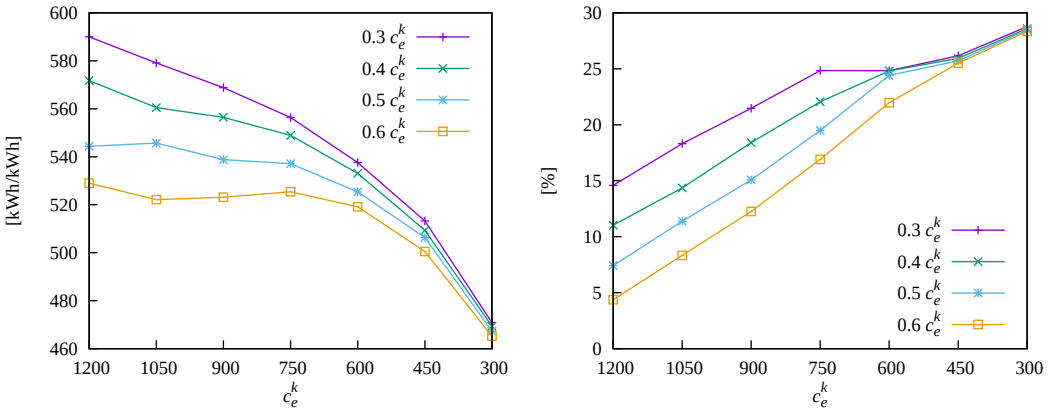

(a) Transit Energy/b_e

(b) Peak reduction

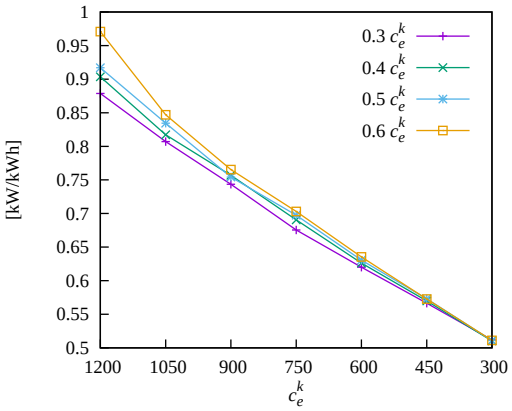

(c) PV peak power ϕ_p/b_e

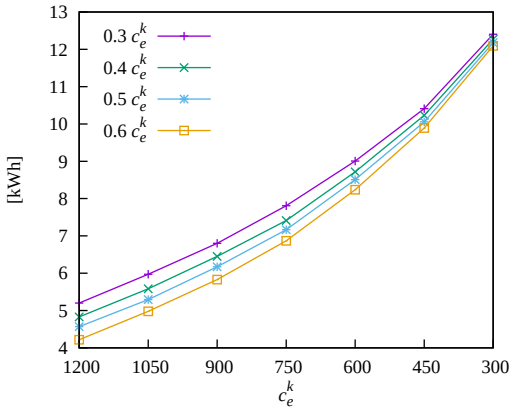

(d) Battery energy capacity b_e

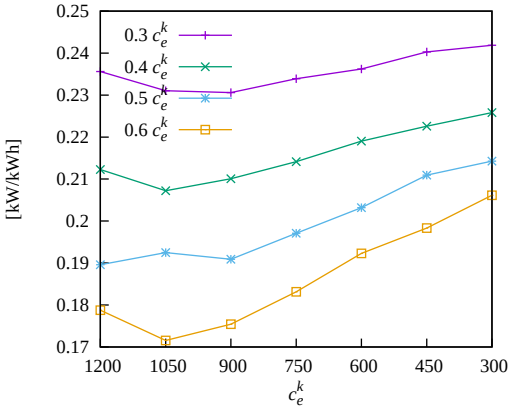

(e) Battery input power b_p^{in}/b_e

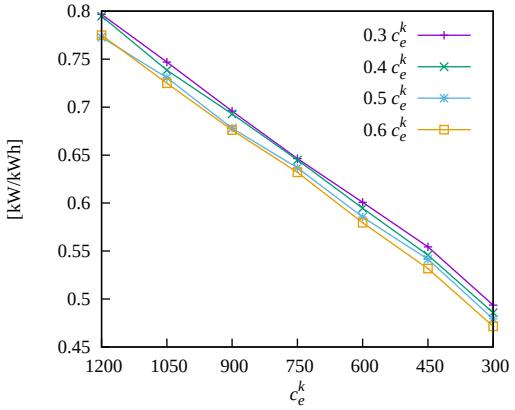

(f) Battery output power b_p^{out}/b_e

Figure 4.8: Battery cost (c_e^k) scenarios for building b0 under tariff p4. Each line represent a power cost (c_p^k) scenario, assumed proportional to c_e^k. Some quantities are normalized to the battery capacity b_e and expressed in kW/kWh or kWh/kWh. PV costs are kept constant, $c_\phi^k = 1400$ €/kW.

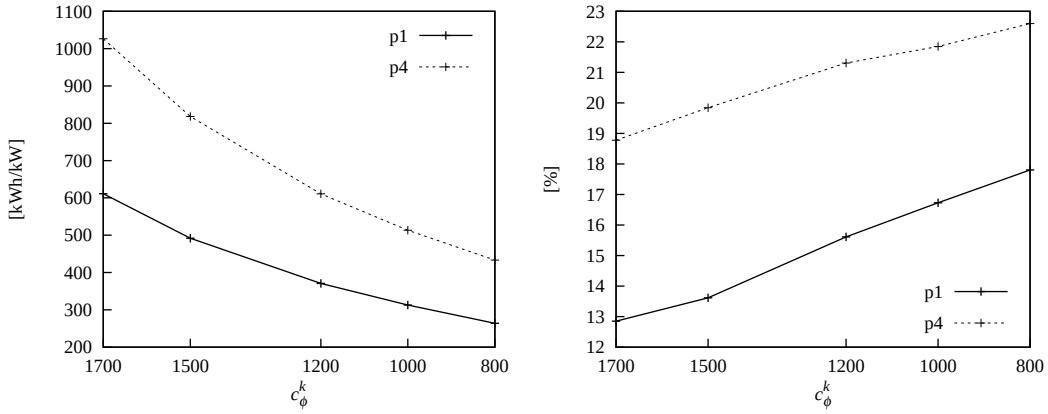

(a) Transit Energy/ϕ_p

(b) Peak reduction

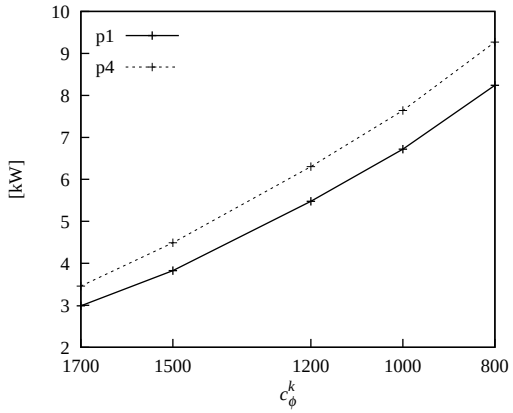

(c) PV peak power ϕ_p

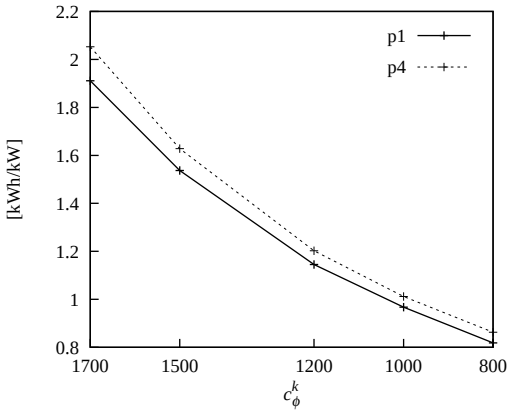

(d) Battery energy capacity b_e/ϕ_p

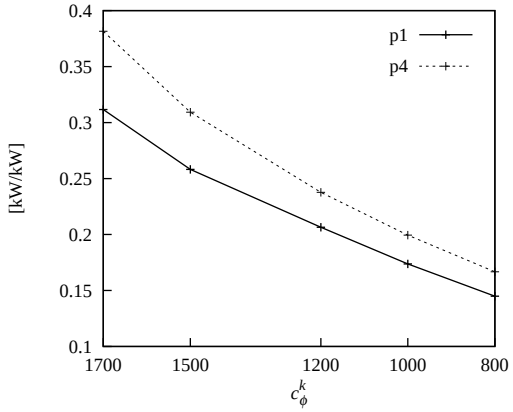

(e) Battery input power b_p^{in}/ϕ_p

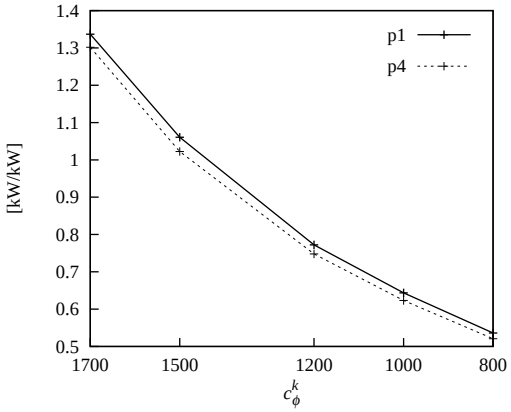

(f) Battery output power b_p^{out}/ϕ_p

Figure 4.9: PV cost (c^k_ϕ) scenarios for building b0 under tariffs p1 and p4. Some quantities are normalized to the PV capacity ϕ_p and expressed in kW/kW or kWh/kW. Battery costs are kept constant, $c^k_e = 650$ €/kWh and $c^k_p = 315$ €/kW.

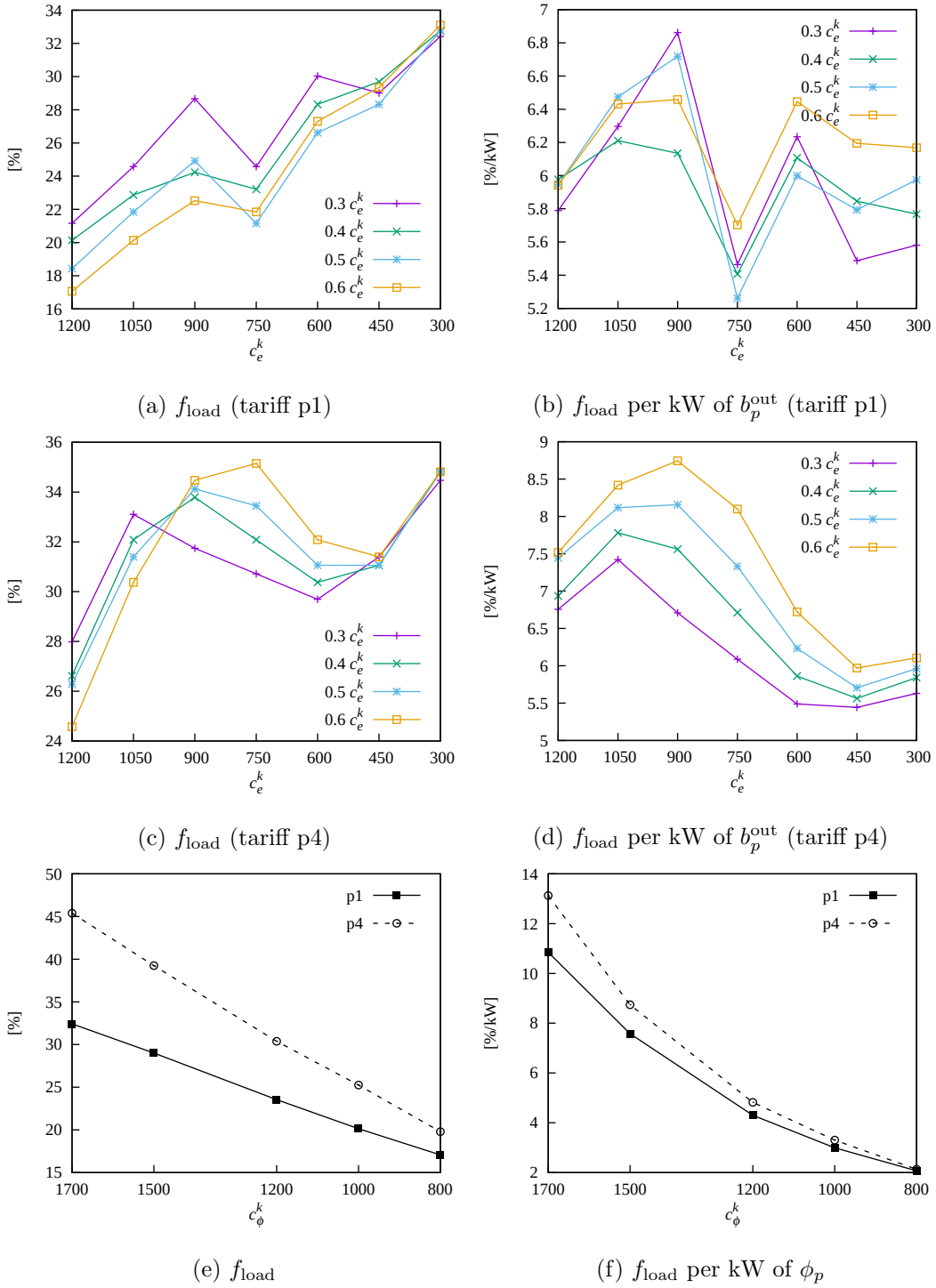

(a) f_{load} (tariff p1)

(b) f_{load} per kW of b_p^{out} (tariff p1)

(c) f_{load} (tariff p4)

(d) f_{load} per kW of b_p^{out} (tariff p4)

(e) f_{load}

(f) f_{load} per kW of ϕ_p

Figure 4.10: Per cent change in the load factor f_{load} as a function of the battery costs (4 upper plots) and PV costs (2 lower plots), for building b0 under tariffs p1 and p4. The different lines in the upper plots represent different scenarios of power cost c_p^k. In the lower plots, the different lines represent the two tariffs.

4.3.5 Investment Shares

This section is devoted to the analysis of the different investment shares incurred by a user facing the cost scenarios enunciated at the beginning of Section 4.3.4. This section analyses both battery and PV cost development scenarios, and concludes with a comparison between different battery technologies.

Figures 4.11 and 4.12 depict the investment shares incurred throughout the battery cost scenarios under tariffs p1 and p4, respectively. Analogously, Figure 4.13 illustrates the case of constant battery and varying PV costs. C_g and $\mathrm{C}_g^{\max}$ reflect the total cost of electricity: energy and power components, respectively. $\mathrm{C}_{b,e}^{m}$ is the total cost paid for storing energy, i.e. the total marginal cost of storage, $\mathrm{C}_{b,e}^{f}$ is the investment in storage capacity, $\mathrm{C}_{b,p}^{\mathrm{in}}$ is the investment in input power, $\mathrm{C}_{b,p}^{\mathrm{out}}$ is the investment in output power, and C_ϕ is the investment in PV. Strictly speaking, C_g and $\mathrm{C}_g^{\max}$ are not investments, but the electricity fee that the users incur. This electricity fee is referred to as an investment and displayed together with the other shares for comparison purposes.

It is interesting to notice that for the whole range of battery costs c_e^k the optimum investment consist of a more or less constant share of battery-related costs, around 15% for the p1, and around 20% for the p4 case, plus a PV investment amount that is inversely proportional to c_e^k. Figure 4.13 shows that in the scenarios with constant battery and varying PV costs, both the investment in battery and PV elements are inversely proportional to the PV cost c_ϕ^k.

In all scenarios, $\mathrm{C}_{b,p}^{\mathrm{in}}$ claims the lowest share and remains more or less constant. Throughout the battery cost scenarios, the investments in battery capacity $\mathrm{C}_{b,e}^{f}$ and in battery output power $\mathrm{C}_{b,p}^{\mathrm{out}}$ decrease with decreasing c_e^k, while the investment in transit energy $\mathrm{C}_{b,e}^{m}$, associated with the marginal cost of storage, increases. This fact is in line with the increment in the PV capacity and the fact that at lower costs the energy component comes closer in importance to the peak component. In the variable battery cost scenarios, investments are larger, both in absolute and per cent figures under tariff p4.

In the scenarios with variable PV costs, illustrated in Figure 4.13, the battery and PV investment percentages are similar between the two tariffs, but $\mathrm{C}_{b,e}^{m}$ is larger under p4, signaling that the energy component acquires more relevance than the peak one.

Regarding the fee paid for the energy component C_g, it can be observed that it is more or less constant for the variable battery cost scenarios, while the fee paid for the peak $\mathrm{C}_g^{\max}$ decreases with decreasing c_e^k. On the other hand, when c_e^k is kept constant and c_ϕ^k changes, it is $\mathrm{C}_g^{\max}$ that remains constant, while C_g decreases with decreasing c_ϕ^k. This fact confirms that the dimension of the PV element is associated with the objective of reducing the electricity consumption, while the dimension of the battery, at least the capacity and the output power, is associated with the objective of reducing the average peak.

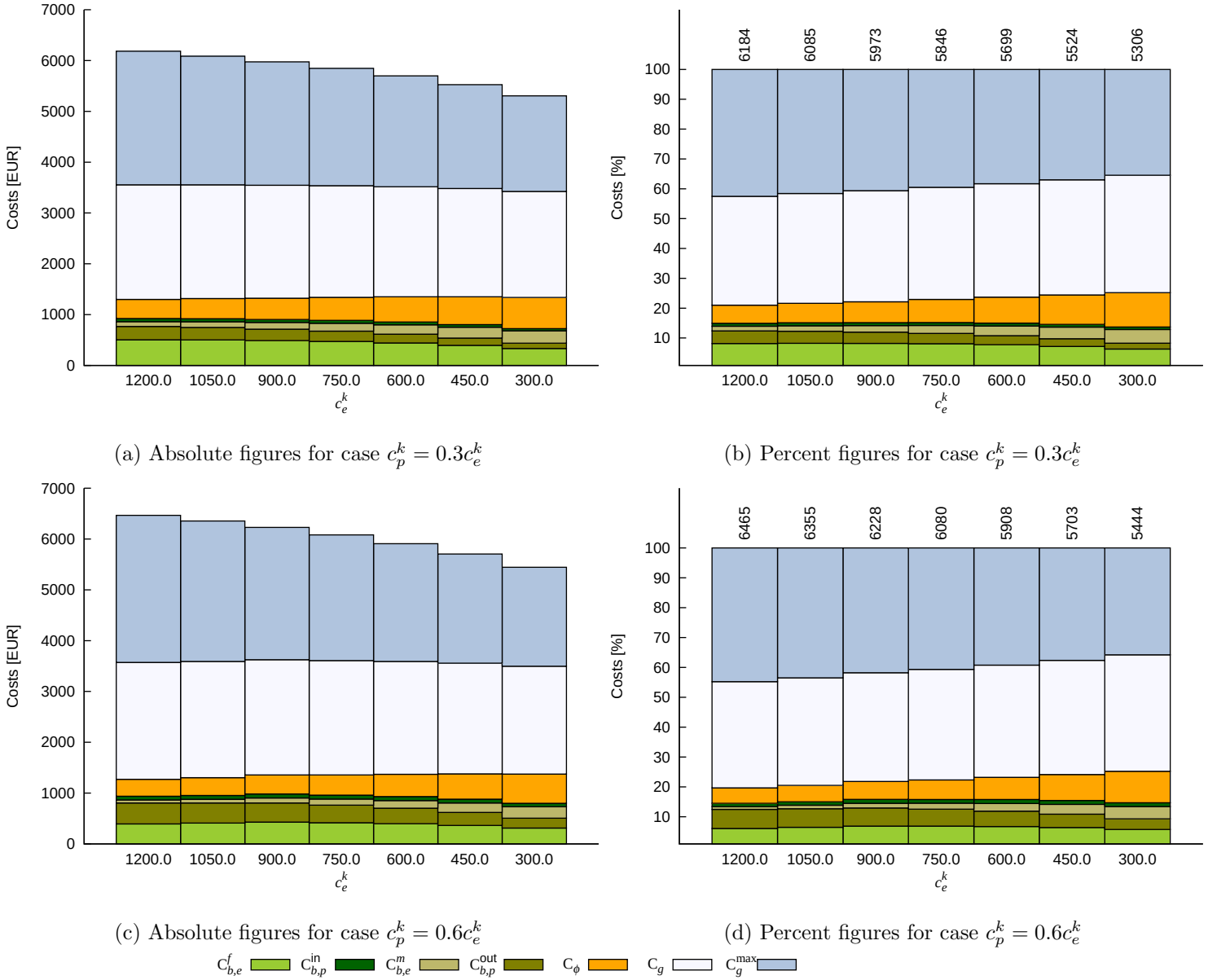

(a) Absolute figures for case $c_p^k = 0.3c_e^k$

(b) Percent figures for case $c_p^k = 0.3c_e^k$

(c) Absolute figures for case $c_p^k = 0.6c_e^k$

(d) Percent figures for case $c_p^k = 0.6c_e^k$

Figure 4.11: Investments as a function of the battery capacity cost c_e^k for building b0 under tariff p1. Numbers on top of the bars are the total cost in €.

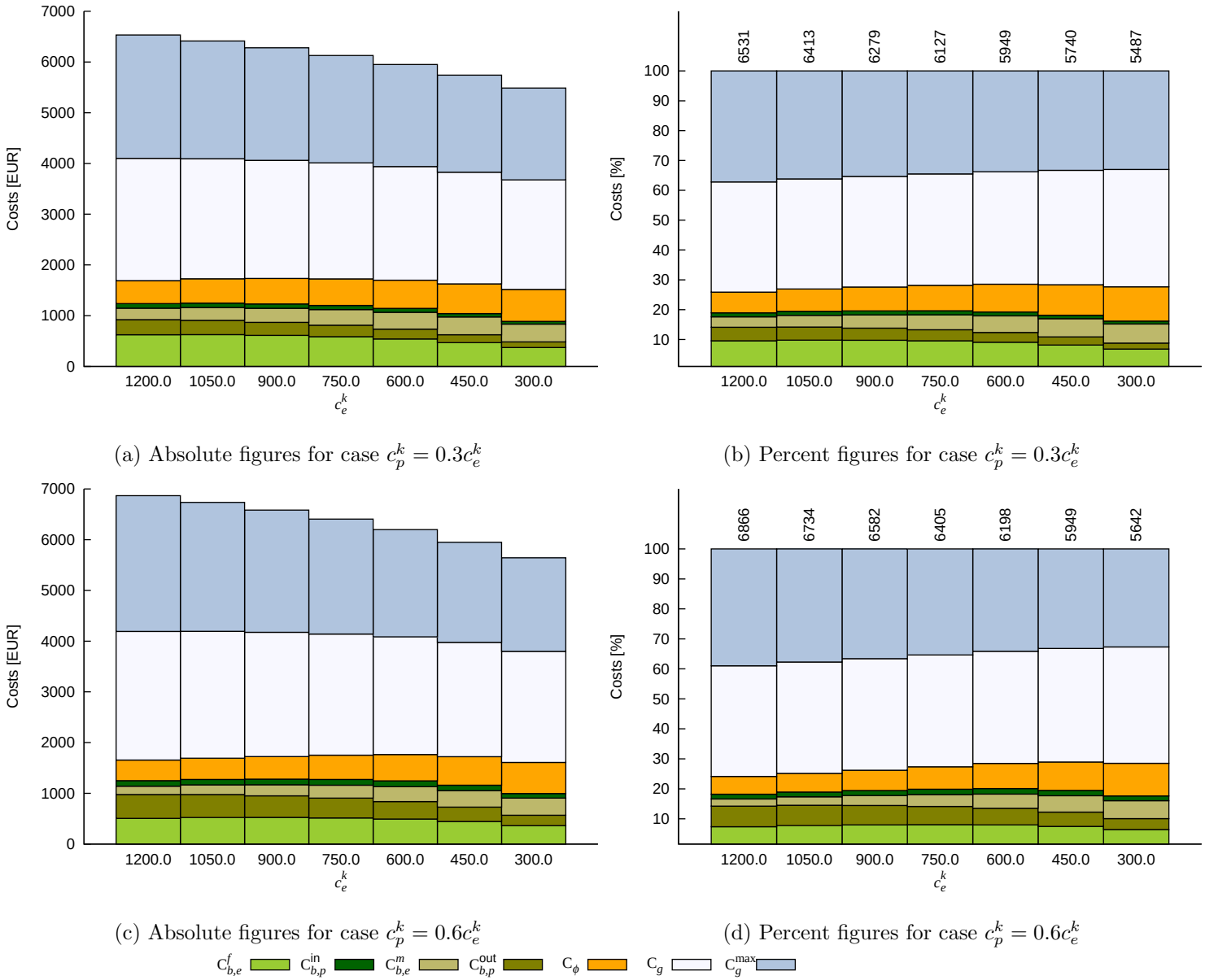

(a) Absolute figures for case $c_p^k = 0.3c_e^k$

(b) Percent figures for case $c_p^k = 0.3c_e^k$

(c) Absolute figures for case $c_p^k = 0.6c_e^k$

(d) Percent figures for case $c_p^k = 0.6c_e^k$

Figure 4.12: Investments as a function of the battery capacity cost c_e^k for building b0 under tariff p4. Numbers on top of the bars are the total cost in €.

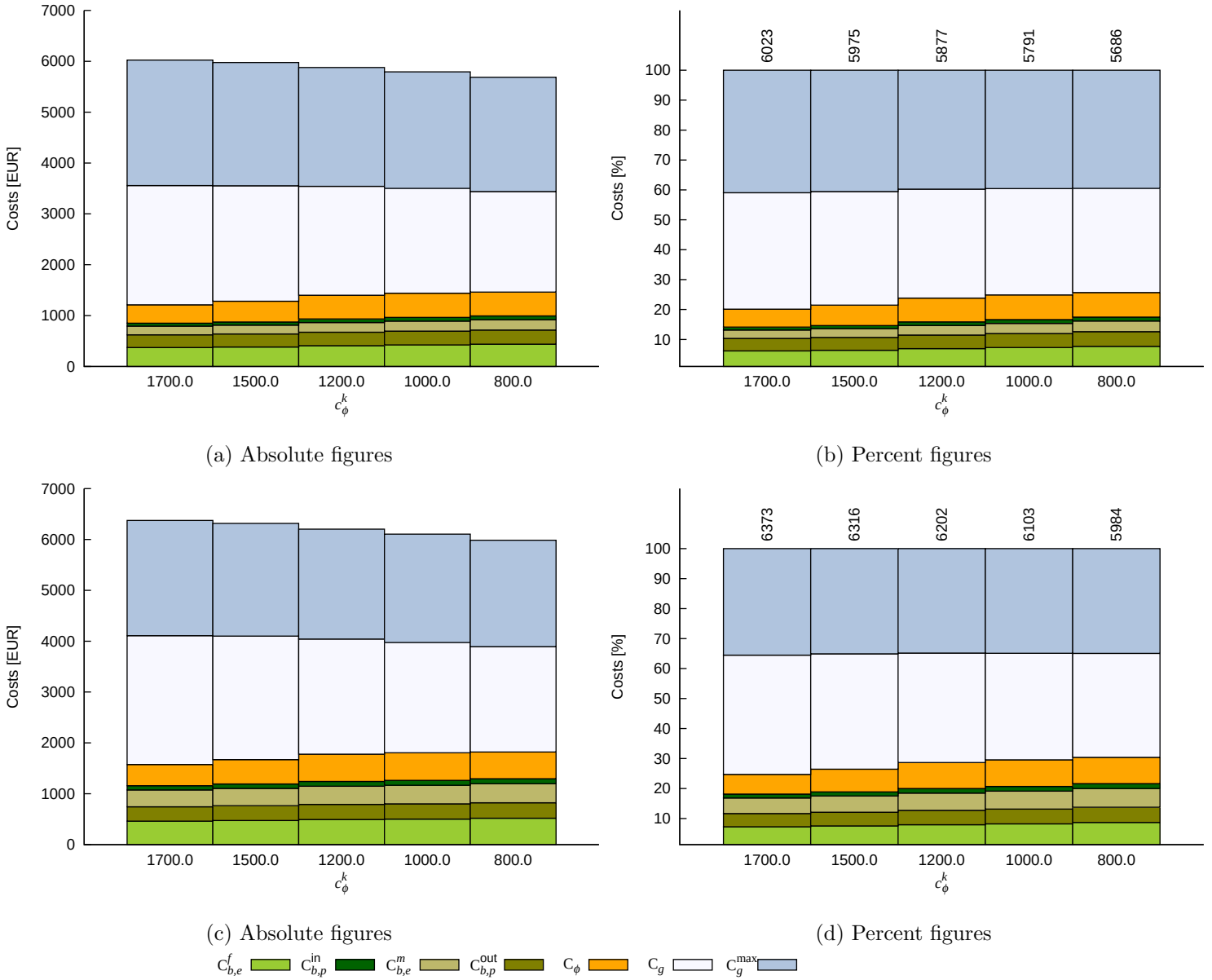

(a) Absolute figures

(b) Percent figures

(c) Absolute figures

(d) Percent figures

Figure 4.13: Investments as a function of the PV cost c_ϕ^k for building b0 under tariffs p1 (upper plots) and p4 (lower plots). Numbers on top of the bars are the total cost in €.

Comparison Between Different Battery Technologies

The analysis on the impact of the battery costs on the model's outcome concludes with a comparison between different battery technologies. Table 4.6 summarizes the results for different model runs corresponding to the costs defined in Table 2.3 on page 31. The PV cost is kept constant at $c_{\phi}^{k} = 1400\,€/\text{kW}$.

Results are ranked according to the total cost C. For the constant tariff p1 case, the largest costs correspond to the "Ni-Cd average", "Li-ion average", and "Ni-Cd best" scenarios, respectively, which are the most expensive technologies. These scenarios feature, additionally, the largest peak component fee $\text{C}_{g}^{\max}$ and the lowest load factors f_{load}. Lead acid is the most competitive technology, mainly due to the profit possibilities offered by the large peak reduction. This fact is clearly reflected in the largest f_{load} factors, resulting from the comparatively larger battery capacities. The greatest PV investment C_{ϕ} corresponds as well to the lead acid technology scenarios. The relatively high PV value is linked to the high battery capacity b_e and transit energy.

The results are similar for the p4 tariff. The biggest average peak reduction is achieved by the "Lead best" technology, but the larger load factors correspond to the "Lead average" and "Ni-Cd best" scenarios.

4.4 Computational Details

All optimizations ran on an 8-core Intel(R) Core(TM) i7-3720QM computer. Each processor core clocks at 2.60GHz. The system has 8Gb of RAM and runs on the GNU/Linux (kernel 3.x.) operating system.

The stochastic LP was implemented in GAMS [15], using the EMP solver facilities [45]. The analysis period of each LP is 1-year, with hourly resolution. The stochastic version includes 10 different realizations of the electrical load. The average time per each stochastic run was 90s. For comparison purposes, the deterministic equivalent (comprising one single scenario) is executed in 4.4s.

4.5 Summary and Conclusions

This chapter introduced a stochastic LP, aimed at determining the optimal investment in DSE and PV incurred by a user facing a demand-based electricity tariff. The demand-based tariff explicitly penalizes both the total energy consumed and the maximum power on a daily basis. The daily peaks are a mapping of the grid utilization component, i.e. the network costs that final consumers pay. The mapping between these two components is not exact, but is an acceptable approximation. For instance, for the 3000 buildings used to model the aggregate load level, the average error in this approximation was found to be +5%.

Scenario	b_e	b_p^{in}	b_p^{out}	ϕ_p	C	C_g	$C_g^{\max}$	$C_{b,e}^{f}$	$C_{b,e}^{m}$	$C_{b,p}^{\text{in}}$	$C_{b,p}^{\text{out}}$	C_ϕ	**Trs**	$\overline{\textbf{peak}}$	f_{load}
Tariff p1															
Ni-Cd average	5.7	1.4	3.6	4.1	6118.8	2364.6	2727.9	316.7	121.3	51.7	127.8	408.6	1655.3	5.0	0.36
Li-ion average	5.8	1.0	4.1	3.7	5982.9	2300.7	2437.9	377.6	174.6	63.8	255.9	372.3	1879.7	4.4	0.38
Ni-Cd best	8.3	2.1	4.5	5.2	5789.5	2322.3	2349.0	331.0	114.1	50.5	109.1	513.5	2851.9	4.2	0.39
Lead average	10.2	1.8	4.9	5.2	5578.4	2265.0	2098.9	177.8	285.0	63.9	171.5	516.1	3421.8	3.8	0.40
Li-ion best	12.4	2.4	6.1	5.5	5204.8	2137.0	1789.3	372.7	135.5	62.4	157.8	550.2	4516.2	3.2	0.40
Lead best	19.4	3.3	6.2	7.0	5103.2	2126.7	1659.1	194.5	191.2	78.2	148.5	704.9	5740.9	2.9	0.42
Tariff p4															
Ni-Cd average	7.3	1.7	4.1	4.6	6516.7	2727.1	2526.9	402.4	196.9	62.6	146.3	454.4	2687.0	4.6	0.40
Li-ion average	7.3	1.4	4.6	4.4	6322.7	2458.1	2226.1	475.4	343.8	90.1	289.7	439.4	3701.3	4.0	0.41
Ni-Cd best	10.6	2.7	5.2	5.6	6081.1	2599.4	2149.1	425.2	165.4	64.0	125.3	552.9	4134.0	3.8	0.43
Lead average	13.0	2.4	5.4	5.6	5828.5	2430.2	1923.3	227.6	414.5	83.6	190.5	558.8	4976.3	3.4	0.43
Li-ion best	12.6	3.0	6.1	5.6	5298.3	2133.4	1782.7	378.8	211.9	78.6	158.5	554.3	7065.2	3.1	0.41
Lead best	20.2	3.7	6.1	7.1	5249.6	2200.3	1674.5	201.9	225.4	89.5	147.3	710.5	6769.1	2.9	0.42

Table 4.6: Model evaluation for building b0 and different battery technologies. These technologies are described in Table 2.3 on page 31. All costs and investments are given in €. C is the total cost, C_g is the energy component fee, $C_g^{\max}$ is the peak component fee, $C_{b,e}^{m}$ is the total cost paid for storing energy, $C_{b,e}^{f}$ is the investment in storage capacity, $C_{b,p}^{\text{in}}$ is the investment in input power, $C_{b,p}^{\text{out}}$ is the investment in output power, C_ϕ is the investment in PV, Trs is the transit energy, $\overline{\text{peak}}$ is the average peak, and f_{load} is the load factor.

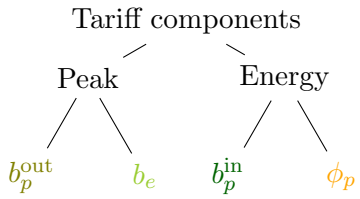

Figure 4.14: Relation between the electrical tariff components and the model variables

The model described in this chapter is linear; consequently, superposition techniques like the OAT methodology can be applied to analyse the model's sensitivity. Additionally, as a further consequence of the model's linearity, changing the costs is equivalent to changing the electricity prices, provided that the ratio between costs and prices remains constant. Throughout the experiments presented in this chapter the mean value of the electricity prices was kept constant.

The model was alternately evaluated under two electricity tariffs, a constant tariff p1, and a 4-level tariff p4. The constant tariff p1 constitutes a base scenario for comparison purposes. It allows studying separately the daily peak component in the demand-based tariff, i.e. illustrating the efficiency of the proposed pricing policy. Tariff p4 is used to illustrate an additional profit possibility; namely, the possibility to reduce the energy component costs. This variability in the price's energy component can also be viewed as an additional control mechanism serving the retailer's profit objectives.

The retailer's ultimate goal is to have the ability to peak-shave the aggregate load level. This objective was measured by means of the load factor metrics f_{load}. It was found that load factors are larger under tariff p4, in part due to the larger peak reduction, but also due to the increasing importance of the energy component in the final equilibrium. Load factors were found to decrease with decreasing PV cost, which indicates that despite the average peak reduction, the difference between the mean and maximum values grows larger with increasing PV size.

The various experiments and analyses were designed bearing in mind the following recurrent questions. The subsequent discussion elaborates on the answers.

1. *What is the optimal investment in batteries and PV in low exergy (lowEx) residential buildings?*

2. *Is the dimension of a battery element affected by the available on-site generation?*

3. *Is the idea of deploying DSEs in line with a massive deployment of rooftop PV? Does it pursue overlapping, complementary, or contradictory objectives?*

From the sensitivity analysis and model evaluation results, it can be conjectured that the different dimension variables can be classified as depicted in Figure 4.14. The battery

energy capacity b_e and output power b_p^{out} were found to be mainly related to the peak reduction objective. Similarly, the battery input power b_p^{in} and the PV power ϕ_p were found to be mainly related to the electricity cost reduction objective. The PV power ϕ_p was found to be the most sensitive variable in the model. There exists a significant influence of the PV cost c_ϕ^k upon the battery input power b_p^{in}, but the influence of the battery costs upon ϕ_p is comparatively smaller.

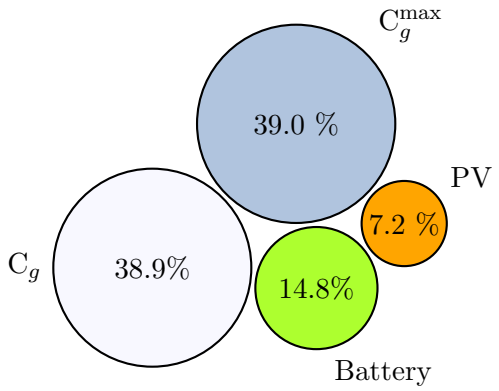

(a) Investment shares, p1

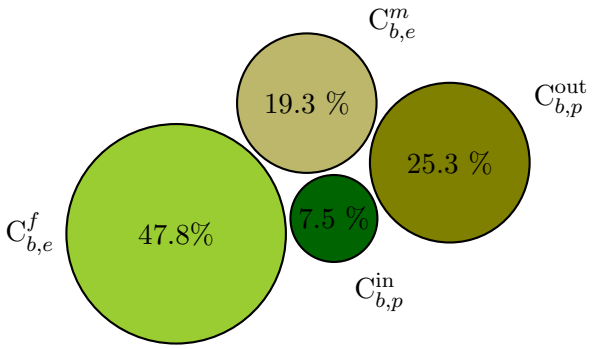

(b) Battery shares, p1

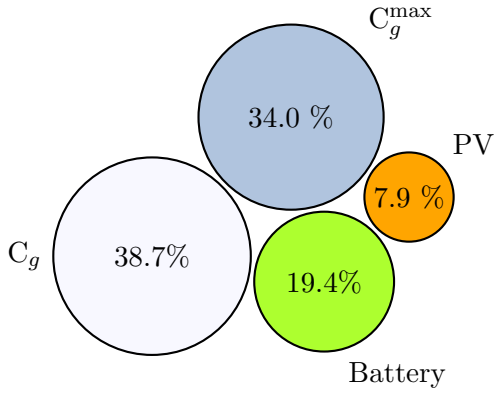

(c) Investment shares, p4

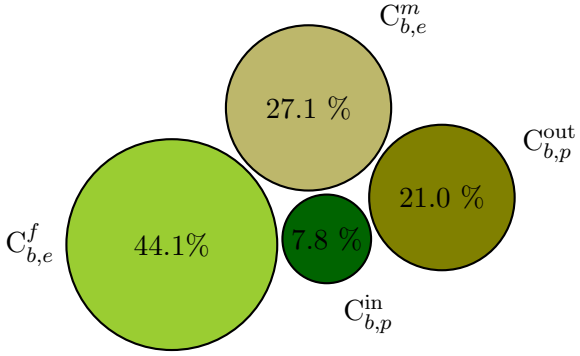

(d) Battery shares, p4

Figure 4.15: Investment shares (left) and battery shares (right) for a reference building and average battery costs ($c_e^k = 600$, $c_p^k = 240$, and $c_\phi^k = 1400$). Upper plots correspond to the constant tariff p1 and lower plots to the 4-level tariff p4. Figures on the right are the split of the battery component within the investment shares. C_g is the energy component fee, $C_g^{\max}$ is the peak component fee, $C_{b,e}^m$ is the total cost paid for storing energy, $C_{b,e}^f$ is the investment in storage capacity, $C_{b,p}^{\text{in}}$ is the investment in input power, and $C_{b,p}^{\text{out}}$ is the investment in output power.

Figure 4.15 exemplifies the investment shares structure for an average cost scenario ($c_e^k = 600$, $c_p^k = 240$, and $c_\phi^k = 1400$). Figures 4.15a and 4.15c represent the investment shares incurred under tariffs p1 and p4, respectively. By comparing these two figures, it

can be inferred that the p4 tariff increases the importance of the energy component, i.e. the peak component fee $C_g^{\max}$ decreases in favor of the battery and PV investments.

The most important observation derived from the investment experiments is that the retailer's profit decreases by the same amount that users invest in battery and PV. The overall investment in battery and PV, besides giving users the possibility to reduce costs, offers the retailer the possibility to control the aggregate load. The main underlying assumption in this dissertation is that the benefit that the retailer can obtain from the ability to control the load is larger than the profit reduction in the sale of electricity. This assumption is further analysed in Chapter 5.

Another important observation is that it is necessary to invest both in batteries and PV, as there is an interplay between the two elements. Nevertheless, the battery component is more than twice as large than the PV one in the investment shares.

From the p1 tariff results in Figure 4.15, where the only control that users have is the possibility to reduce the daily peaks, it can be observed than the solution to the problem is an equilibrium between the energy and peak fees: $C_g \approx C_g^{\max}$. The investment in battery and PV are the minimum necessary shares to achieve this equilibrium. This equilibrium was found to have different forms in different experiments. In the scenarios with variable battery costs, the cost associated with the energy component fee C_g is approximately constant, while the cost associated with the peak component fee $C_g^{\max}$ decreases with decreasing battery costs. The situation was found to be the opposite in the scenarios with variable PV cost.

Figures 4.15b and 4.15d are the exploded version of the battery share in Figures 4.15a and 4.15c, respectively. They illustrate how the battery investment is split into different components. The investment in battery capacity $C_{b,e}^{f}$ claims the largest share, approximately one half. It is followed by the investments in output power $C_{b,p}^{\text{out}}$ and transit energy $C_{b,e}^{m}$. This is the situation in the p1 case, where the peak reduction is the primary objective. In the p4 case, as the two tariff components come closer in importance, $C_{b,e}^{m}$ becomes larger than $C_{b,p}^{\text{out}}$. The investment in battery input power $C_{b,p}^{\text{in}}$ claims always the lowest share. This fact indicates that contrary to a battery usage driven only by the volatility in the price signal, under the price structure proposed in this dissertation, the battery is used as an energy to power buffer. Energy is slowly stored in the battery and rapidly released at the critical peak hours. The size of the battery input power depends on the volatility, i.e. the standard deviation, of the price signal's energy component.

Finally, in the comparison between different battery technologies, lead-acid was found to be the most competitive one. The comparatively larger amounts of installed battery capacity and peripherals result in larger peak reductions. The less competitive technology is Ni-Cd, mainly due to the high costs and low efficiency. Li-ion batteries were assumed *a priori* to be the default technology, motivated mainly by the market situation, and the greater compactness and versatility provided by this technology.

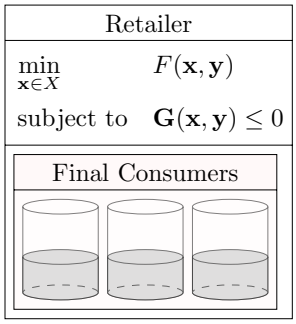

Chapter 5

Battery and PV Selection Model, the Retailer's Perspective

The equilibrium presented in the previous chapter is entirely determined by the battery and PV costs, the structure of the electrical load, and the users' reaction to the pricing policy. The pricing policy introduced by the retailer is effective, in that it reduces the maximum peak. However, even though the retailer is the policy maker, it lacks a mechanism to directly control the final electricity profile. In the model studied in the previous chapter, it is implicitly assumed that from the retailer's perspective, the peak reduction is worth the decrease in profit. In that model, the profit reduction in the sale of electricity depends on the equilibrium conditions only and cannot be influenced by the retailer, simply because the retailer's controls are not modelled.

This chapter is an attempt to explicitly account for the retailer's objectives and viewpoint. The mathematical model presented in this chapter provides an extra level of control that allows the retailer to impact the final equilibrium. This extra level of control is achieved by superimposing additional control signals on the price vectors. The resulting problem is a hierarchical optimization, or BLP, which is reformulated as an NLP.

This chapter is organized as follows: Section 5.1 addresses the reduction of the problem's time horizon; the model presented in Chapter 4 has to be simplified in order to reduce the number of variables and equations. Section 5.2 explores the retailer's profit possibilities. The BLP is defined in Section 5.3, and some details on its solution are illustrated in Section 5.4. Section 5.5 is dedicated to discussing the results. Section 5.6 provides a brief description of the computational issues. This chapter concludes with the summary and conclusions in Section 5.7.

5.1 Clustering

The model presented in Chapter 4 is an LP, which is relatively easy to solve, even in its stochastic form. This kind of problem can be scaled up to millions of variables and millions of constraints [29]. Conversely, the problem presented in this chapter is an NLP, which can be solved up to a few thousands of variables and constraints, provided it does not contain binary variables, in which case it is hard to solve and requires the use of decomposition

techniques [29].

Ideally, the BLP formulation should implement a structure in which the retailer is the leader, or upper level player, and each building is a follower, or lower level player. If the time horizon of model (4.1) is preserved (8760h), this formulation would result in approximately $70000 \cdot n$ additional variables and $36000 \cdot n$ additional equations, where n is the number of buildings. If the number of buildings is $n > 500$, it can be easily inferred than the resulting NLP is hard to solve and becomes intractable.

The clustering methodology pursues a twofold objective. On one hand, we are interested in representing a large number of buildings — $n > 500$ — without explicitly modelling each. On the other hand, the problem's time horizon has to be compressed, in a way that the resulting NLP can be solved without recurring to decomposition techniques. The compressed problem, however, has to be representative of the original one, encapsulate its temporal and structural characteristics, and conduct to approximately the same results. All in all, the clustering procedure consist in: first, reducing the number of days τ_d in the analysis to a smaller number that still encapsulates the year dynamics. And second, representing the total number of buildings in a simplified way.

We start by running model (4.1) for each of 700 buildings in a random subsample, which is extracted from the 3000 buildings that were simulated to model the prices in Chapter 3. This number of buildings is large enough to be representative of the aggregate pattern resulting from the distributions depicted in Figure 3.10 on page 49. The stochastic LP's results for each of the 700 buildings, for an average cost scenario[1] and under the 4-level tariff described in Section 4.3, are summarized in Figure 5.1. Figure 5.2 indicates that the total electricity consumption without considering DHW production is the best predictor for the model's variables. These first results constitute the reference scenario against which the clustering approach will be compared.

As it is not possible to represent each building individually in the BLP formulation, we approximate the 700 buildings as a single superbuilding, whose load is the summation of all individual buildings' loads. All individual vectors are added linearly. The total solar radiation $\mathbf{E}_e$ is the average of all radiation series, weighted by the respective buildings' areas. Table 5.1 contrasts the results between the individual building model evaluation and the aggregate one.

It can be observed that the aggregate equivalent constitutes a conservative representation of the individual building evaluations. The magnitude of all dimension variables is approximately one half in the aggregate version. On the other hand, the cost structure is accurately preserved. Variables C, C_g, and $\mathrm{C}_g^{\max}$ are very similar in all scenarios. It is possible to exploit the relation between the different variables and the total consumed electricity, illustrated in Figures 5.2, to bring these variables closer to the reference case. The aggregation can be split into different building categories, each one corresponding to a different range, e.g., the quantiles of the electrical load distribution. On the whole, the

[1] $c_e^k = 650$,$c_p^k = 315$, and $c_\phi^k = 1400$ €; and $\gamma = 7000$, $\eta_d = \eta_c = 0.92$.

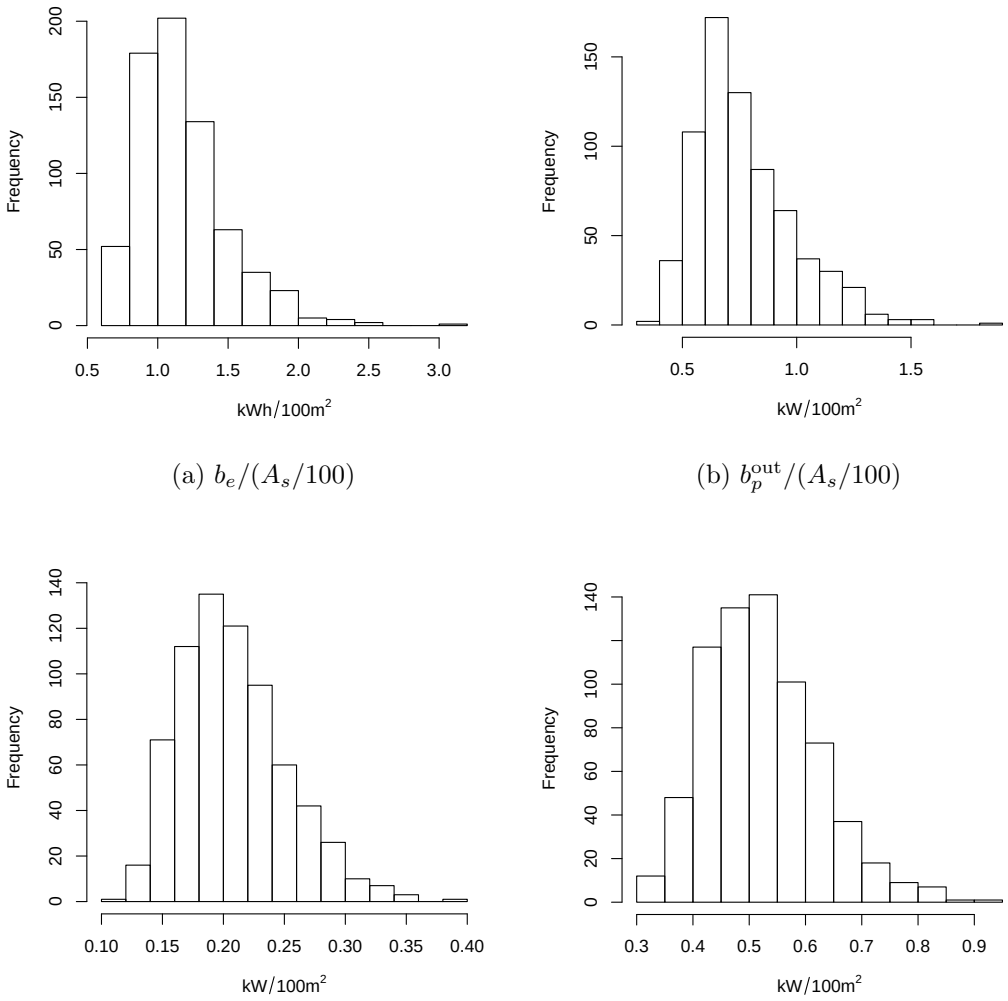

(a) $b_e/(A_s/100)$

(b) $b_p^{\text{out}}/(A_s/100)$

(c) $b_p^{\text{in}}/(A_s/100)$

(d) $\phi_p/(A_s/100)$

Figure 5.1: Model (4.1) evaluation results for a 700-building subsample

Scenario	b_e MWh	b_p^{in} MW	b_p^{out} MW	ϕ_p MW	C k€	C_g k€	$C_g^{\max}$ k€
Individual	2.88	0.52	1.88	1.38	2206.4	824.8	777.6
Aggregated stochastic	1.56	0.28	0.98	1.53	1907.1	840.7	648.3
Aggregated average	1.50	0.27	0.95	1.52	1901.2	844.0	647.7

Table 5.1: Comparison between the 700 buildings' individual and aggregate model evaluation results

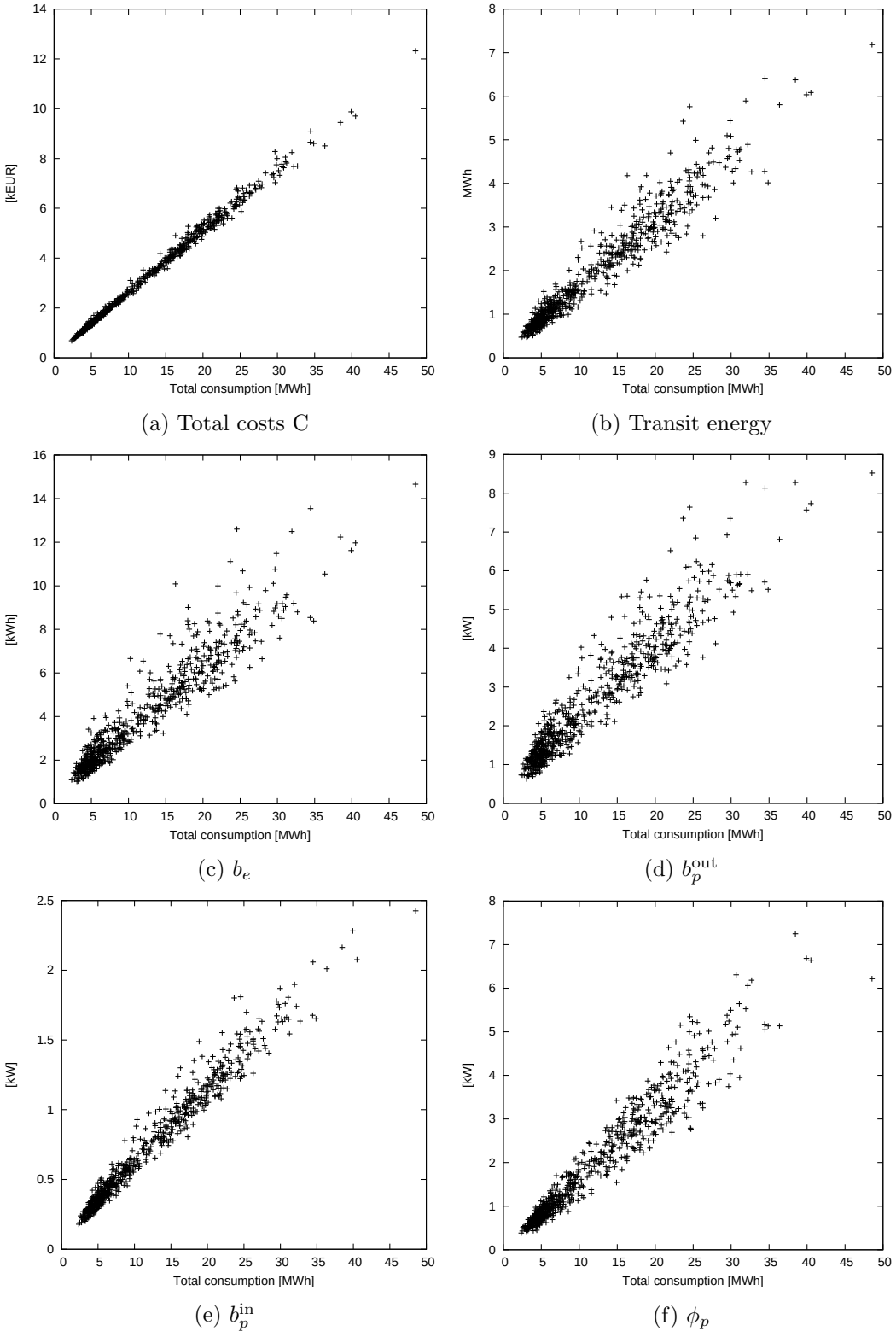

(a) Total costs C

(b) Transit energy

(c) b_e

(d) b_p^{out}

(e) b_p^{in}

(f) ϕ_p

Figure 5.2: The best estimator for model (4.1) variables is the total consumption excluding DHW preparation

approximation given by the aggregate superbuilding is considered acceptable and is used in the following analyses. We use the average approach, as there is not significant difference between the stochastic and the average case. The average case is the deterministic evaluation of the average of all stochastic scenarios.

The second part of the clustering procedure consists in the reduction of the problem's time horizon. The dimension of the different variables in model (4.1) is determined by the price dynamics and the load structure. As several days feature similar price and load patterns, there is redundant information that can be removed. Some days are more important than others in contributing to determine the decision variables. The classification and subsequent reduction of the time horizon is based on the results and not on the input vectors. The ranking is carried out using the aggregate superbuilding described above. Model (4.1) is run over 21 cost scenarios, first for the total length ($\tau_d = 365$), and then for each individual day. The results of each run are the same 7 variables presented in Table 5.1. The whole procedure results in 366 time series, one for the total length, referred to as reference series, and one for each individual day. Each series has a length of 21 scenarios $\times$ 7 variables = 147 items. Each of the per-day 365 series is compared against the reference series using the Euclidean distance. The selected days are those for which the quadratic errors are the smallest. We found that the 7 most significant days are enough to encapsulate the dynamics found in the whole year. In the subsequent analysis, the 10 most significant days are used. The selected days are depicted in Figure 5.3.

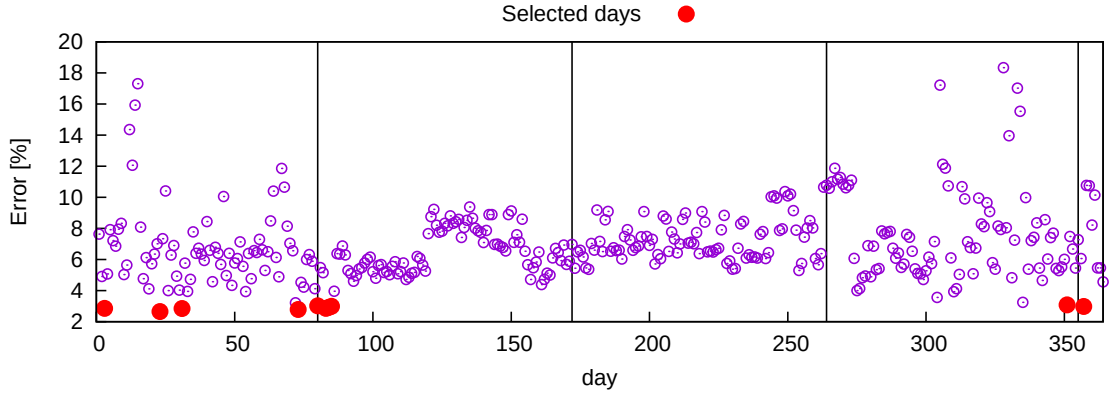

Figure 5.3: Clustering results. The selected days encapsulate the whole year dynamics. The vertical lines represent the division between the different seasons.

Summing up, the 700 buildings used in the analysis are represented by an equivalent superbuilding consisting of the aggregate load, and the time horizon is reduced from $\tau_d = 365$ to $\tau_d = 10$, resulting in vectors of length $10 \times 24 = 240$. The modified discontinuous set D is redefined as $D = d_3, d_{23}, d_{31}, d_{73}, d_{80}, d_{83}, d_{84}, d_{85}, d_{351}, d_{357}$.

5.2 Retailer's Profit Possibilities

In order to incorporate the retailer's viewpoint in the equilibrium construction, it is necessary to identify its profit possibilities and to model its objective function. This section explores different revenue possibilities and proposes an objective function.

Modelling the retailer's profit function implies making assumptions and estimations about its profit margin. This section does not provide a detailed analysis of the retailer's objective function, but a mere approximation that attempts to represent its goals and revenue possibilities. The availability of electrical storage results in several benefits for the retailer and, overall, for the electrical system. Among others, these benefits include: avoided distribution outages, deferred transmission and distribution investments, production cost saving, avoided capacity investments, line loss savings, avoided energy cost at the wholesale market, grid security and reliability, and power system adequacy [17].

Contrary to the final electricity consumers, who can react to the electricity prices and accommodate their consumption accordingly, the retailer has to make bids at the wholesale market and agree in advance on the amount of energy traded and the corresponding price. The retailer trades energy at two different markets: it buys electricity at the wholesale market, and sells electricity to the final consumers.

There are two main drivers shaping the retailer's revenues. The first one is the benefit derived from the sale of electricity. As users react to the retailer's prices, the retailer's objective is concerned with reducing the gap between the cost at the wholesale market and the profit reduction in the sale of electricity. This reduction is the consequence of the user's investment in DSEs and PV. The second driver encompasses all possible benefits derived from the ability to peak-shave the load, which amounts to assigning a value to the overall peak reduction.

In order to represent the gap between the retailer's costs and revenue, it is necessary to model the cost paid by the retailer at the wholesale market. We assume that the retailer pays a price that is proportional to the electricity consumed. In this approach, the merit order curve is modelled as an affine function of the consumed power. The resulting cost is then a quadratic function of the total electricity consumption. If the prices are normalized to their mean value, the function's slope is irrelevant. Following this approach and considering the 700 buildings described in the previous section, the difference between the costs at the wholesale market and the price paid by the users, if no investment in PV and DSEs is incurred, is 3.4%. This number, which is equivalent to a profit of 83€/MWh, is in line with the figures reported in [24].

Assigning a value to the peak reduction is less straightforward. The electrical grid is a complex and highly interconnected system; it is very difficult to identify a unique figure that characterizes the marginal cost of enhancing the installed capacity. There does not exist a figure in €/kW expressing the cost of deferring the grid expansion investments. Nevertheless, the benefit of future transmission investment deferrals can be approximated.

For instance, it is possible to approximate this cost using the average annual transmission costs, as suggested in [17]. We implement this latter approach.

Summing up, the retailer's objective function consist of two terms. 1) The maximization of the difference between the revenue and the costs, and 2) the minimization of the overall peak.

5.3 Model Formulation

A model simultaneously accounting for the retailer's and users' objectives has the hierarchical BLP structure described in Section 2.7. The upper level represents the retailer's objectives and the lower levels represent the final consumers' perspective. Each level influences the outcome of the other level. The lower level is equivalent to the model studied in Chapter 4. This section describes the resulting BLP's topology.

The lower level problem has identical structure with model (4.1). The notation is slightly different though. The notation is modified to distinguish each follower's variables sets from one another. Each follower has its own and unique sets of variables. In order to differentiate the variables pertaining to each follower, the subscript $_\omega$ is introduced. This subscript uniquely labels the variables according to the follower to which they belong. $\omega \in \{1, 2, \cdots, n_{\text{LL}}\}$, where n_{LL} is the number of followers. For instance, vector $\mathbf{x}_{g,1}$ defines the electricity withdrawn from the grid by follower 1. Equations (4.1) are recast in the form of (5.1), where the new notation is incorporated. The scalars and vectors involved in the definition of (5.1), despite the extended ω-notation, are the same defined in Tables 4.1 and 4.2. The $_\omega$ subscript simply defines different instances of those variables sets for each follower.

$$\min_{\chi^*_\omega} \sum_{d=d_1}^{d_{\tau_d}} \sum_{h=h_1}^{h_{24}} c_{g_i} x_{g_i,\omega} + \sum_{d=d_1}^{d_{\tau_d}} c^{\max}_{g_d} \cdot \kappa^d_{g,\omega} + \frac{1}{2} c^m_{b_e} \sum_{d=d_1}^{d_{\tau_d}} \sum_{h=h_1}^{h_{24}} (x^{\text{in}}_{b_i,\omega} + x^{\text{out}}_{b_i,\omega}) \tag{5.1a}$$
$$+ \tau_d \big(c^f_{b_e} b_{e,\omega} + c^f_{b_p} b^{\text{in}}_{p,\omega} + c^f_{b_p} b^{\text{out}}_{p,\omega} \big) + \tau_d \cdot c^f_\phi \cdot \phi_{p,\omega}$$

subject to

$$b_{e,\omega} - b_{\text{soc}_i,\omega} \geq 0, \quad \forall b_{\text{soc}_i,\omega} \in \mathbf{b}_{\text{soc},\omega} \tag{5.1b}$$
$$b_{\text{soc}_i,\omega} - b^{\min}_{\text{soc}} \cdot b_{e,\omega} \geq 0, \quad \forall b_{\text{soc}_i,\omega} \in \mathbf{b}^{\bar{0}}_{\text{soc},\omega} \tag{5.1c}$$
$$b_{\text{soc}_i,\omega} - b^{\min}_{\text{soc}} \cdot b_{e,\omega} = 0, \quad \forall b_{\text{soc}_i,\omega} \in \mathbf{b}^{0}_{\text{soc},\omega} \tag{5.1d}$$
$$x^{\text{out}}_{b_i,\omega} = 0, \quad \forall x^{\text{out}}_{b_i,\omega} \in \mathbf{x}^{\text{out}^0}_{b,\omega} \tag{5.1e}$$
$$b^{\text{in}}_{p,\omega} - \xi x^{\text{in}}_{b_i,\omega} \geq 0, \quad \forall x^{\text{in}}_{b_i,\omega} \in \mathbf{x}^{\text{in}}_{b,\omega} \tag{5.1f}$$
$$b^{\text{out}}_{p,\omega} - \xi x^{\text{out}}_{b_i,\omega} \geq 0, \quad \forall x^{\text{out}}_{b_i,\omega} \in \mathbf{x}^{\text{out}}_{b,\omega} \tag{5.1g}$$
$$x^{\text{out}}_{b_i,\omega} + \phi_{a,\omega} E_{e_i,\omega} + x_{g_i,\omega} - x^{\text{in}}_{b_i,\omega} - x_{l_i,\omega} \geq 0, \tag{5.1h}$$

$$\forall x_{g_i,\omega} \in \mathbf{x}_{g,\omega}, \forall x^{\text{in}}_{b_i,\omega} \in \mathbf{x}^{\text{in}}_{b,\omega}, \forall x^{\text{out}}_{b_i,\omega} \in \mathbf{x}^{\text{out}}_{b,\omega}, \forall x_{l_i,\omega} \in \mathbf{x}_{l,\omega}, \forall E_{e_i,\omega} \in \mathbf{E}_{e,\omega}$$

$$\Delta b_{\text{soc}_i,\omega} - b_{\eta_c} x^{\text{in}}_{b_i,\omega} + \frac{1}{b_{\eta_d}} x^{\text{out}}_{b_i,\omega} = 0, \quad \forall b_{\text{soc}_i,\omega} \in \mathbf{b}^{+1}_{\text{soc},\omega}, \forall x^{\text{in}}_{b_i,\omega} \in \mathbf{x}^{\text{in}^{+1}}_{b,\omega}, \forall x^{\text{out}}_{b_i,\omega} \in \mathbf{x}^{\text{out}^{+1}}_{b,\omega} \tag{5.1i}$$

$$\phi_{p,\omega} - \xi \phi_{a,\omega} E_{e_i,\omega} \geq 0, \quad \forall E_{e_i,\omega} \in \mathbf{E}_{e,\omega} \tag{5.1j}$$

$$\kappa^d_{g,\omega} - \xi x^d_{g_j,\omega} \geq 0, \quad \forall \kappa^d_{g,\omega} \in \mathbf{k}^d_{g,\omega}, \forall x^d_{g_j,\omega} \in \mathbf{x}^d_{g,\omega}, \forall \mathbf{x}^d_{g,\omega} \in \mathbf{x}^{\Delta}_{g,\omega} \tag{5.1k}$$

$$b_{e,\omega} \geq 0, \quad b^{\text{in}}_{p,\omega} \geq 0, \quad b^{\text{out}}_{p,\omega} \geq 0, \quad \phi_{a,\omega} \geq 0, \quad \phi_{p,\omega} \geq 0 \tag{5.1l}$$

$$x^{\text{out}}_{b_i,\omega} \geq 0, \forall x^{\text{out}}_{b_i,\omega} \in \mathbf{x}^{\text{out}^0}_{b,\omega}; \quad x^{\text{in}}_{b_i,\omega} \geq 0, \forall x^{\text{in}}_{b_i,\omega} \in \mathbf{x}^{\text{in}}_{b,\omega}; \quad x_{g_i,\omega} \geq 0, \forall x_{g_i,\omega} \in \mathbf{x}_{g,\omega} \tag{5.1m}$$

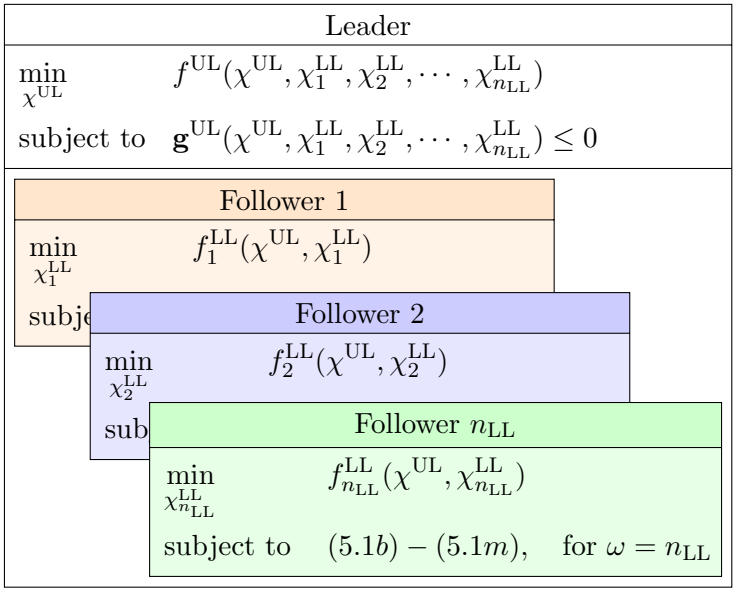

Figure 5.4: Bilevel program (BLP) structure

The retailer's controls are given by set χ^{UL}, and the followers' controls by sets $\chi^{\text{LL}}_{\omega}$.

$$\chi^{\text{LL}}_{\omega} = \{\mathbf{x}_{g,\omega}, \mathbf{x}^{\text{in}}_{b,\omega}, \mathbf{x}^{\text{out}}_{b,\omega}, \mathbf{k}^d_{g,\omega}, \mathbf{b}_{\text{soc},\omega}, b_{e,\omega}, b^{\text{out}}_{p,\omega}, b^{\text{in}}_{p,\omega}, \phi_{a,\omega}, \phi_{p,\omega}\}, \quad \omega \in \{1, 2, \cdots, n_{\text{LL}}\}$$

$$\chi^{\text{UL}} = \{\mathbf{c}^{\text{UL}}_g, \mathbf{c}^{\text{UL,max}}_g\}$$

The resulting BLP has to have the structure depicted in Figure 5.4. The retailer plays the leader role and can influence the users' outcome by modifying the χ^{UL} controls. This ability to influence the resulting equilibrium, which model (4.1) lacks, is achieved by extending the price signal definition. Vectors $\mathbf{c}^{\text{UL}}_g$ and $\mathbf{c}^{\text{UL,max}}_g$ are superimposed on the price's energy and peak components, respectively, as illustrated in (5.2). The new prices, $\mathbf{c}''_g$ for the energy component and $\mathbf{c}^{\text{max}''}_g$ for the daily peaks, are passed down to the final

consumers.

Table 5.2 summarizes the additional components added on top of the price signals. Vector $\mathbf{c}^{\text{UL}}_{g,\Delta}$ is the clustered-by-day subset of hourly prices in the additional price's energy component $\mathbf{c}^{\text{UL}}_{g}$; $\mathbf{c}^{\text{UL}}_{g,\Delta} \subseteq \mathbf{c}^{\text{UL}}_{g}$. All the elements in $\mathbf{c}^{\text{UL}}_{g,\Delta}$ are of length 24. Each of the vectors in $\mathbf{c}^{\text{UL}}_{g,\Delta}$ is denoted $\mathbf{c}^{\text{UL}}_{g,d}$, where the additional subscript $_d$ indicates the corresponding day. For instance, $\mathbf{c}^{\text{UL}}_{g,d_3}$ is the vector containing the 24 prices for day d_3.

Description	**Symbol**	**Set**	$\{\cdot\}$	**Units**
Extended prices (energy component)	$\mathbf{c}''_g$	Ω	c''_{g_i}	€/kWh
Extended prices (peak component)	$\mathbf{c}^{\max''}_g$	D	$c^{\max''}_{g_d}$	€/kW
Additional prices' energy component	$\mathbf{c}^{\text{UL}}_g$	Ω	$c^{\text{UL}}_{g_i}$	€/kWh
Additional prices' peak component	$\mathbf{c}^{\text{UL,max}}_g$	D	$c^{\text{UL,max}}_{g_d}$	€/kW
Additional prices' energy component per days	$\mathbf{c}^{\text{UL}}_{g,\Delta}$	D	$\mathbf{c}^{\text{UL}}_{g,d}$	€/kWh
Additional prices' energy component for day d	$\mathbf{c}^{\text{UL}}_{g,d}$	H	$c^{\text{UL}}_{g_j,d}$	€/kWh

Table 5.2: Additional vectors in the retailer's extended price formulation. These signals can be positive or negative.

.

$$c''_{g_i} = c_{g_i} + c^{\text{UL}}_{g_i}, \quad \forall c''_{g_i} \in \mathbf{c}''_g, \forall c_{g_i} \in \mathbf{c}_g, \forall c^{\text{UL}}_{g_i} \in \mathbf{c}^{\text{UL}}_g \tag{5.2a}$$

$$c^{\max''}_{g_d} = c^{\max}_{g_d} + c^{\text{UL,max}}_{g_d}, \quad \forall c^{\max''}_{g_d} \in \mathbf{c}^{\max''}_g, \forall c^{\max}_{g_d} \in \mathbf{c}^{\max}_g, \forall c^{\text{UL,max}}_{g_d} \in \mathbf{c}^{\text{UL,max}}_g \tag{5.2b}$$

The extended prices are incorporated into the resulting BLP formulation given by (5.3).

$$\begin{aligned} \max_{\chi^{\text{UL}}} \quad & -\frac{1}{\overline{\mathbf{x}}_{g,\Omega}} \sum_{d=d_1}^{d_{\tau_d}} \sum_{h=h_1}^{h_{24}} \left(\sum_{\omega=1}^{n_{\text{LL}}} x_{g_i,\omega} \right)^2 \quad + \\ & \sum_{d=d_1}^{d_{\tau_d}} \sum_{h=h_1}^{h_{24}} \sum_{\omega=1}^{n_{\text{LL}}} c''_{g_i} x_{g_i,\omega} \quad + \\ & \xi \sum_{d=d_1}^{d_{\tau_d}} \sum_{\omega=1}^{n_{\text{LL}}} c^{\max''}_{g_d} \cdot \max \mathbf{x}^d_{g,\omega} \quad - \\ & \xi \cdot \iota \cdot \max \mathbf{x}_{g,\Omega} \end{aligned} \tag{5.3a}$$

subject to

$$\sum_{j=h_1}^{h_{24}} c^{\mathrm{UL}}_{g_j,d} = 0, \quad \forall \mathbf{c}^{\mathrm{UL}}_{g,d} \in \mathbf{c}^{\mathrm{UL}}_{g,\Delta} \tag{5.3b}$$

$$\sum_{d=d_1}^{d_{\tau_d}} c^{\mathrm{UL,max}}_{g_d} = 0 \tag{5.3c}$$

$$c^{\mathrm{UL}}_{g_i} + c_{g_i} \geq 0, \quad \forall c^{\mathrm{UL}}_{g_i} \in \mathbf{c}^{\mathrm{UL}}_{g}, \forall c_{g_i} \in \mathbf{c}_{g_i} \tag{5.3d}$$

$$c^{\mathrm{UL,max}}_{g_d} + c^{\max}_{g_d} \geq 0, \quad \forall c^{\mathrm{UL,max}}_{g_d} \in \mathbf{c}^{\mathrm{UL,max}}_{g}, \forall c^{\max}_{g_d} \in \mathbf{c}^{\max}_{g} \tag{5.3e}$$

$$\left|c^{\mathrm{UL,max}}_{g_d}\right| \leq \rho_{\max}, \quad \forall c^{\mathrm{UL,max}}_{g_d} \in \mathbf{c}^{\mathrm{UL,max}}_{g} \tag{5.3f}$$

$$\left|c^{\mathrm{UL}}_{g_i}\right| \leq \rho, \quad \forall c^{\mathrm{UL}}_{g_i} \in \mathbf{c}^{\mathrm{UL}}_{g} \tag{5.3g}$$

$$\text{Follower 1} \begin{cases} \min\limits_{\chi^{\mathrm{LL}_1}} \quad \sum\limits_{d=d_1}^{d_{\tau_d}} \sum\limits_{h=h_1}^{h_{24}} c''_{g_i} x_{g_i,1} + \sum\limits_{d=d_1}^{d_{\tau_d}} c^{\max''}_{g_d} \cdot \kappa^{d}_{g,1} \\ \qquad +\frac{1}{2} c^{m}_{b_e} \sum\limits_{d=d_1}^{d_{\tau_d}} \sum\limits_{h=h_1}^{h_{24}} (x^{\mathrm{in}}_{b_i,1} + x^{\mathrm{out}}_{b_i,1}) \\ \qquad +\tau_d \big(c^{f}_{b_e} b_{e,1} + c^{f}_{b_p} b^{\mathrm{in}}_{p,1} + c^{f}_{b_p} b^{\mathrm{out}}_{p,1}\big) + \tau_d \cdot c^{f}_{\phi} \cdot \phi_{p,1} \\ \text{subject to} \\ \qquad (5.1b) - (5.1m), \qquad \text{for } \omega = 1 \end{cases} \tag{5.3h}$$

$$\vdots$$

$$\text{Follower } n_{\mathrm{LL}} \begin{cases} \min\limits_{\chi^{\mathrm{LL}_{n_{\mathrm{LL}}}}} \quad \sum\limits_{d=d_1}^{d_{\tau_d}} \sum\limits_{h=h_1}^{h_{24}} c''_{g_i} x_{g_i,n_{\mathrm{LL}}} + \sum\limits_{d=d_1}^{d_{\tau_d}} c^{\max''}_{g_d} \cdot \kappa^{d}_{g,n_{\mathrm{LL}}} \\ \qquad +\frac{1}{2} c^{m}_{b_e} \sum\limits_{d=d_1}^{d_{\tau_d}} \sum\limits_{h=h_1}^{h_{24}} (x^{\mathrm{in}}_{b_i,n_{\mathrm{LL}}} + x^{\mathrm{out}}_{b_i,n_{\mathrm{LL}}}) \\ \qquad +\tau_d \big(c^{f}_{b_e} b_{e,n_{\mathrm{LL}}} + c^{f}_{b_p} b^{\mathrm{in}}_{p,n_{\mathrm{LL}}} + c^{f}_{b_p} b^{\mathrm{out}}_{p,n_{\mathrm{LL}}}\big) + \tau_d \cdot c^{f}_{\phi} \cdot \phi_{p,n_{\mathrm{LL}}} \\ \text{subject to} \\ \qquad (5.1b) - (5.1m), \qquad \text{for } \omega = n_{\mathrm{LL}} \end{cases} \tag{5.3i}$$

Equation (5.3a) is the objective function introduced in Section 5.2. The first term in this equation represents the total cost paid by the retailer at the wholesale market. The quantity $\overline{\mathbf{x}}_{g,\Omega}$, defined in (5.4), is the ratio between the aggregate electricity consumption's mean value and the prices' average. The second and third terms are the revenue obtained from the sale of electricity, they account for the energy and power components, respectively. The fourth term is the cost associated with the maximum peak, and is used to estimate the benefit resulting from the overall peak reduction. $\mathbf{x}_{g,\Omega}$ is the aggregate load vector, whose elements are defined as $x_{g_i,\Omega} = \sum\limits_{\omega=1}^{n_{\mathrm{LL}}} x_{g_i,\omega}$. The peak value factor ι is approximated as the average grid utilization component costs: $\iota = 14 \times (1-\alpha) \times 0.2[€/\mathrm{kW}]$, where 14 represents the average network costs and 0.2 is the average electricity price. The average

network costs are calculated using the total load levels defined in Section 3.5.

$$\overline{\mathbf{x}}_{g,\Omega} = \frac{\sum_{d=d_1}^{d_{\tau_d}} \sum_{h=h_1}^{h_{24}} \sum_{\omega=1}^{n_{\mathrm{LL}}} x_{g_i,\omega}}{\tau_d \cdot 24 \cdot 0.2 \text{€/kWh}} \tag{5.4}$$

Equations (5.3b) and (5.3c) impose the constraint that the signals modulated on top of the price's energy and power components have mean value 0. The idea of these constraints is to preserve the equilibrium structure and avoid that the retailer abuse the price controls. Equations (5.3d) and (5.3e) ensure that the price's energy and power components are always positive. These constraints are intended to preserve the feasibility of the follower's dual formulation (see Section 5.4). Equations (5.3f) and (5.3g) set upper and lower caps on the additional superimposed price signals. The caps are chosen to be approximately two standard deviations of the respective signal, i.e $\rho = 1.0 \times \alpha \times 0.2$ [€/kWh] and $\rho_{\max} = 4.0 \times (1 - \alpha) \times 0.2$ [€/kW]. Finally, (5.3h)-(5.3i) represent the BLP's followers defined in (5.1) and described in detail in Chapter 4.

5.4 Model Solution

Contrary to model (4.1), model (5.3) cannot be routinely solved. The model has to be first transformed. As explained in Section 2.7, we opted for an approach in which the followers are replaced by their dual representations and strong duality condition [29,35,36]. In order to obtain the dual representation, it is convenient to write the followers in their canonical matrix form, as illustrated in Tables 5.3 and 5.4. Essentially, the dual formulation is obtained by transposing the matrix depicted in Table 5.3.

The followers in the BLP formulation can be used to represent different building categories, or to account for uncertainty [29]. We implement a single follower, obeying mainly computational issues (see Section 5.6), but also because it was found that the PV value is underestimated when several followers are considered. Uncertainty is indirectly taken into account, as the vectors passed to the model are the average of all stochastic scenarios, and the load itself is the summation of all buildings' loads. As it can be appreciated in Table 5.1, the aggregate superbuilding's stochastic and average solutions are virtually equivalent. The resulting model is an NLP that for the size resulting from the reduced time horizon can be routinely solved.

5.5 Experiments and Results

This section summarizes the main findings and results following the BLP's evaluation. The main focus of this section is on illustrating the retailer's ability to influence the equilibrium conditions.

		b_e	b_p^{in}	b_p^{out}	$\mathbf{k}_g^d$	$\mathbf{x}_{g_1}$	$\mathbf{x}_{g_2}$	$\mathbf{x}_{g_n}$	$\mathbf{x}_{b_1}^{\text{in}}$	$\mathbf{x}_{b_2}^{\text{in}}$	$\mathbf{x}_{b_n}^{\text{in}}$	$\mathbf{x}_{b_1}^{\text{out}}$	$\mathbf{x}_{b_2}^{\text{out}}$	$\mathbf{x}_{b_n}^{\text{out}}$	$\mathbf{b}_{\text{soc}_1}$	$\mathbf{b}_{\text{soc}_2}$	$\mathbf{b}_{\text{soc}_n}$	ϕ_p	ϕ_a		b
	1	1	·	·	·	·	·	·	·	·	·	·	·	·	−1	·	·	·	·	≥	0
(5.1b)	2	1	·	·	·	·	·	·	·	·	·	·	·	·	·	−1	·	·	·	≥	0
	n	1	·	·	·	·	·	·	·	·	·	·	·	·	·	·	−1	·	·	≥	0
(5.1d)	1	−0.2	·	·	·	·	·	·	·	·	·	·	·	·	1	·	·	·	·	=	0
(5.1d)	2	−0.2	·	·	·	·	·	·	·	·	·	·	·	·	·	1	·	·	·	=	0
(5.1c)	n	−0.2	·	·	·	·	·	·	·	·	·	·	·	·	·	·	1	·	·	=	0
	1	·	1	·	·	·	·	·	−1	·	·	·	·	·	·	·	·	·	·	≥	0
(5.1f)	2	·	1	·	·	·	·	·	·	−1	·	·	·	·	·	·	·	·	·	≥	0
	n	·	1	·	·	·	·	·	·	·	−1	·	·	·	·	·	·	·	·	≥	0
	1	·	·	1	·	·	·	·	·	·	·	−1	·	·	·	·	·	·	·	≥	0
(5.1g)	2	·	·	1	·	·	·	·	·	·	·	·	−1	·	·	·	·	·	·	≥	0
	n	·	·	1	·	·	·	·	·	·	·	·	·	−1	·	·	·	·	·	≥	0
	1	·	·	·	1	−1	·	·	·	·	·	·	·	·	·	·	·	·	·	≥	0
(5.1k)	2	·	·	·	1	·	−1	·	·	·	·	·	·	·	·	·	·	·	·	≥	0
	n	·	·	·	1	·	·	−1	·	·	·	·	·	·	·	·	·	·	·	≥	0
	1	·	·	·	·	1	·	·	−1	·	·	1	·	·	·	·	·	·	E_{e_1}	≥	x_{l_1}
(5.1h)	2	·	·	·	·	·	1	·	·	−1	·	·	1	·	·	·	·	·	E_{e_2}	≥	x_{l_2}
	n	·	·	·	·	·	·	1	·	·	−1	·	·	1	·	·	·	·	E_{e_n}	≥	x_{l_n}
(5.1i)	2	·	·	·	·	·	·	·	·	$-b_{\eta_c}$	·	·	$\frac{1}{b_{\eta_d}}$	·	−1	1	·	·	·	=	0
(5.1i)	n	·	·	·	·	·	·	·	·	·	$-b_{\eta_c}$	·	·	$\frac{1}{b_{\eta_d}}$	·	−1	1	·	·	=	0
(5.1e)	1	·	·	·	·	·	·	·	·	·	·	1	·	·	·	·	·	·	·	=	0
(5.1e)	2	·	·	·	·	·	·	·	·	·	·	·	1	·	·	·	·	·	·	=	0
	1	·	·	·	·	·	·	·	·	·	·	·	·	·	·	·	·	1	$-E_{e_1}$	≥	0
(5.1j)	2	·	·	·	·	·	·	·	·	·	·	·	·	·	·	·	·	1	$-E_{e_2}$	≥	0
	n	·	·	·	·	·	·	·	·	·	·	·	·	·	·	·	·	1	$-E_{e_n}$	≥	0

Table 5.3: Dual representation of model (5.1)

	$\kappa_g^{d_1}$	$\kappa_g^{d_2}$	$\kappa_g^{d\tau_d}$	$\mathbf{x}_{g_1}$	$\mathbf{x}_{g_2}$	$\mathbf{x}_{g_3}$	$\mathbf{x}_{g_4}$	$\mathbf{x}_{g_5}$	$\mathbf{x}_{g_6}$	$\mathbf{x}_{g_7}$	$\cdots$	$\mathbf{x}_{g_n}$
1	1	·	·	-1	·	·	·	·	·	·	·	·
⋮	1	·	·	·	-1	·	·	·	·	·	·	·
24	1	·	·	·	·	-1	·	·	·	·	·	·
1	·	1	·	·	·	·	-1	·	·	·	·	·
⋮	·	1	·	·	·	·	·	-1	·	·	·	·
24	·	1	·	·	·	·	·	·	-1	·	·	·
1	·	·	1	·	·	·	·	·	·	-1	·	·
⋮	·	·	1	·	·	·	·	·	·	·	-1	·
24	·	·	1	·	·	·	·	·	·	·	·	-1

Table 5.4: Matrix representation of Equations (5.1k)

Scenario	ρ €/kWh	$\rho_{\max}$ €/kW	ι €/kW
Scenario 1	0.0	0.0	0.0
Scenario 2	0.1	0.4	0.0
Scenario 3	0.1	0.4	0.7
Scenario 4	0.1	0.4	1.4
Scenario 5	0.1	0.4	2.1
Scenario 6	0.15	0.4	1.4
Scenario 7	0.1	0.6	1.4
Scenario 8	0.15	0.6	1.4

Table 5.5: Evaluation scenarios for model (5.3)

In order to study the effect of the retailer's controls on the final equilibrium, we define the 8 scenarios presented in Table 5.5. All scenarios correspond to an average cost: $c_e^k = 650$, $c_p^k = 315$, and $c_\phi^k = 1400$; and $\gamma = 7000$, $\eta_d = \eta_c = 0.92$. Scenario 1 is the reference scenario. In this scenario, the retailer's controls are disabled and no value is assigned to the peak reduction. In Scenario 2, the retailer's controls are enabled, but no value is given to the peak reduction objective. In Scenarios 3-5, the retailer's controls are enabled and a value is assigned to the peak reduction; each scenario features a different peak reduction value. Scenarios 6-8 keep the peak value constant and vary the cap on the price's energy and peak components. The cap values are incremented by 1σ.

Scenario 1 is supposed to resemble the LP formulation. This fact is confirmed by comparing the investment shares resulting from this scenario with the LP's evaluation. This comparison is depicted in Figure 5.5, where both the complete and reduced LP versions are included.

The results for the scenarios defined in Table 5.5 are presented in Figures 5.6 and

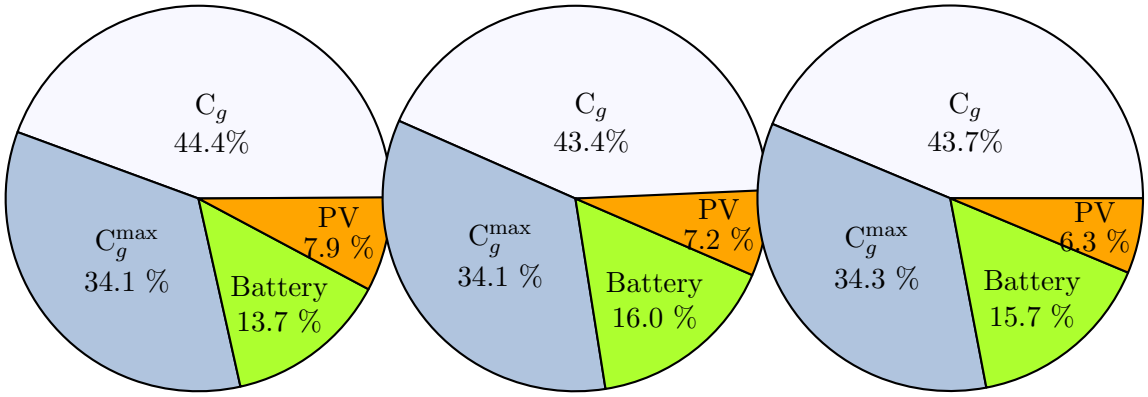

(a) Average LP, $\tau_d = 365$ (b) Average LP, $\tau_d = 10$ (c) BLP, Scenario 1

Figure 5.5: Comparison between the total length LP problem, the reduced LP problem, and the BLP without additional controls.

	Profit											
	LL	UL	Δ	C	C_g	C_g^{max}	$C_{b,e}^{f}$	$C_{b,e}^{m}$	$C_{b,p}^{in}$	$C_{b,p}^{out}$	C_ϕ	**Peak↓**
Scenario	k€	k€	%	k€	%	%	%	%	%	%	%	%
1	42.2	47.1	-10.4	54.1	43.7	34.3	6.2	5.7	1.0	2.7	6.3	32.9
2	46.5	48.6	-4.5	54.9	46.5	38.1	3.8	3.2	1.1	2.1	5.2	25.9
3	43.5	45.7	-4.9	54.8	44.1	35.3	5.5	4.3	1.7	2.5	6.5	31.5
4	44.0	46.2	-4.8	54.8	44.5	35.8	5.3	3.9	1.4	2.5	6.6	30.9
5	44.3	46.6	-5.1	54.9	44.9	35.8	5.1	3.8	1.5	2.7	6.2	33.5
6	44.4	46.3	-4.0	54.9	44.3	36.7	4.6	3.7	1.4	2.5	6.7	27.7
7	44.6	46.5	-4.0	54.8	44.4	37.0	4.7	3.4	1.0	2.2	7.3	31.6
8	44.4	46.0	-3.5	54.8	43.7	37.4	4.3	3.5	1.0	2.3	7.8	28.7

Table 5.6: Results of the scenarios presented in Table 5.5. All Costs are expressed as percentages of the total cost C. Peak↓ is the peak reduction.

Table 5.6. LL represents the total electricity fee paid by the final consumers, i.e. the retailer's revenue, UL represents the retailer's costs at the wholesale market, and Δ is the difference between them, i.e. the retailer's profit. The different investment shares are defined in Section 4.3.5. Figure 5.6a summarizes the investment shares incurred by the final electricity consumers (lower level players). Figure 5.6b presents the costs incurred by the retailer at the spot market, i.e. the upper level player's costs, and the revenue obtained from the sale of electricity, i.e. the lower level player's costs. Figure 5.6c describes the overall peak reduction achieved across the different scenarios.

The total investment in DSE and PV incurred by the users is more or less constant across the scenarios, evidencing that the solution is indeed an equilibrium. The only exception is Scenario 2, where no value is assigned to the peak reduction and the total investment is

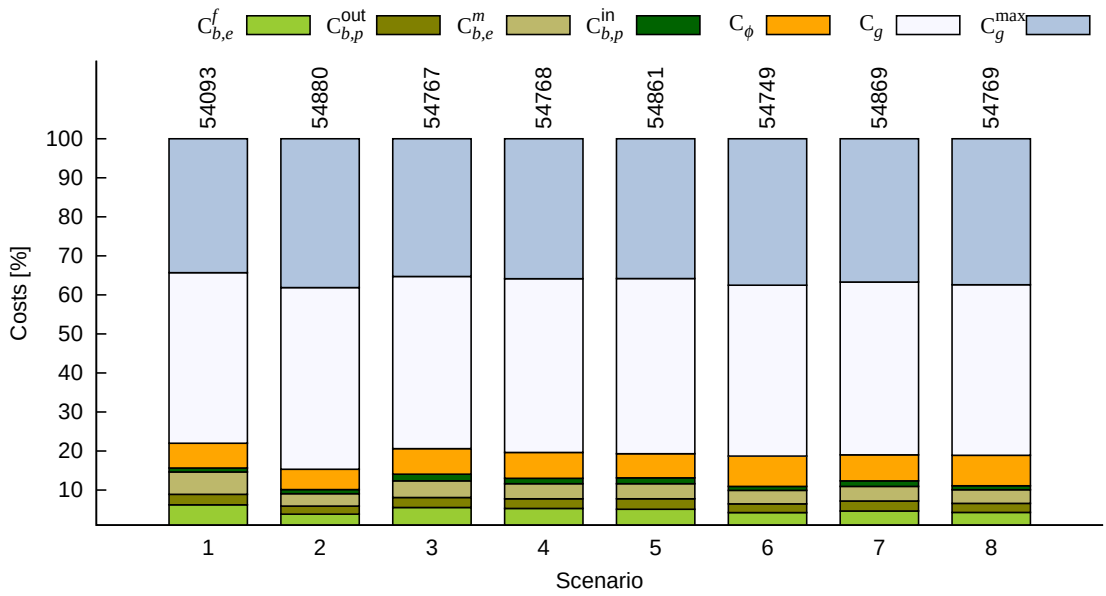

(a) Investment shares. Numbers on top of the bars are the absolute costs in €.

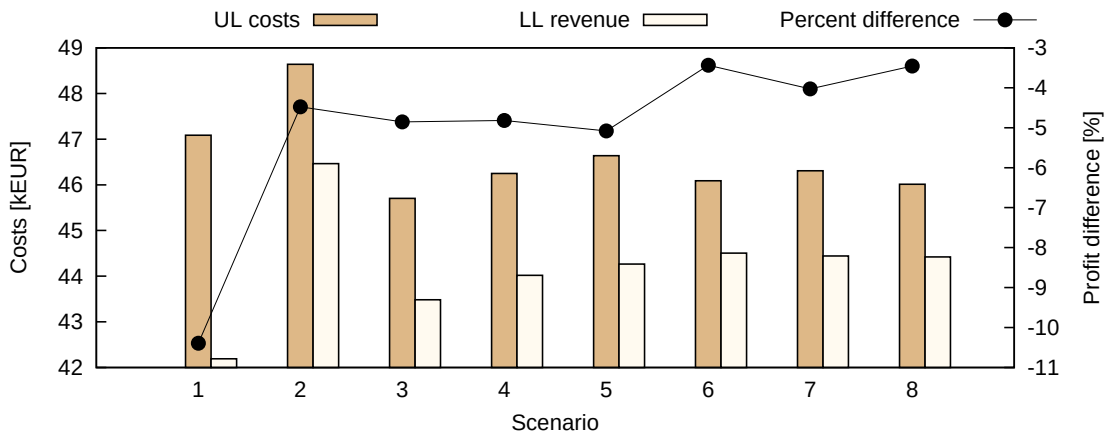

(b) Difference between the upper level costs and lower level revenue

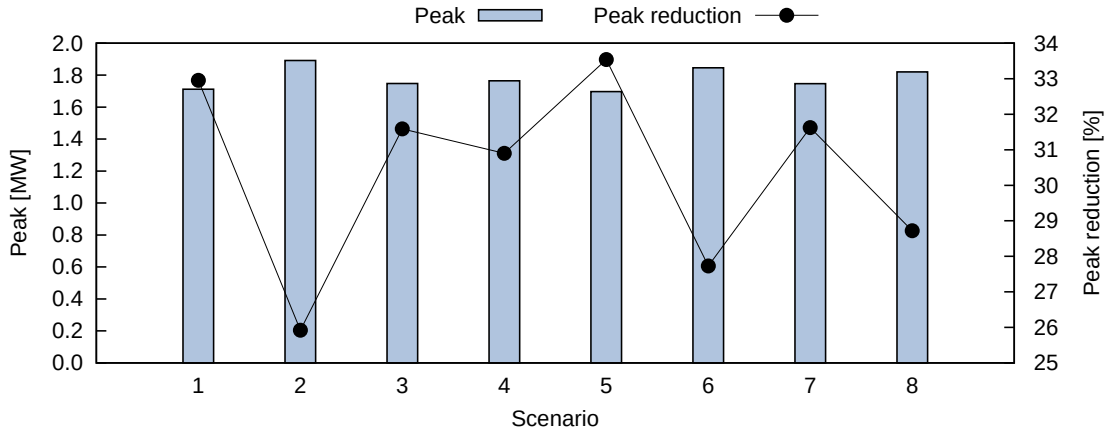

(c) Peak reduction

Figure 5.6: Results for the BLP (5.3) evaluation under the scenarios defined in Table 5.5

correspondingly lower. Scenario 2 features, as expected, the lowest peak reduction. The effect of the retailer's control on the user's costs can be appreciated by comparing Scenario 1 to the other scenarios in Figure 5.6b. The difference between the upper level cost and the low level revenue becomes smaller when the superimposed controls are introduced on top of the prices. In the scenarios with constant price caps and varying peak value, i.e. Scenarios 3-5, the investment shares remain approximately constant, while the upper and lower level costs increase proportionally to the peak value. The peak reduction does not increase linearly with the peak reduction value ι even though a larger peak reduction is evident in Scenario 5. Scenarios 6-7 are to be compared with Scenario 4. The peak value ι is kept constant, and the price caps —ρ and $\rho_{\max}$— are increased. The overall observation of these three scenarios evidences an increment in the cost paid by the users, i.e. higher LL revenue in Figure 5.6b, and a larger PV share C_ϕ in Figure 5.6a. The increment in C_ϕ seems to be proportional to the increment in the price' peak component cap $\rho_{\max}$.

5.6 Computational Details

All optimizations and scripts ran on an 8-core Intel(R) Core(TM) i7-3720QM computer. Each processor core clocks at 2.60GHz. The system has 8Gb of RAM and runs on the GNU/Linux (kernel 3.x.) operating system.

The NLP was implemented in GAMS [15]. The analysis period of each NLP is 10-day, with hourly resolution. The average time per run was between 1.2 and 5min, depending on the input parameters.

The BLP is reformulated as an NLP by replacing the followers by their dual representation and strong duality equation. Building the dual matrix, which is the transpose of the matrix displayed in Table 5.3, is error prone due to the large matrix's size: 1921×975. We tackled this problem by creating a python [55] script that automatically generates the GAMS models describing each follower. This approach is validated by comparing the primal and dual solutions, which were found to be identical. By the theory of linear programming, the primal and the dual solutions are identical, unless the problems are unfeasible [60].

We opted for modelling the aggregate consumption as a single follower, obeying mainly the long time that takes to solve the BLP with more than one follower. For instance, solving the BLP for two followers takes 45 min per run.

5.7 Summary and Conclusions

This chapter extended the results presented in Chapter 4 to incorporate the retailer's viewpoint. The retailer's perspective is accounted for by introducing a new control mechanism, which allows the retailer to influence the final equilibrium's outcome. The new problem's dynamics results in a hierarchical BLP formulation.

In a preparatory step, the data size and time horizon had to be reduced. The 700-building subsample used in the analysis is represented by an equivalent superbuilding consisting of the aggregate load. Our assumptions regarding the individual building modelling are inferred based on the aggregate scenario. We used the average deterministic equivalent, which was found to have very similar results with the stochastic representation. The time horizon was reduced to a lower number of days that still encapsulate the dynamics of the whole year. The reduced time horizon comprises winter days mainly. Interestingly, some of them are located at the very threshold between winter and spring, and autumn and winter.

The most important assumption in this chapter is regarding the costs incurred by the retailer at the wholesale market. We assumed that the wholesale market prices are an affine function of the electricity transacted, which results in a quadratic cost function. The retailer's objective consists in the overall peak reduction, plus the reduction of the gap between the costs at the wholesale market and the revenue obtained from the sale of electricity to the final consumers. The maximum peak reduction objective accounts for all benefits resulting from the ability to peak-shave the aggregate load level.

The additional controls that the retailer can use to influence the final equilibrium are zero-mean capped signals, superimposed on top of the price vectors.

We presented 8 different scenarios to evaluate the effect of the additional controls. When no investments are incurred by the users, the quadratic cost approach results in a 3.4% profit for the retailer, which is similar to the profits reported for retailers in countries such as Germany and Norway [24]. Once the users invest in DSEs and PV to reduce their costs, the retailer's profit decreases to -10.4%. The additional controls provided in the BLP formulation allow the retailer to increase this profit up to -3.5%.

By and large, we found that the cluster methodology used to reduce the problem's complexity is effective in that it captures the structure of the complete problem and leads to very similar results. The scenarios used to evaluate the BLP's outcome illustrate the effectiveness of the retailer's controls in bringing the equilibrium closer to the retailer's interests.

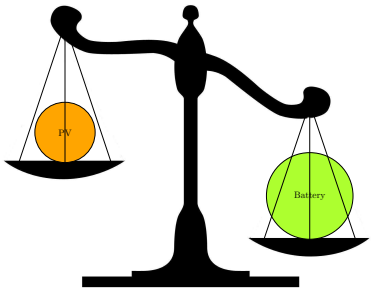

Chapter 6

Final Conclusions and Remarks

The challenges appearing at the interface between the buildings and the electrical grid are not only in regard to the availability of generation resources, but to the stringent timing imposed by the supply-demand balance, and the limited capacity of the transmission and distribution infrastructure. The only way to decouple the consumption from the grid's operational conditions without affecting users' habits and comfort levels is by introducing electrical storage. This thesis presented a distributed electricity storage strategy consisting of three milestones. 1) The proposition of a pricing policy. 2) The extrapolation of the $2Sol$ building paradigm to the aggregate view of a community, and 3) the formulation of mathematical models aimed at determining the optimal battery and PV investments.

The pricing policy introduced in this dissertation is effective, in that users confronted to it, conforming with the principles of rational economic behavior, decide to invest in a DSE and PV in order to reduce their costs. The demand-based electricity tariff, and the users' reaction to it result in an equilibrium, in which the users' and retailer' objectives, namely cost minimization and peak reduction, respectively, are met. Provided that the overall peak reduction is worth the profit reduction perceived by the retailer in the sale of electricity, the equilibrium is beneficial for both the retailer and the final electricity consumers.

The two-component electricity tariff's effectiveness was assessed by introducing a reference tariff with constant energy component. This tariff evidenced the importance of splitting and separately accounting for energy and power. The mere differentiation of these two products creates a scenario that is propitious for the adoption of DSEs and PV. The reference constant tariff was compared against a 4-level tariff, which illustrates the second profit possibility, namely the possibility of reducing the energy component costs. A variable tariff's energy component provides a more versatile control signal. This 4-level tariff was exploited in the model that considers the retailer's perspective. This model revealed that the retailer can use the prices as a control signal, and influence, but not entirely determine, the final equilibrium's outcome.

The four variables sized in the model, namely PV size and battery energy capacity, input and output power can be classified in two main categories. If the variables contribute to reducing the energy component, they are referred to as energy variables. Analogously, if

the variables contribute to mitigating the maximum peak, they are referred to as power variables. The battery energy capacity and output power belong to the former, and the PV power and the battery input power to the latter category. This division was established by analysing the sensitivity of the parameters to the relative weights between the tariff's energy and the peak components. Battery and PV are interdependent upon each other. There exists a significant influence of the PV cost upon the battery input power. The models' results evidence that both battery and PV are necessary, but the battery investment was found to be consistently larger than for PV.

The equilibrium between the fee paid for the energy and peak components was found to have different forms under different conditions. When the battery costs are varied, while the PV costs are fixed, the fee paid for the energy component remains approximately constant, while the fee associated with the peak decreases with decreasing battery costs. On the other hand, when the battery costs are kept constant, while the PV costs vary, the situation is the opposite. This fact again evidences the coupling between PV and the reduction in the energy component, or the inefficacy of the PV at actively controlling the peak.

In the first model, formulated from the user's perspective, the tariff alone provides equilibrium conditions. The investments in battery elements and PV constitute the necessary incurred costs to achieve this equilibrium. The retailer's objective of reducing the peak is automatically attained, at expenses of a profit reduction in the sale of electricity. The retailer perceives a profit reduction in the sale of electricity proportional to the investment incurred by the users. When users invest between 20% and 25% of the total cost in batteries and PV, the retailer achieves 15% and 20% peak reductions under the constant and 4-level tariffs, respectively.

When the retailer objectives are specified and the two players simultaneously taken into account in the equilibrium construction, the investment shares are similar. However, the retailer can use the electricity prices to influence the final equilibrium. In this model, the cost paid by the retailer at the spot market was approximated by a quadratic function. In the base scenario, when no DSEs or PV are deployed, the difference between the retailer's costs and revenue is approximately between +3% and + 4%, that is, the retailer obtains a 3% to 4% profit for delivering electricity to the final consumers. However, users facing the demand-based tariff decide to invest in battery and PV. When the retailer exerts no control upon the energy and power prices, the difference between the price paid at the spot market and the revenue obtained from the demand-based tariff is approximately -10.5%, that is, the investment incurred by the users, between 20% and 25%, results in a negative profit for the retailer. The introduction of a superimposed signal in both the energy and power tariff components allows the retailer to mitigate this negative profit and decrease it to -4.0%. The underlying assumption is that this profit reduction is acceptable if the benefit derived from the overall peak reduction is more valuable.

As the equilibrium resulting from the distributed adoption of DSEs and PV can accrue

benefits for both the final electricity consumers and the retailer simultaneously, it can be concluded that it is advantageous for society. Relying on a distributed electrical storage capacity for grid regulation provides a previously non-existent level of controllability.

The electrical system seems to be following the path of the telecom companies, in that it is likely that it converges to a scenario in which users are charged for power and not for energy. This dissertation contributes to paving the path in that direction, by providing an active and efficient mechanism to differentiate and individually control two variables; namely, energy and power. The demand-based electricity tariff introduced in this dissertation provides two superimposed control dimensions, an hourly and a seasonal one.

Buildings are not isolated entities, they feature very many interfaces with larger and more complex systems. The analysis and planning of the building's exergetic performance necessarily has to include these boundaries, especially when the ultimate goal is to mitigate the environmental impact of buildings upon the largest system under consideration: the Earth. The boundary condition considered in this dissertation is the one between the buildings and the electrical grid. The challenges appearing at this interface are mainly associated with the timing and magnitude of the aggregate consumption. This dissertation showed —controverting the idea of a policy fostering a massive and general deployment of rooftop PV— that an orchestrated deployment of DSEs and rooftop PV, together with a power-aware pricing policy, can bring technical and economic benefits to society.

6.1 Implications of the Results and Findings for the $2Sol$ System

The $2Sol$ system strives to secure the provision of the building's thermal load without increasing the instantaneous electrical power by more than 10-15% [43]. This dissertation showed that a *lowEx* community can achieve this objective. The power addition can be actually 0, or even negative. The HPs can be scheduled in such a way that their operation does not exacerbate the maximum peak already imposed by the building. Once a DSE has been integrated, the maximum power withdrawn by the building is considerably lower. The electrification of the heating and cooling systems is expected to impact the electrical system in terms of the additional energy required, but not in terms of the required instantaneous power. Tackling the energy problem requires enlarging the boundary condition to consider a global perspective.

The implicit assumption regarding the self-consumption of the PV electricity has important consequences for the distribution grid planning and operation. This assumption also raises important questions in regard to the building operation; namely, how to better utilize the battery and PV when, from the user's perspective, they are idle. The DSE and PV could be used, even during vacation periods, to inject heat into the MBHE.

6.2 Future Work

There are several ways in which this dissertation can be continued or enhanced. This section is very brief and is by no means exhaustive of the list of possibilities. The BLP's formulation and solution offer a large potential. The problem could be extended to represent a larger variety of buildings' characteristics, weather patterns, occupancy regimes, or operational conditions. The use of advanced solution methods, like decomposition techniques, might also be advisable. The single aspect that requires more attention is the modelling of the retailer's profit. The simulation of occupancy is another aspect that has to be further developed and validated with real data. Another important aspect is the definition of the ownership structure. Who owns the battery and PV? Who owns the electricity meter? And other similar questions. Similar to the latter topic is the definition of the electrical connection between the battery and the mains, the necessary power electronics, algorithms, and so forth. The models presented in this dissertation can be incorporated in larger systems; for instance, systems comprising representations of the electrical grid and district facilities.

The price scheme used in this dissertation does not consider the impact of renewables in the merit order curves. More elaborated price structures can be developed that better reflect the real market and electrical system conditions.

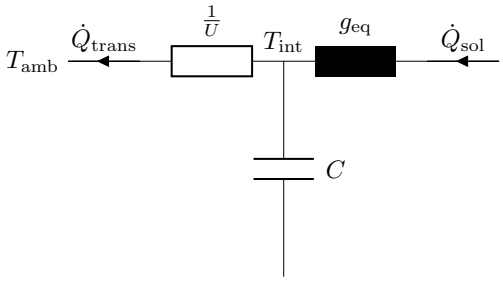

Appendix A

Load Generator Thermal Model

This appendix provides additional details on the simulations carried out within the load generator described in Chapter 3. The different blocks are implemented as a collection of software routines, which are designed for fast and computationally efficient profiling of the different buildings' electricity consumption patterns.

The load generator structure is depicted in Figure 3.4 on page 42. The parameters and vectors are summarized in Tables 3.2, 3.3, and 3.4. Besides the building's physical parameters, the location-dependent parameters, i.e. temperature and solar radiation vectors, play an important role in defining the building's final electricity consumption. Solar gains are calculated for a vertical surface facing south, and the specific solar radiation at the rooftop is calculated for a 30-degree tilted surface also facing south. These calculations are based on the equations derived in [53].

This appendix is organized as follows: Section A.1 describes the mathematical model employed to dispatch the HPs in a way that contributes to reduce the building's maximum daily peaks. Section A.2 documents the constant values assumed in the load generator calculations.

A.1 Heat Pump Dispatch Model

The HPs dispatch presented in Section 3.4 is based on the MIP described in this section. In addition to the parameters and vectors presented in Tables 3.2, 3.3, and 3.4, the model includes the vectors described in Table A.1. The underlying assumption is that the building's thermal mass can be modelled as a thermal battery. Vectors $\mathbf{th}_{\text{soc}}$, $\mathbf{q}_{\theta}^{\text{in}}$, and $\mathbf{q}_{\theta}^{\text{out}}$ can be thought of as the thermal counterpart of vectors $\mathbf{b}_{\text{soc}}$,$\mathbf{x}_{b}^{\text{in}}$, and $\mathbf{x}_{b}^{\text{out}}$, respectively, in model (4.1).

The HPs scheduling model is given by (A.1). Superscripts ^{0},$^{\bar{0}}$, or $^{+1}$ indicate that the vectors are defined for the domains Ω^{0}, $\Omega^{\bar{0}}$, and Ω^{+1}, respectively, as defined in Table 2.6 on page 34. For instance, $\mathbf{th}_{\text{soc}}^{0} = \{\mathbf{th}_{\text{soc}}(d_1 h_1), \mathbf{th}_{\text{soc}}(d_1 h_2)\}$.

Description	**Symbol**	**Set**	$\{\cdot\}$	**Units**
Thermal capacity state of charge	$\mathbf{th}_{\text{soc}}$	Ω	θ_{soc_i}	kWh_{th}
Heat injected into the building C	$\mathbf{q}_{\theta}^{\text{in}}$	Ω	$q_{\theta_i}^{\text{in}}$	kWh_{th}
Heat extracted from the building C	$\mathbf{q}_{\theta}^{\text{out}}$	Ω	$q_{\theta_i}^{\text{out}}$	kWh_{th}
Electrical load per days	$\mathbf{x}_l^{\Delta}$	D	$\mathbf{x}_l^d$	kWh
Electrical load in day d	$\mathbf{x}_l^d$	H	$x_{l_j}^d$	kWh
DHW HP electricity per days	$\mathbf{x}_{\text{hp,dhw}}^{\Delta}$	D	$\mathbf{x}_{\text{hp,dhw}}^d$	kWh
DHW HP electricity in day d	$\mathbf{x}_{\text{hp,dhw}}^d$	H	$x_{\text{hp,dhw}_j}^d$	kWh

Table A.1: Additional vectors involved in the definition of model (A.1)

$$\min_{x\in\chi^{\text{th}}} \frac{1}{\text{hp}} \sum_{d=d_1}^{d_{\tau_d}} \sum_{h=h_1}^{h_{24}} x_{\text{hp}_i} + \frac{1}{\text{hp}_{\text{dhw}}} \sum_{d=d_1}^{d_{\tau_d}} \sum_{h=h_1}^{h_{24}} x_{\text{hp,dhw}_i} + \nu \sum_{d=d_1}^{d_{\tau_d}} \max \mathbf{x}_l^d \tag{A.1a}$$

subject to

$$\theta_{\text{soc}_i} = 0, \quad \forall \theta_{\text{soc}_i} \in \mathbf{th}_{\text{soc}}^0 \tag{A.1b}$$

$$q_{\theta_i}^{\text{out}} = 0, \quad \forall q_{\theta_i}^{\text{out}} \in \mathbf{q}_{\theta}^{\text{out}^0} \tag{A.1c}$$

$$\Delta\theta_{\text{soc}_i} - \frac{1}{\xi} \cdot \frac{UHA}{C} \theta_{\text{soc}_i} - q_{\theta_i}^{\text{in}} + q_{\theta_i}^{\text{out}} = 0, \tag{A.1d}$$
$$\forall \theta_{\text{soc}_i} \in \mathbf{th}_{\text{soc}}^{+1}, \forall q_{\theta_i}^{\text{in}} \in \mathbf{q}_{\theta}^{\text{in}^{+1}}, \forall q_{\theta_i}^{\text{out}} \in \mathbf{q}_{\theta}^{\text{out}^{+1}}$$

$$\left| \frac{1}{C} \theta_{\text{soc}_i} \right| \leq 3, \quad \forall \theta_{\text{soc}_i} \in \mathbf{th}_{\text{soc}} \tag{A.1e}$$

$$q_{\theta_i}^{\text{out}} + x_{\text{hp}_i}\text{cop} - q_{\theta_i}^{\text{in}} - Q_{\text{vent}_i} - Q_{\text{infl}_i} - Q_{\text{trans}_i} + Q_{\text{sol}_i} + Q_{\text{per}_i} + Q_{\text{ap+li}_i} \geq 0, \tag{A.1f}$$
$$\forall x_{\text{hp}_i} \in \mathbf{x}_{\text{hp}} \in \{0, \text{hp}\}, \forall q_{\theta_i}^{\text{in}} \in \mathbf{q}_{\theta}^{\text{in}}, \forall q_{\theta_i}^{\text{out}} \in \mathbf{q}_{\theta}^{\text{out}}, \forall Q_{\text{vent}_i} \in \mathbf{Q}_{\text{vent}},$$
$$\forall Q_{\text{trans}_i} \in \mathbf{Q}_{\text{trans}}, \forall Q_{\text{infl}_i} \in \mathbf{Q}_{\text{infl}}, \forall Q_{\text{sol}_i} \in \mathbf{Q}_{\text{sol}}, \forall Q_{\text{ap+li}_i} \in \mathbf{Q}_{\text{ap+li}}, \forall Q_{\text{per}_i} \in \mathbf{Q}_{\text{per}}$$

$$\sum_{j=h_1}^{h_{24}} x_{\text{hp,dhw}_j}^d \text{cop} \geq \text{dhw}_d, \quad \forall \mathbf{x}_{\text{hp,dhw}}^d \in \mathbf{x}_{\text{hp,dhw}}^{\Delta}, \forall \text{dhw}_d \in \mathbf{dhw} \tag{A.1g}$$

$$q_{\theta_i}^{\text{out}} \geq 0, \quad \forall q_{\theta_i}^{\text{out}} \in \mathbf{q}_{\theta}^{\text{out}^{\bar{0}}}; \quad q_{\theta_i}^{\text{in}} \geq 0, \quad \forall q_{\theta_i}^{\text{in}} \in \mathbf{q}_{\theta}^{\text{in}}; \quad \theta_{\text{soc}_i} \geq 0, \quad \forall \theta_{\text{soc}_i} \in \mathbf{th}_{\text{soc}}; \tag{A.1h}$$
$$x_{\text{hp,dhw}_i} \in \{0, \text{hp}_{\text{dhw}}\}, \quad \forall x_{\text{hp,dhw}_i} \in \mathbf{x}_{\text{hp,dhw}}; \quad x_{\text{hp}_i} \in \{0, \text{hp}\}, \quad \forall x_{\text{hp}_i} \in \mathbf{x}_{\text{hp}}$$

Equation (A.1a) is the objective function, it penalizes the maximum daily electricity peak. The HPs' electricity consumption are modelled as binary variables. The weighting factor ν is necessary to assign the two objective terms, i.e. the HPs' electricity consumption and the appliances + lighting consumption, the same importance.

Equations (A.1b)-(A.1e) model the building thermal capacity C as a battery, which can be charged to ± 3°C. The second term in (A.1d) represents the additional losses incurred

Description	Symbol	Units	Value		
			Standard	From	To
Area per person	A_s/P	m^2/P	40	30	50
Air heat capacity	C_{air}	$kWh_{th}/(kg\,K)$	2.811×10^{-4}	—	—
Air density	ρ_{air}	kg/m^3	1.225	—	—
Water heat capacity	C_{water}	$kWh_{th}/(kg\,K)$	1.16×10^{-3}	—	—
Water density	ρ_{water}	kg/m^3	1000	—	—
Ventilation volume (day)	V_{vent}	$m^3/(P\,h)$	30	—	—
Ventilation volume (night)	V^n_{vent}	$m^3/(P\,h)$	15	—	—
Infiltration volume	V_{infl}	$m^3/(m^2\,h)$	0.1	—	—
Metabolic heat gains	$\dot{Q}_{per}$	W	70	—	—
Lighting elec. power (rooms)	p^r_{li}	W/m^2	6.3	3	10
Lighting elec. power (kitchen)	p^k_{li}	W/m^2	12	6	18
Appliances elec. power (rooms)	p^r_{ap}	W/m^2	2	1	3
Appliances elec. power (kitchen)	p^k_{ap}	W/m^2	40	30	50
DHW consumption (rooms)	V^r_{dhw}	l/P	40	30	50
DHW consumption (kitchen)	V^k_{dhw}	l/P	30	10	50

Table A.2: Constants involved in the load generator calculation [62–64]

when increasing or decreasing the temperature of the building's thermal mass.

The energy balance is enforced in (A.1f), and (A.1g) ensures that the DHW production is satisfied.

A.2 Module Constants

Table A.2 describes the different constants assumed in the calculations. The different heat components used in the thermal balance are given by (A.2), where t is the time in hours.

$$Q_{trans} = UHA_s\,(hdd + cdd)\,t \tag{A.2a}$$

$$Q_{vent} = \rho_{air} C_{air} V_{vent} P\,(hdd + cdd)\,t \tag{A.2b}$$

$$Q_{infl} = \rho_{air} C_{air} V_{infl} A_s\,(hdd - cdd)\,t \tag{A.2c}$$

Nomenclature

Models' Scalars

b_e	Battery energy capacity
b_p^{in}	Battery input power
b_p^{out}	Battery output power
b_{η_c}	Battery charging efficiency
b_{η_d}	Battery discharging efficiency
b_η	Battery roundtrip efficiency $b_{\eta_c} b_{\eta_d}$
$b_{\text{soc}}^{\min}$	Minimum SOC (maximum DOD)
ϕ_p	PV peak power
ϕ_a	PV effective area and efficiency
γ	Battery maximum number of cycles
τ_y	Battery calendar life
τ_ϕ	PV calendear life

Models' Costs and Parameters

ξ	Power conversion factor
α	Ratio between grid and peak costs
r	Discount rate
m	Maintenance rate
τ_d	Length of the analysis period
c_e^k	Cost per storage capacity unit
c_p^k	Cost per storage power unit
$c_{b_e}^f$	Daily per-unit battery energy fixed cost
$c_{b_p}^f$	Daily per-unit battery power fixed cost
$c_{b_e}^m$	Marginal cost of battery storage
c_ϕ^k	Cost per PV power unit
c_ϕ^f	Daily per-unit PV power fixed cost

Models' Vectors

$\mathbf{b}_{\text{soc}}$	Battery SOC

$\mathbf{x}_b^{\text{in}}$	Electricity flowing into the battery
$\mathbf{x}_b^{\text{out}}$	Electricity flowing out of the battery
$\mathbf{x}_l$	Building's electrical load
$\mathbf{x}_l^d$	Building's electrical load for day d
$\tilde{\mathbf{x}}_l$	Stochastic version of the building's electrical load
$\mathbf{x}_g$	Electricity withdrawn from the grid
$\mathbf{x}_g^d$	Electricity withdrawn from the grid for day d
$\mathbf{c}_g'$	Electricity prices (energy and power components)
$\mathbf{c}_g$	Electricity prices (energy component)
$\mathbf{c}_g^d$	Electricity prices (energy component) for day d
$\mathbf{c}_g^{\max}$	Peak prices (power component)
$\mathbf{k}_g^{\Delta}$	Maximum daily peaks
$\mathbf{c}_g^{\text{spot}}$	Spot market prices
$\mathbf{x}_l^{\text{total}}$	Total electrical load (all buildings)
$\mathbf{x}_g^{\text{total}}$	Total electricity withdrawn from the grid (all buildings)
$\mathbf{x}_g^{d,\text{total}}$	Total electricity withdrawn from the grid for day d

Models' Investments

C	Total cost
C_g	Total fee due to grid electricity (energy component)
$\text{C}_g^{\max}$	Total fee due to daily peaks (power component)
$\text{C}_{b,e}^f$	Investment in battery storage $c_e^k b_e$
$\text{C}_{b,e}^m$	Total cost of transit energy
$\text{C}_{b,p}^{\text{in}}$	Investment in battery input power $c_p^k b_p^{\text{in}}$
$\text{C}_{b,p}^{\text{out}}$	Investment in battery output power $c_p^k b_p^{\text{out}}$
C_ϕ	Investment in PV power $c_\phi^k \phi_p$

Bilevel Program's scalars

n_{LL}	Number of followers
ι	Yearly average power peak component cost
ρ	Cap for the absolute value of the additional price's energy component
$\rho_{\max}$	Cap for the absolute value of the additional price's power component

Bilevel Program's vectors

$\mathbf{c}_g^{\mathrm{UL}}$	Additional energy component prices
$\mathbf{c}_g^{\mathrm{UL,max}}$	Additional peak component prices
$\mathbf{c}_{g,\Delta}^{\mathrm{UL}}$	Additional energy component prices per days
$\mathbf{c}_{g,d}^{\mathrm{UL}}$	Additional energy component prices for day d
$\mathbf{x}_{g,\Omega}$	Aggregated load vector, summation of all followers
$\mathbf{c}_g''$	Extended price's energy component
$\mathbf{c}_g^{\mathrm{max}''}$	Extended price's power (grid utilization) component

Load Generator's Configuration Parameters

btype	Building type
loc	Location
markov	Markov type
sd	Mechanical shading factor
$\mathrm{sd}_{\mathrm{pol}}$	Shading factor for the shades polygon
g_{eq}	Equivalent orientation and solar transmission
s_{ap}	Appliances consumption scenario
s_{li}	Lighting consumption scenario
s_{dhw}	DHW consumption scenario
s_{ap}^r	Room appliances consumption scenario
s_{ap}^k	Kitchen appliances consumption scenario

Load Generator's Scalars

P	Number of persons
A_s	Constructed area
A_f	Facade area
A_w	Glazing area
H	Shape factor
U	U-value
A_s^r	Rooms area
A_s^k	Kitchen area
hp	HP electrical power
$\mathrm{hp}_{\mathrm{dhw}}$	DHW HP electrical power
cop	COP
C	Thermal capacity

Load Generator's Vectors

$\mathbf{T}_{\text{amb}}$	Ambient temperature
$\mathbf{T}_{\text{ind}}$	Indoor temperature
cdd	Cooling Degree Days
hdd	Heating Degree Days
p	Normalized occupancy
$\mathbf{Q}_{\text{infl}}$	Infiltration losses
$\mathbf{Q}_{\text{ap+li}}$	Internal gains due to appliances and lighting
$\mathbf{Q}_{\text{per}}$	Internal gains due to persons
$\mathbf{Q}_{\text{trans}}$	Transmission losses
$\mathbf{Q}_{\text{vent}}$	Ventilation losses
$\mathbf{Q}'_{\text{sol}}$	Normalized solar radiation on a vertical surface
$\mathbf{Q}_{\text{sol}}$	Equivalent total solar gains
$\mathbf{E}'_e$	Normalized solar irradiance on a horizontal plane
$\mathbf{E}_e$	Normalized corrected solar irradiance
sd	Normalized shades
$\mathbf{x}_{\text{hp}}$	HP electricity consumption
$\mathbf{x}_{\text{hp,dhw}}$	DHW HP electricity consumption
$\mathbf{x}^{\Delta}_{\text{hp,dhw}}$	DHW HP electricity consumption per days
$\mathbf{x}^{d}_{\text{hp,dhw}}$	DHW HP electricity consumption in day d
$\mathbf{x}_{\text{ap+li}}$	Total appliances plus lighting consumption
$\mathbf{x}^{r}_{\text{ap}}$	Appliances consumption (rooms)
$\mathbf{x}^{k}_{\text{ap}}$	Appliances consumption (kitchen)
$\mathbf{x}^{r}_{\text{li}}$	Lighting consumption (rooms)
$\mathbf{x}^{k}_{\text{li}}$	Lighting consumption (kitchen)
dhw	DHW daily consumption
dl	Daylight hours (from,to)
$\mathbf{th}_{\text{soc}}$	Thermal battery SOC
$\mathbf{q}^{\text{in}}$	Heat injected into the building thermal capacity
$\mathbf{q}^{\text{out}}$	Heat extracted from the building thermal capacity

Load Generator's Markov Probabilities

`A`	Absent state
`P`	Present state
p_t	Probability that an occupant is present
μ	Mobility parameter
t_{00}	Transition probability: probability of staying away
t_{01}	Transition probability: probability of arriving home

t_{10}	Transition probability: probability of leaving home
t_{11}	Transition probability: probability of staying at home

Bibliography

[1] Klaus-Henning Ahlert. Assessing the Economics of Distributed Storage Systems at the End Consumer Level. In *Proceedings of the 4th International Renewable Energy Storage Conference (IRES-4) (24.-25.11.)*, Berlin, Germany, 2009.

[2] Klaus-Henning Ahlert. *Economics of Distributed Storage Systems*. PhD thesis, Karlsruher Institut für Technology KIT, 2010.

[3] Klaus-Henning Ahlert and van Clemens Dinther. Definition of an Optimization Model for Scheduling Electricity Storage Devices. In *Proceedings of the Web 2008 - 7th Workshop on e-Business*, Paris, France, 2008.

[4] Philip Delff Andersen, Anne Iversen, Henrik Madsen, and Carsten Rode. Dynamic modeling of presence of occupants using inhomogeneous markov chains. *Energy and Buildings*, 69(0):213 – 223, 2014.

[5] Rainer Bacher. System optimization of liberalized electric power systems. Class Text ETH Zurich (unpublished), May 2012.

[6] J.F. Bard. *Practical Bilevel Optimization: Algorithms and Applications*. Nonconvex Optimization and Its Applications. Springer, 1998.

[7] L. Baringo and A.J. Conejo. Strategic offering for a wind power producer. *Power Systems, IEEE Transactions on*, 28(4):4645–4654, Nov 2013.

[8] Cajsa Bartusch, Fredrik Wallin, Monica Odlare, Iana Vassileva, and Lars Wester. Introducing a demand-based electricity distribution tariff in the residential sector: Demand response and customer perception. *Energy Policy*, 39(9):5008 – 5025, 2011.

[9] The Boston Consulting Group BCG. Batteries for electric cars, challenges, opportunities and the outlook for 2020. Technical report, The Boston Consulting Group, 2009.

[10] Sebastina Beer, Tomás Gómez, David Dallinger, Ilan Momber, Chris Marnay, Michael Stadler, and Judy Lai. An economic analysis of used electric vehicle batteries integrated into commercial building microgrids. *IEEE Transactions on Smart Grid*, 3(1):517–525, March 2012.

[11] BFE. Schweizerische elektrizitätsstatistik 2013. Technical report, Bundesamt für Energie BFE, 2014.

[12] Severin Borenstein. The long-run efficiency of real-time electricity pricing. *The Energy Journal*, pages 93–116, 2005.

[13] BPIE. Europe's buildings under the microscope. a country-by-country review of the energy performance of buildings. Technical report, Buildings Performance Institute Europe, 2011.

[14] Diane Broad and Ken Dragoon. Chapter 20 - {DR} for integrating variable renewable energy: A northwest perspective. In Lawrence E. Jones, editor, *Renewable Energy Integration*, pages 253 – 264. Academic Press, Boston, 2014.

[15] A. Brooke, D.A. Kendrick, A. Meeraus, and R.E. Rosenthal. *GAMS: A User's Guide*. Scientific Press, 1988.

[16] Michel Broussely. {CHAPTER} {THIRTEEN} - battery requirements for hevs, phevs, and evs: An overview. In Gianfranco Pistoia, editor, *Electric and Hybrid Vehicles*, pages 305 – 345. Elsevier, Amsterdam, 2010.

[17] Judy Chang, Ioanna Karkatsouli, Johannes Pfeifenberger, Lauren Regan, Kathleen Spees, James Mashal, and Matthew Davis. The value of distributed electricity storage in texas. proposed policy for enabling grid-integrated storage investments. Technical report, Oncor, November 2014.

[18] Haisheng Chen, Thang Ngoc Cong, Wei Yang, Chunqing Tan, Yongliang Li, and Yulong Ding. Progress in electrical energy storage system: A critical review. *Progress in Natural Science*, 19(3):291 – 312, 2009.

[19] Federal Energy Regulatory Comission. Staff report: Demand response and advance meetering. Technical report, Federal Energy Regulatory Comission, August 2006.

[20] Gaëtan Masson (CARES Consulting), Sinead Orlandi, and Manoël Rekinger. Global market outlook for photovoltaics 2014-2018. Technical report, EPIA, European Photovoltaic Industry Association, 2014.

[21] Paul Denholm and Maureen Hand. Grid flexibility and storage required to achieve very high penetration of variable renewable electricity. *Energy Policy*, 39(3):1817 – 1830, 2011.

[22] Paul Denholm and Maureen Hand. Grid flexibility and storage required to achieve very high penetration of variable renewable electricity. *Energy Policy*, 39(3):1817 – 1830, 2011.

[23] digitalSTROM. *digitalSTROM Manual, including Introduction, Operation and Settings*, 2013. `http://www.digitalstrom.com/`.

[24] London Economics. Energy retail markets comparability study. Technical report, London Economics, April 2012.

[25] Konferenz Kantonaler Energiedirektoren. Mustervorschriften der kantone im energiebereich (muken). Technical report, Konferenz Kantonaler Energiedirektoren, 2014.

[26] V.M. Fthenakis and T. Nikolakakis. 1.11 - storage options for photovoltaics. In Ali Sayigh, editor, *Comprehensive Renewable Energy*, pages 199 – 212. Elsevier, Oxford, 2012.

[27] Bundesamt für Energie BFE. Erste Massnhamen Energiestrategie 2050: Faktenblatt 1. Technical report, Schweizerisches Bundesamt für Energie BFE, April 2012.

[28] Bundesamt für Energie BFE. Photovoltaik-grossanlagen in der schweiz, branchenstruktur und preisentwicklung. Technical report, Schweizerisches Bundesamt für Energie BFE, May 2014.

[29] S.A. Gabriel, A.J. Conejo, J.D. Fuller, B.F. Hobbs, and C. Ruiz. *Complementarity Modeling in Energy Markets*. International Series in Operations Research & Management Science. Springer New York, 2012.

[30] C.W. Gellings. The concept of demand-side management for electric utilities. *Proceedings of the IEEE*, 73(10):1468–1470, Oct 1985.

[31] Joern Hoppmann, Jonas Volland, Tobias S. Schmidt, and Volker H. Hoffmann. The economic viability of battery storage for residential solar photovoltaic systems – a review and a simulation model. *Renewable and Sustainable Energy Reviews*, 39(0):1101 – 1118, 2014.

[32] M. Ibrahim, M.Z. Jaafar, and M.R.A. Ghani. Demand-side management. 4:572–576 vol.4, Oct 1993.

[33] Antiono Sánchez Ihl. *Enhancing the Quality of Ground Coupled Heat Pumps*. PhD thesis, ETH Zurich, 2014.

[34] D.P. Jenkins, J. Fletcher, and D. Kane. Model for evaluating impact of battery storage on microgeneration systems in dwellings. *Energy Conversion and Management*, 49(8):2413 – 2424, 2008.

[35] S.J. Kazempour, A.J. Conejo, and C. Ruiz. Strategic generation investment using a complementarity approach. *Power Systems, IEEE Transactions on*, 26(2):940–948, May 2011.

[36] S.J. Kazempour, A.J. Conejo, and C. Ruiz. Strategic generation investment considering futures and spot markets. *Power Systems, IEEE Transactions on*, 27(3):1467–1476, Aug 2012.

[37] Andreas Kemmler, Alexander Piégsa, Andrea Ley (Prognos AG), Philipp Wüthrich, Mario Keller (Infras AG), Martin Jakob, and Giacomo Catenazzi (TEP Energy GmbH). Analyse des schweizerischen energieverbrauchs 2000 - 2013 nach verwendungszwecken. Technical report, Schweizerisches Bundesamt für Energie BFE, Prognos AG, Infras AG, TEP Energy GmbH, September 2014.

[38] Daniel Kirschen and Goran Strbac. *Markets for Electrical Energy*. John Wiley & Sons, Ltd, 2005.

[39] J. Zico Kolter and Matthew J. Johnson. REDD: A Public Data Set for Energy Disaggregation Research. In *SustKDD Workshop on Data Mining Applications in Sustainability*, 2011. `http://redd.csail.mit.edu/`.

[40] Albert R. Landgrebe and Samuel W. Donley. Battery storage in residential applications of energy from photovoltaic sources. *Applied Energy*, 1983.

[41] Jason Leadbetter and Lukas Swan. Battery storage system for residential electricity peak demand shaving. *Energy and Buildings*, 55(0):685 – 692, 2012. Cool Roofs, Cool Pavements, Cool Cities, and Cool World.

[42] Hansjürg Leibundgut. *LowEx Building Design*. vdf Hochschulverlag AG, 2011.

[43] Hansjürg Leibundgut, Niklaus Haller, and Nico Abt. Ze-2sol concept booklet, 2013.

[44] Mark Levine, Diane Ürge Vorsatz, Kornelis Blok, Luis Geng, Danny Harvey, Siwei Lang, Geoffrey Levermore, Anthony Mongameli Mehlwana, Sevastian Mirasgedis, Aleksandra Novikova, Jacques Rilling, and Hiroshi Yoshino. *Residential and commercial buildings*, chapter 6. Cambridge University Press, Cambridge, United Kingdom and New York, NY, USA, 2007.

[45] Martha Lowe and Michael Ferris. *Stochastic Programming with EMP*. GAMS, June 2014.

[46] J. I. San Martín, I. Zamora, J. J. San Martín, V. Aperribay, and P. Eguía. Energy storage technologies for electric applications. In *International Conference on Renewable Energies and Power Quality*, Las Palmas de Gran Canaria, Spain, 2011.

[47] Forrest Meggers, Volker Ritter, Philippe Goffin, Marc Baetschmann, and Hansjürg Leibundgut. Low exergy building systems implementation. *Energy*, 41:48–55, August 2011.

[48] M. Parsa Moghaddam, A. Abdollahi, and M. Rashidinejad. Flexible demand response programs modeling in competitive electricity markets. *Applied Energy*, 88(9):3257 – 3269, 2011.

[49] European Network of Transmission System Operators for Electricity. Statistical database. `https://www.entsoe.eu/data/data-portal/Pages/default.aspx`. last checked on 01.02.2014.

[50] F. Oldewurtel, A. Ulbig, A. Parisio, G. Andersson, and M. Morari. Reducing peak electricity demand in building climate control using real-time pricing and model predictive control. In *Decision and Control (CDC), 2010 49th IEEE Conference on*, pages 1927–1932, Dec 2010.

[51] Andrew Ott. Chapter 21 - case study: Demand-response and alternative technologies in electricity markets. In Lawrence E. Jones, editor, *Renewable Energy Integration*, pages 265 – 274. Academic Press, Boston, 2014.

[52] J. Page, D. Robinson, N. Morel, and J.-L. Scartezzini. A generalised stochastic model for the simulation of occupant presence. *Energy and Buildings*, 40(2):83 – 98, 2008.

[53] Volker Quaschning. Sonnenstrahlung. In *Regenerative Energiesysteme : Technologie - Berechnung - Simulation ; mit 117 Tabellen*, chapter 2, pages 55–88. Hanser, 8 edition, 2013.

[54] Robert G. Quayle and Henry F. Diaz. Heating degree day data applied to residential heating energy consumption. *Journal of applied metheorology*, 19(3):241–246, March 1980.

[55] Guido Rossum. Python reference manual. Technical report, Amsterdam, The Netherlands, The Netherlands, 1995.

[56] Jonas Ruggle. Optimizing the design and operation of ground source heat pumps in the european context. Master's thesis, ETH Zurich, November 2014.

[57] Andrzej Ruszczyński and Alexander Shapiro. *Handbooks in OR & MS*, volume 10. Elsevier, 2003.

[58] Diego Sandoval and Hansjürg Leibundgut. Introduction of electrical batteries in the operation of lowex buildings. *Energy and Buildings*, 81(0):105 – 114, 2014.

[59] Suvrajeet Sen and Julia L. Higle. And introductory tutorial on stochastic linear programming models. *Interfaces*, 29(2):36–61, 1999.

[60] Alexander Shapiro, Andrzej Ruszczyński, and Darinka Dentcheva. *Lectures on Stochastic Programming, Modelling and Theory*. Society of Industrial and Applied Mathematics, Philadelphia, 2009.

[61] Fereidoon P. Sioshansi. Chapter 22 - the implications of distributed energy resources on traditional utility business model. In Lawrence E. Jones, editor, *Renewable Energy Integration*, pages 275 – 283. Academic Press, Boston, 2014.

[62] Swiss society of engineers and architects. Elektrische energie im hochbau, 1995.

[63] Swiss society of engineers and architects. Standard-nutzungsbediungungen für die energie- und gebäudetechnik, sia 2024, 2006.

[64] Swiss society of engineers and architects. Thermische energie im hochbau, 2007.

[65] David Spiers. Chapter iib-2 - batteries in {PV} systems. In Augustin McEvoy, Tom Markvart, and Luis Castañer, editors, *Practical Handbook of Photovoltaics (Second Edition)*, pages 721 – 776. Academic Press, Boston, second edition edition, 2012.

[66] Goran Strbac. Demand side management: Benefits and challenges. *Energy Policy*, 36(12):4419 – 4426, 2008. Foresight Sustainable Energy Management and the Built Environment Project.

[67] J. Taneja, K. Lutz, and D. Culler. The impact of flexible loads in increasingly renewable grids. In *Smart Grid Communications (SmartGridComm), 2013 IEEE International Conference on*, pages 265–270, Oct 2013.

[68] The European Commission. *Energy Prices and Costs in Europe*. The European Commission, January 2014.

[69] Energy Systems Research Unit. *The ESP-r System for Building Energy Simulation User Guide Version 10 Series*. University of Strathclyde, October 2012. `http://www.esru.strath.ac.uk/Programs/ESP-r.htm`.